THE UNIVERSITY OF WESTERN AUSTRALIA

School of Mechanical, Materials and Mechatronics Engineering

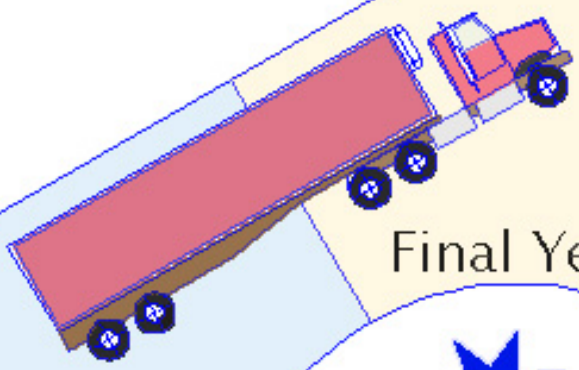

Final Year Project 2003

In-Service Testing of Road Friendly Suspensions

by Ian Peters

Supervisor: Brian Stone

sponsored by Main Roads WA

Acknowledgements

to Brian Stone, for his encouragement and excellent guidance

to Kevin Sands, for being more than helpful in providing a testing vehicle and facilities in which to really make headway into this project

to Siva Thillainath, Hamptons Transport and the guys from Doug Gould's, for the use of their facilities and equipment for testing

to Dante Travaglini, for providing an excellent foundation paper and background information from which to work

to John Marcolina and Andrew Lambert from Main Roads for their knowledge, field help, and assistance in matters clerical

to Peter Robertson of Robbo's Contracting, and Phil Baruffi and Steve Camarri of Giacci's, for providing useful opinions early on

to Emi, for helping me through a very critical period

to Mum, Mark and Kate, for always being helpful and positive

to Dad, for being the best sounding board on Earth, for his excellent reviewing, opinions and all around advice, and his unwilting support

SYNOPSIS

The development of a field test for determining the performance characteristics of heavy vehicle trailer suspensions is considered in this thesis. A regulatory concern exists that some particular types of suspensions, known as 'road friendly' suspensions, are not being maintained or designed properly. Road friendly suspensions offer productivity benefits and economic savings to road users and providers alike, and it is of interest to the transport community to be able to know when they are performing inadequately.

However, the lack of an inexpensive and simple method with which to quantifiably determine the performance of road friendly suspensions has hampered their forward progress. Of critical interest is the chassis' vertical sprung natural frequency and damping ratio, which must meet certain performance parameters. Currently, assessing a suspension for these performance parameters is either expensive or unreliable.

This thesis details the development of a simple in-service (on-the-road) field test. A drop test, involving the rolling of a suspension over a set of raised bumps is developed. Recording of chassis performance is accomplished with a magnet-mounted low-G accelerometer, which itself is attached to a portable computer. Analysis of performance data is accomplished via a graphical-user-interface, designed for quickly determining the natural frequency and damping ratio after a test.

Four individual field testing sessions involving heavy vehicles are held, and the qualitative and quantitative results gained from each included in the development of the in-service test. The evidence from these testing sessions shows that a suspension with performing dampers can be easily identified from a suspension with non-performing dampers.

A mechanical suspension is easily identified from an air suspension using the test, by comparing individual sets of results with well established performance guidelines. Testing on loaded suspensions is found to be a requirement, as testing unloaded provides results which are not directly comparable.

The test appears to meet the requirements of being repeatable and quick. It is simple to administer, non-intrusive, highly portable, inexpensive, and does not pose a safety threat to personnel.

22 October 2003

Ian Peters
9 Millington St
Ardross
Western Australia
6153

Faculty of Engineering, Computing and Mathematics
School of Mechanical, Materials and Mechatronics Engineering
Crawley
Western Australia
6009

Attn: Dean of Engineering

Dear Sir

Re: Transmittal of mechanical engineering final year thesis

I am proud to present for your consideration, my honours thesis, entitled *'In-service testing of road friendly suspensions'*. It is the culmination of a year's hard yet rewarding work.

This work has shown me that with a little initiative, almost anything is possible. I leave the university with a sense of being able to accomplish real work, and do real research which can provide useful results and information.

I thank the University for providing a stimulating cultural and intellectual environment, and for giving me the opportunity to work for and learn from a teacher of whom I have had none better, Professor Brian Stone.

Yours faithfully

Ian Peters
991999/5

LIST OF FIGURES

LIST OF EQUATIONS

LIST OF TABLES

TABLE OF CONTENTS

◈ ◈ ◈ ◈

NOMENCLATURE

ω_n	natural frequency (Hz)
ζ	damping ratio
k_{spring}	spring rate of an airbag (N/m)
c_{damper}	damping rate of a truck damper (Ns/m)
k_{tyre}	constant spring rate of a truck tyre (N/m)
c_{tyre}	constant damping rate of a truck tyre (Ns/m)
g	constant gravity rate on Earth (m/s^2)
M	quarter axle model sprung mass (kg)
m	quarter axle model axle mass (kg)
P	pressure inside an airbag (N/m^2)
V	volume inside an airbag (m^3)
γ	constant polytropic gas coefficient
y1	modelled vertical position of bottom of truck tyre with respect to Earth (m)
y2	modelled vertical position of centre of axle mass with respect to Earth (m)
y3	modelled vertical position of centre of sprung mass with respect to Earth (m)
F_{spring}	force exerted on an airbag during modelled transient oscillation (N)
Δt	time increment used in modelling transient oscillation (s)
t_n	individual times at which accelerations are recorded (s)
a_n	vertical acceleration of sprung mass at individual time increments t_n (m/s^2)
v_n	vertical velocity of sprung mass at individual time increments t_n (m/s)
dt	time increment between recorded accelerations (s)
K	constant adjustment to acceleration data used in removal of bias (m/s^2)
α,β	stretching factors applied to acceleration data to correct under and over peaking
δ	logarithm of ratio of adjacent peaks in a transient decay curve (m/s^2)

1 INTRODUCTION AND BACKGROUND

1.1 INTRODUCTION

The development of a field test suitable for determining the in service performance of certain heavy vehicle suspensions is considered in this thesis. The ability to quickly and simply determine whether a truck or trailer suspension is performing within specified operating parameters is an ability that road maintenance authorities, such as Main Roads Western Australia (MRWA), currently lack. It is a concern that some parts of the Australian transport industry are not adequately maintaining 'road friendly' airbag suspensions (RFS), which are a relatively new and encouraged technology. With the advent of Performance Based Standards for the Australian road transport industry, it is essential that regulators have suitable tools and methods for carrying out the compliance and enforcement task.

1.2 AUSTRALIAN ROAD TRANSPORT REFORM

The Australian road transportation industry has been undergoing a steady reform process over the past decade. Part of this process has been an increase in permitted mass limits (also known as concessional loading) for heavy vehicles fitted with road-friendly suspensions (RFS). Mass limits are statutorily imposed for safety reasons and to limit premature wear and failure of roads and bridges.

Mass limits for particular heavy vehicle combinations are determined based upon their axle configuration. In Western Australia, typical mechanical leaf-sprung tri-axle groups are permitted to carry 20 tonne, with twin-axle groups permitted 16.5 tonne. Other states have permitted additional loading on air suspensions, given proper accreditation. However, Western Australia has not pursued concessional loading on RFS, but instead allowed concessional loading on any suspension type, given proper accreditation.

Extensive research continues into the impact of and interaction of vehicles and road surfaces. Of particular interest is minimising fatigue-induced damage to road pavements, often associated with gross overloading. Part of the transport reform process aims to encourage transport operators to adopt quality management systems, thereby encouraging good loading practices. Increased mass limits could be used as encouragement to operators to adopt RFS, which are considered to cause less fatigue damage than conventional suspensions. Alternatively, reduced fees and charges could be levied on operators of air suspensions. Much research has confirmed the benefits of RFS in terms of road fatigue when carrying the same load as mechanical suspensions [01, 02, 03, 04].

1.3 ROAD FRIENDLY SUSPENSIONS

In 1992, OECD (Organisation for Economic Co-Operation and Development) Expert Group IR6 recommended research into the significant issues associated with how vehicle dynamics affect roads. The project, Dynamic Interaction between Vehicles and Infrastructure Experiment (DIVINE) [01] concluded in 1997, and the findings showed clearly that heavy vehicle suspensions equipped with airbags and dampers generated 15% less road wear compared to mechanical suspensions. Such suspensions could be characterised as having low spring stiffness, low coulomb friction, and sufficient viscous damping. The performance characteristics of road friendly suspensions are described in Chapter 3.

Suspension units, minus chassis, are generally purchased from one of several major international manufacturers, such as BPW, Hendrickson and others. The suspension units are then customised and fitted to a custom chassis. The construction, customisation and chassis fitting are usually performed locally, so as to minimise international transportation costs.

In Australia, the Department of Transport and Regional Services (DOTARS) has a list of certified road-friendly suspensions[1], which are automatically certified as road friendly based upon historical testing and documentation. However, during fitting, suspensions are often customised, with key functional components such as the dampers repositioned. This factor, along with damper maintenance concerns, are the prime reasons behind doubts regulators have over the sustained road friendly performance of air suspensions.

1.4 THIS INVESTIGATION

The work covered concerns the development of a simple field test capable of determining the performance characteristics of a suspension. The approach taken was that of a bump test, with measurement of the sprung mass motion performed using an accelerometer. In conjunction, a computer graphical-user-interface (GUI) was developed to facilitate the rapid dissemination of information following a test. The system was tested and developed over four testing sessions, culminating in an arrangement that can provide repeatable and reliable tests.

[1] *DOTARS Transport Regulation Certified Road-Friendly Suspensions,* [Online], DOTARS, Available from http://www.dotars.gov.au/transreg/str_certroad_friendly.htm [14 August 2003]

Changes in suspension performance depending on the presence or absence of damping were measured and compared to check for discernable differences. Also, mechanical-leaf suspensions were compared in performance to airbag suspensions.

The results of this investigation are intended to be used as a cornerstone in the development of a field test of airbag suspensions, which may be deployed by regulatory bodies. The developed test is not intended to be packaged as a complete operational system at this stage, and requires further development to increase operator friendliness and reliability. However, it is shown that the methods and results obtained are useful and practical.

2 PREVIOUS WORK AND LITERATURE REVIEW

The primary topic covered is the useful measurement of free transient oscillation of a heavy vehicle trailer airbag suspension. In this regard, previous work involving the assessment of possible suspension testing methods, and analysis of the operational characteristics of airbag suspensions was considered relevant. Work already completed on the assessment and practicality of heavy vehicle suspension testing methods was limited and not to the level of depth covered in this investigation.

2.1 IN-SERVICE ASSESSMENT SPECIFIC LITERATURE

Sweatman et al [05] report on many of the issues surrounding the adoption and usage of airbag suspensions. It is broad, and includes shock absorber testing to gauge what influence shock absorber degradation has on whole-of-suspension performance. The finding that the region of shock absorber performance up to a velocity of 0.1 m/s is critical to suspension performance, has implications for suspension setups where shock absorber range of travel is restricted. The report suggests maintenance regimes for suspensions meeting original-equipment road-friendliness criteria. Such regimes would involve the inspection of shock absorbers and if necessary, testing and replacement at intervals up to 400,000 km based on operating conditions.

Sweatman et al [05] identify a governmental agency need for a 'low-cost, accurate, reliable and repeatable' field test to identify underperforming suspensions. Such a test is identified as needing the ability to determine suspension frequency, damping ratio and load sharing. In covering testing options, it outlines the problems with bump testing, such as the need to measure relative acceleration between axle and chassis, thereby eliminating tyre frequencies from a purely sprung trailer mass response. It also identifies issues such as testing of sensitive loads. No development work on a field test was completed other than an identification of the issues involved.

Sweatman et al [05] build on the DIVINE [01] findings, which originally identified the critical operational performance characteristics of a road-friendly suspension. It found road-friendly suspensions, ceteris paribus, generate 15% less road wear than mechanical-leaf suspensions. Sweatman et al [05] generally agree with the DIVINE [01] findings, although suggests additional criteria for road friendliness and relaxation of the damping ratio tolerance specified in DIVINE [01].

MM Starrs et al [03] discuss the options of drop testing suspensions, such as annually in a workshop or as part of an inspection, or randomly. Emphasis is placed on the need for vehicles to be laden. The conclusions are that such testing regimes are not economically warranted. However, this is qualified with a statement that should jurisdictions wish to proceed with field test, the need exists for the development of such a test.

Cebon [06] broadly rejects the drop test procedure recommended in DIVINE [01], that being the European drop test covered by *Council Directive 92/7/EEC* [02]. It is the test adopted in Australia under Federal Office of Road Safety [07] guidelines. Cebon [06] states that such a test is not reliable in assessing 'road-friendliness', and simulates a drop test under varying scenarios of suspension type and drop test input amplitude. Cebon [06] fails to recommend a similar yet superior testing method.

Prem et al [04] as part of research into heavy vehicle suspension performance, look at various testing methods. Simulated quarter axle models of mechanical and airbag suspensions traversing the EC test bump are demonstrated. The usefulness of such a test is not broadly rejected. However, a sinusoidal-sweep 'shaking' test is rejected as a means of assessing road friendliness.

The available literature made common references to the lack of a simple suspension testing procedure. This indicates that the research and development of such a testing procedure would be beneficial. The development and trialling of such a test is the main content of this thesis.

2.2 WESTERN AUSTRALIAN PERSPECTIVE

MRWA, whose responsibility it is to regulate heavy road transport in Western Australia, has chosen to adopt several concessional loading schemes for heavy vehicle operators. The maximum standard operating weight for heavy vehicles in Western Australia is set out in Table 2.1.

Axle Group	Maximum Mass
Steer axle	6t
Twin steer axles	11t
Loaded single axle group	9t
Loaded tandem axle group	16.5t
Loaded triple load axle group	20t

Table 2.1: Axle group mass limits for heavy vehicles in Western Australia

However, under the concessional loading scheme, vehicles with the necessary permits may load up to 23.5t on triple axle groups. However, historical oversight has led to there being no requirement for such concessionally loaded axle groups to operate air suspensions, and many operate with mechanical suspensions.

Despite this, MRWA encourages the use of air suspensions for concessional loading, and would like to be in the position of offering incentives to operators choosing air suspensions. The revoking of concessional loading on mechanically sprung vehicles is unlikely to occur. However, MRWA may change its policy with regards to concessional loading and air suspensions, should a field test of air suspensions be developed. The current situation is brought about by an air of scepticism with regards to the continued reliability of air suspensions.

3 THEORY AND MODELLING

3.1 ROAD FRIENDLY PERFORMANCE

Following research by the OECD Dynamic Interaction between Vehicles and Infrastructure (DIVINE) experiment, it was established that a truck (or truck-trailer) suspension could be characterised as 'road-friendly' providing it met the following performance parameters when fully loaded:

Natural mass sprung frequency < 2 Hz

Equation 3.1: Natural frequency performance requirement

Damping > 20% of critical damping

Equation 3.2: Damping ratio performance requirement

Viscous damping > 50% of all damping

Equation 3.3: Viscous damping level performance requirement

Suspension is fitted with dual tyres in preference to single tyres

While these parameters in themselves do not specify that a road-friendly suspension need consist of airbags and viscous dampers, it is virtually impossible for a mechanical-leaf suspension to meet the required sprung frequency performance requirement. Arguably, the performance equations were, in part, designed to eliminate mechanical-leaf suspensions from being designated road-friendly. Thus, a road-friendly suspension is synonymous with an airbag or air suspension, and the terms are used interchangeably henceforth. However, it is important to remember that in the extremely unlikely scenario of a mechanical-leaf suspension meeting the above performance parameters, it may be deemed road-friendly.

To verify an individual suspension's performance, it was considered necessary to perform a test. However, recent times have seen most air suspensions certified as road friendly, providing that adequate documentation and proof of performance of like suspensions is known to authorities. There are three valid methods for testing a new suspension. Fully loaded, the chassis may be lifted down or pulled up by 80mm from its resting position, or it may be driven over an 80mm bump. Data logging linear potentiometers, such as string gauges, are fitted between the chassis and the axle. By fitting between the chassis and axle, potential influence of tyre bounce is eliminated. The obtained time series data is then analysed to isolate the natural frequency and damping ratio.

A critique and analysis of the road-friendly performance parameters and testing methods is not presented in this thesis, but is adequately covered by Cebon [06] and the DIVINE Proceedings [01]. However, it is important to explain the relevance of these performance parameters.

3.2 MODELLING

A quarter-axle suspension is often considered as the first step to modelling a suspension group. A quarter-axle system comprises one wheel (which may be twin or single tyred), one spring and one damper. A diagram of mechanical-leaf and airbag quarter-axle systems is shown in Figure 3.1 and Figure 3.2.

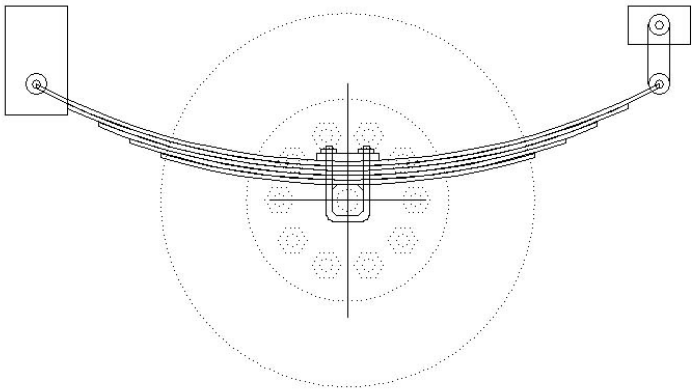

Figure 3.1: Typical mechanical leaf suspension arrangement

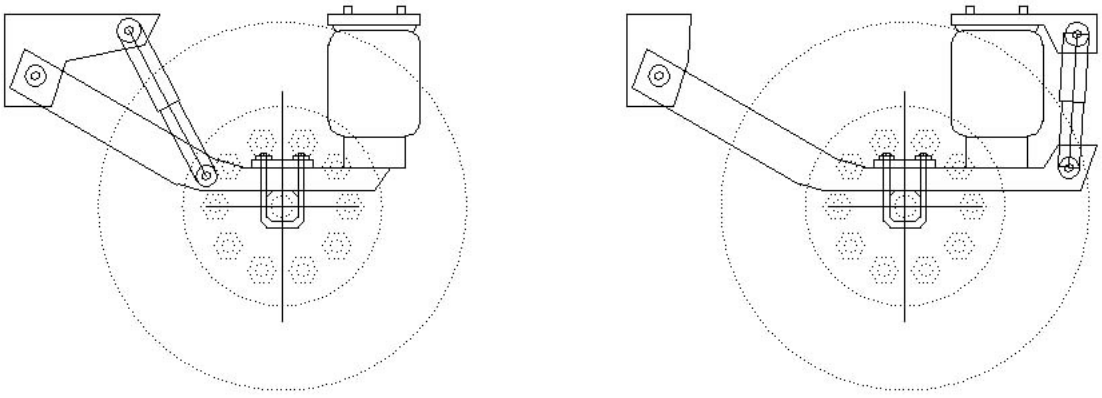

Figure 3.2: Typical airbag suspension arrangements

An air suspension system can be approximated as a two degree of freedom model, where the motion is in the vertical direction. This allows for direct comparison of the performance parameters. Such a system is shown modelled as in Figure 3.3.

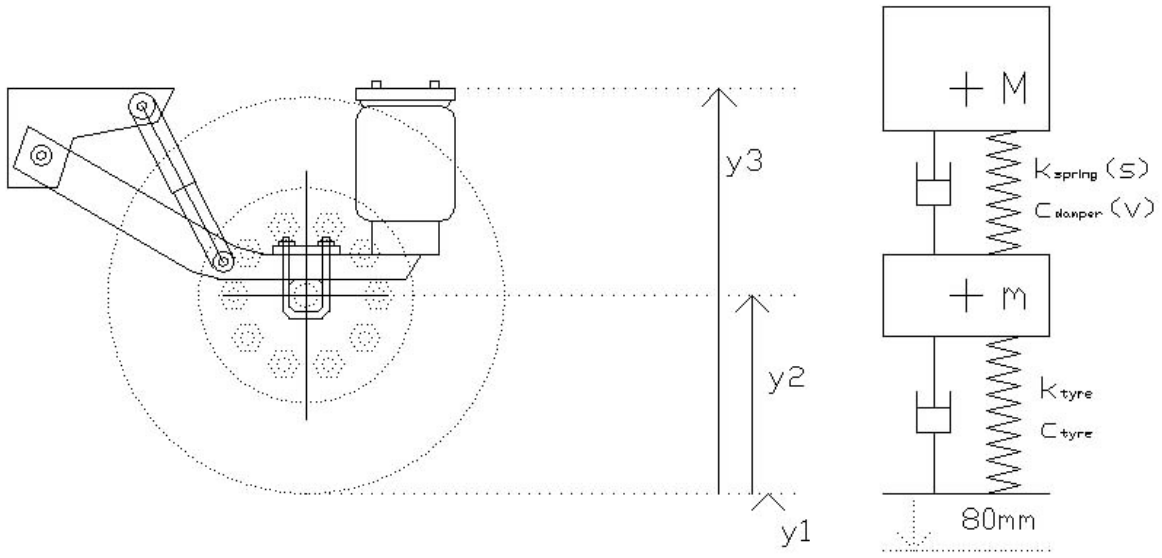

Figure 3.3: Modelling of air suspension as two degree of freedom system

The performance of such models is dependent on the masses *M* the loaded mass, and *m* of the axle-tyre assembly. They are also dependent on spring rates k_{spring} and k_{tyre}, and damping rates c_{damper} and c_{tyre}. For the purposes of modelling an airbag suspension, the following assumptions were made.

$$g = 9.81 \text{ m/s}$$
$$M = 4000 \text{ kg}$$
$$m = 400 \text{ kg}$$

Values of tyre stiffness were assumed constant and taken as an average of values used in Prem et al [04], Cebon [06] and Travaglini [08].

$$k_{tyre} = 1.7 \times 10^6 \text{ N/m}$$

Tyre damping was assumed constant and taken from Prem et al [04].

$$c_{tyre} = 1.755 \times 10^3 \text{ Ns/m}$$

It was assumed that k_{spring} and c_{damper} were not constant. k_{spring} was taken as a function of displacement, and c_{damper} a function of velocity. As the spring movements for an airbag take place rapidly, there is little time for heat transfer from or to the air in the spring. Thus the compression and expansion of air is taken as adiabatic, and the following relationship is assumed:

$$P_1 V_1^{\gamma} = P_n V_n^{\gamma}$$

Given this adiabatic relationship, where γ is the polytropic gas coefficient, the pressure inside the airbag can be calculated for known airbag geometry and initial volume and pressure. Typical dimensions of an airbag are shown in Figure 3.4.

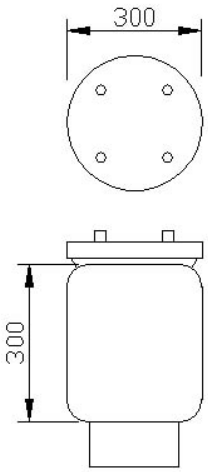

Figure 3.4: Typical dimensions of a truck airbag

Thus, $V_1 = 0.0212m^3$, $P_1 = 5.55 * 10^5 Pa$ and assuming that $\gamma = 1.4$, $P_1 V_1^{\gamma} = 1.65 * 10^4$. Subsequent values for V can be calculated as the displacement of the spring is known.

The performance of the damper is non-linear, and is taken as the performance curve calculated by Travaglini [08] for a new shock absorber operating at 50°C. It is specified as in Table 3.1 and shown in Figure 3.5.

Damper force (N) as a function of velocity (m/s)			
	v^2 term	v term	Constant
velocity < -0.046m/s	0	+ 5410v	- 905
-0.046m/s < velocity < 0.053m/s	$447000v^2$	+ 45600v	+ 0
0.053m/s < velocity < 0.095m/s	$-720000v^2$	+ 169000v	- 3280
velocity > 0.095m/s	0	+ 32500v	+ 3190

Table 3.1: Performance of damper as dependent on velocity (negative velocity is damper extension, positive velocity is damper compression)

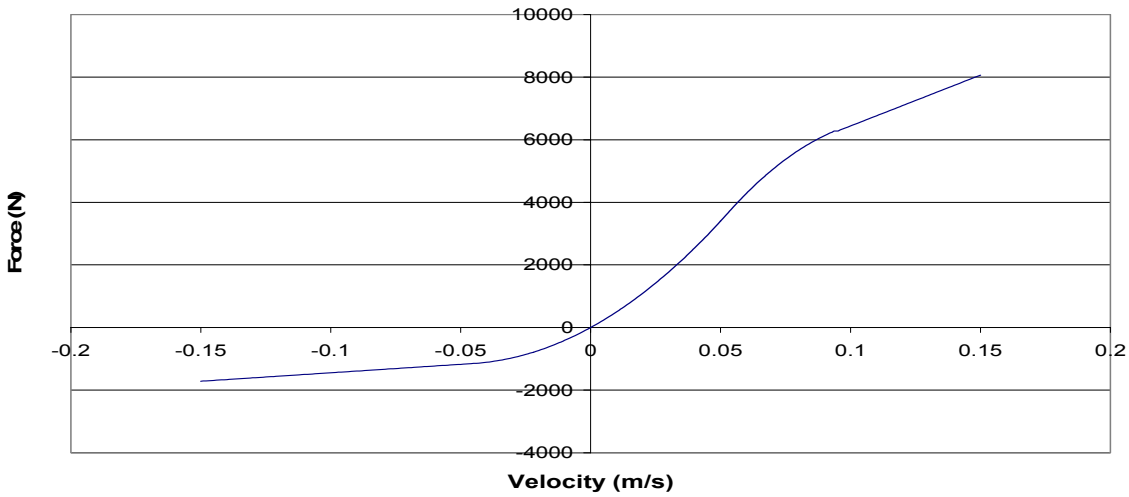

Figure 3.5: Force-Velocity relationship of a new truck damper (negative force implies damper in tension, positive force implies damper in compression)

Calculation with the model is based upon the assumption that the system starts balanced at rest. Thereafter, the conditions applied are that the level of earth is dropped by 0.08m, and the complete system is allowed to fall under the effect of gravity until the tyre touches the ground. During this process, the forces present in the springs and dampers at one instant are used to calculate the new position of the system at an instant Δt later. This is known as the method of small increments. Its precision is based upon the duration of Δt, and improves as $\Delta t \rightarrow 0$. For the simulation, $\Delta t = 10^{-5}$ seconds was chosen, and yielded indicative results.

The results of the quarter axle model being subjected to an 80mm drop test of duration 2s are shown in Figure 3.6.

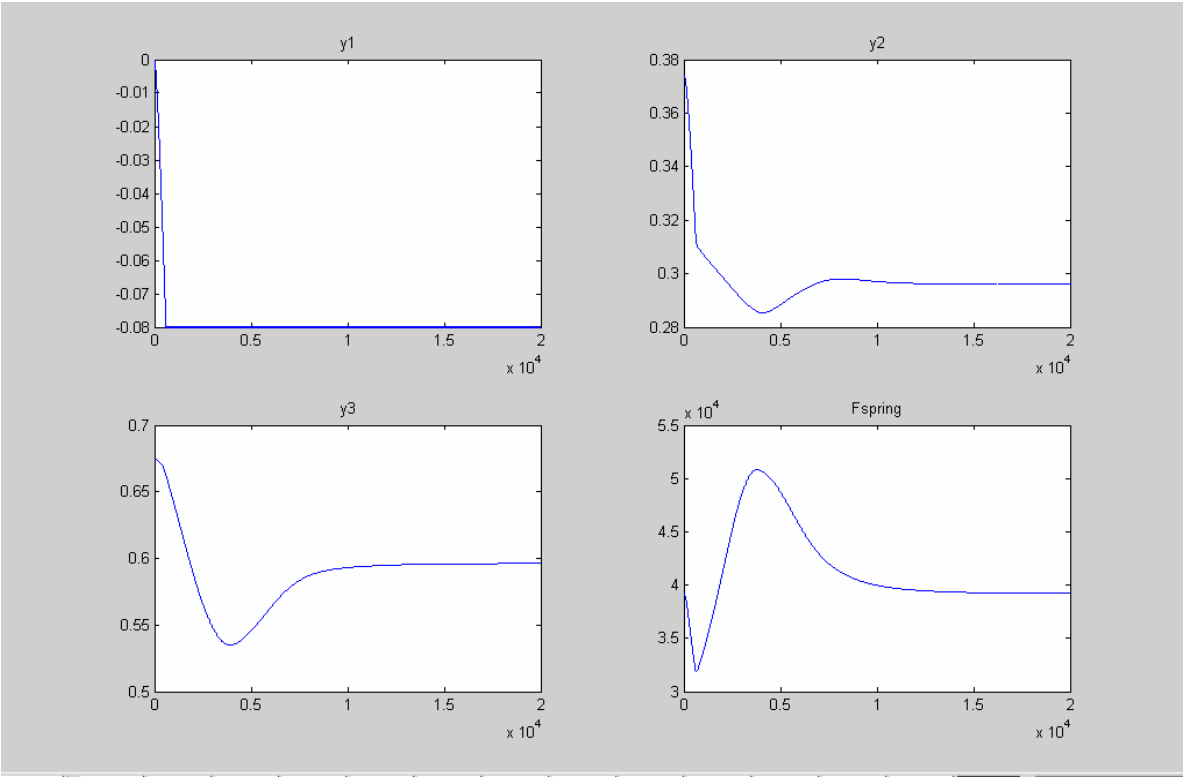

Figure 3.6: Values of y1, y2, y3 and F_{spring} for quarter axle model subjected to a drop test

It can be seen from Figure 3.6 that the displacement of the sprung mass represented by y3 damps very well, such that it is overdamped. This is noted from the positive gradient resulting from the gradual extension of the shock absorber, following its compression phase. During freefall, F_{spring} drops as the spring pushes the axle away from the chassis. However, upon contact with the ground, F_{spring} rises and then settles as it acts to return the sprung mass M back to rest.

The results are compared to where shock absorber damping is removed (tyre damping remains) in Figure 3.7. It can be seen that such as system is underdamped.

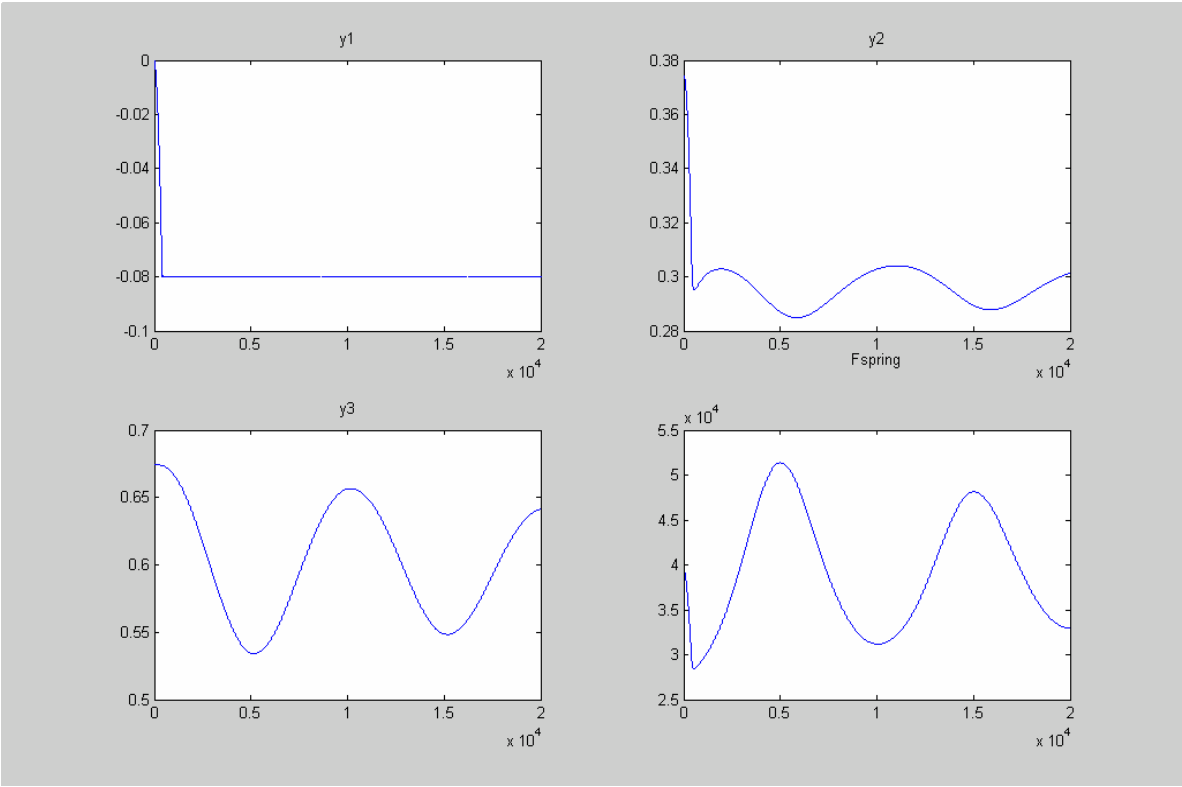

Figure 3.7: Values of y1, y2, y3 and F_{spring} for quarter axle without damping model subjected to a drop test

The usefulness of the quarter axle model is mainly in understanding of the system. The actual results of the quarter axle model are not compared to results from testing, as the quarter axle model is an over simplification of a highly complex system. A good application of shock absorber performance to a quarter axle model is provided in Travaglini [08], which goes into more modelling detail than is provided here.

3.3 AIR SUSPENSION OPERATION

Airbag suspensions operate as a combination of between 2 and 8 quarter axles. They are pressurised via high pressure air lines connected to the vehicle's compressor unit. Such a system is designed to pressure equalise, meaning that under static conditions, the pressures in each airbag are the same. This also means that when there is an air leak and the compressor unit is turned off or the pressure lines are cut, all airbags of a suspension will depressurize rather than a single airbag. This poses some safety and operational maintenance problems.

When a vehicle is started and its compressor unit engaged, self-levelling devices attached to a suspension will determine whether the airbag pressures need raising or lowering. In this way, a ride

height is set depending upon the internal airbag pressure. The ride height of a vehicle is maintained at a constant setting for dynamics reasons. When a vehicle is unloaded, its airbag pressure is lower than for when it is loaded, thereby maintaining constant ride height.

The suspension includes viscous dampers (shock absorbers) mounted either forward or rear of the airbag (see Figure 3.2). Such dampers have a non-linear performance profile, and their performance characteristics change throughout their lifetime. A typical, new-from-shop truck damper operating at 50°C was tested as having a performance curve such as that shown in Figure 3.5 (Travaglini [08]).

Travaglini [08] concluded that the critical region of performance for dampers is that in the low-velocity region. Any loss of performance in this region will have an undesirable effect on suspension performance in a drop test. That investigation also concluded that at elevated temperatures there is a loss of damper performance due to falling viscosity. However, the current work is not focused on damper failure mechanisms, but rather whole-of-suspension performance.

◈ ◈ ◈ ◈

4 TESTING

A bump form of drop test was chosen as the most suitable given the objectives of the research. Other forms of testing were considered. The potential of using hydraulic lifters was considered, but ruled out on grounds of cost, complexity, and potential invasiveness. It was considered undesirable to have testing equipment contact chassis or non-tyre surfaces due to the potential for damage. The potential using of heat-guns to measure damper temperature was considered, but ruled out on grounds of repeatability and such a test's qualitative nature. A measurement of damper temperature may give some indication of level of performance under strict laboratory testing conditions, but the quite varied and random nature of field conditions ruled out this approach.

As such, a test involving the towing of a suspension over a set of bumps was chosen, on a simplicity and repeatability basis. This test achieves the goal of dropping a tri-axle group a distance of 80mm. The use of an accelerometer to measure chassis movement was chosen on the grounds of simplicity and operator safety, and the intrusiveness of measurement devices such as string gauges.

4.1 TESTING SITE REQUIREMENTS

It is proposed that the test sites should be approximately level in both the longitudinal and lateral directions, with any longitudinal grade being positive (uphill). The grade should be marginally uphill either side of the site. The requirement for marginal uphill grades is to assist with natural deceleration of the vehicle after dropping off the bumps. The effect of a slight grade on the vertical drop distance is marginal and thus neglected. A side-on view of the testing setup, with correct longitudinal grade, is shown in Figure 4.1.

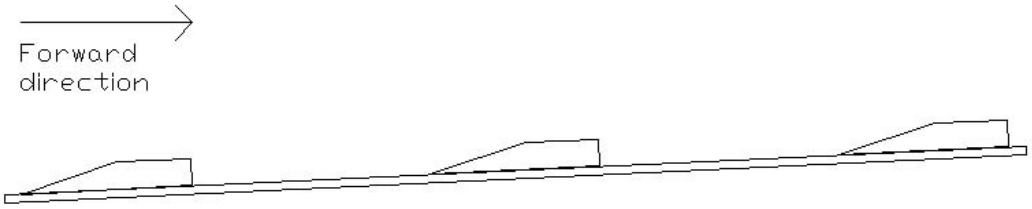

Figure 4.1: Side view showing incline direction of bumps

It is necessary to test slightly uphill rather than slightly downhill as the application of brakes immediately after a suspension is dropped is unsatisfactory, as their application causes additional excitation and vibration. The effect of brake application is shown in Figure 4.2.

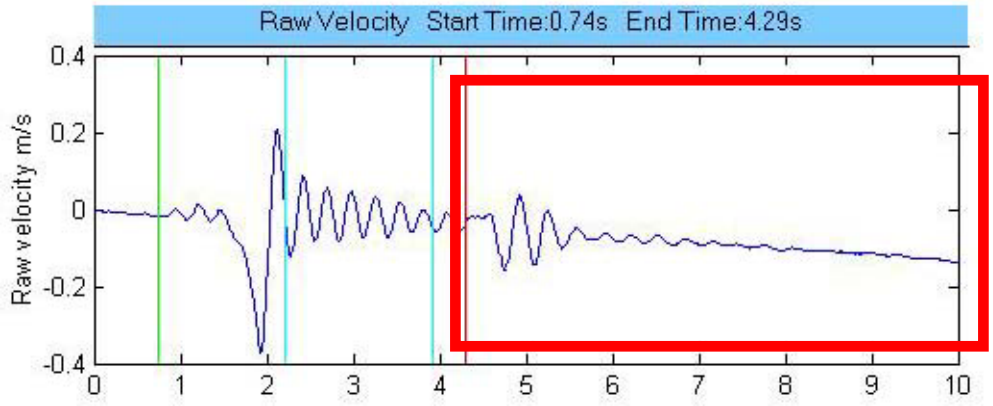

Figure 4.2: Transient oscillations induced into a suspension oscillation signal due to braking, after useful data has finished

Additionally, the momentum in a heavy vehicle (which may be up to 194 tonnes gross mass with 25 axles) following a bump test is substantial, even at small speeds. The ideal scenario is for heavy vehicles to roll to a natural stop just as the rear axle approaches or rolls slightly onto the next bump. When the grade is slightly downhill, the vehicle will tend to roll over the following bumps and not stop until brakes are applied, due to the momentum. Rolling over additional bumps adds additional complications to the data signal, such that it may not be useful.

There should be good approaches, allowing for a heavy vehicle to move in a straight line for at least 20 metres plus the length of the vehicle either side of the site. Figure 4.3 demonstrates an overhead view of the testing arrangement.

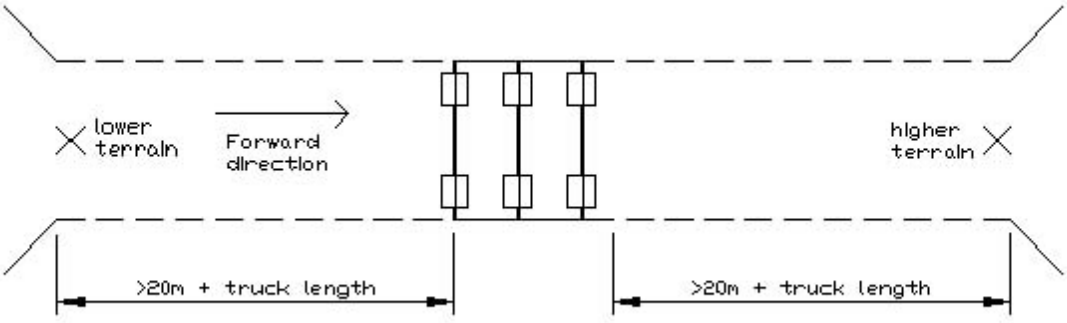

Figure 4.3: Overhead view of testing frame with bumps setup

It is necessary to have a frame bolted or nailed to the surface at two points. In cases of hard surfaces, it is necessary to drill into the surface with a hammer drill. For these occasions, the use of a 6mm / ¼" drill bit and dynabolts may be appropriate.

Sites meeting such specifications are likely to be found in roadside pullover bays and rest areas. Kerbside sites are likely to be unsatisfactory due to problems with levels and grades, and also from a safety standpoint. It is a requirement that the grade at any testing site be known. A preliminary survey is considered necessary. It is also suggested that survey records of useful sites be kept.

4.2 TESTING EQUIPMENT SETUP PROCEDURES

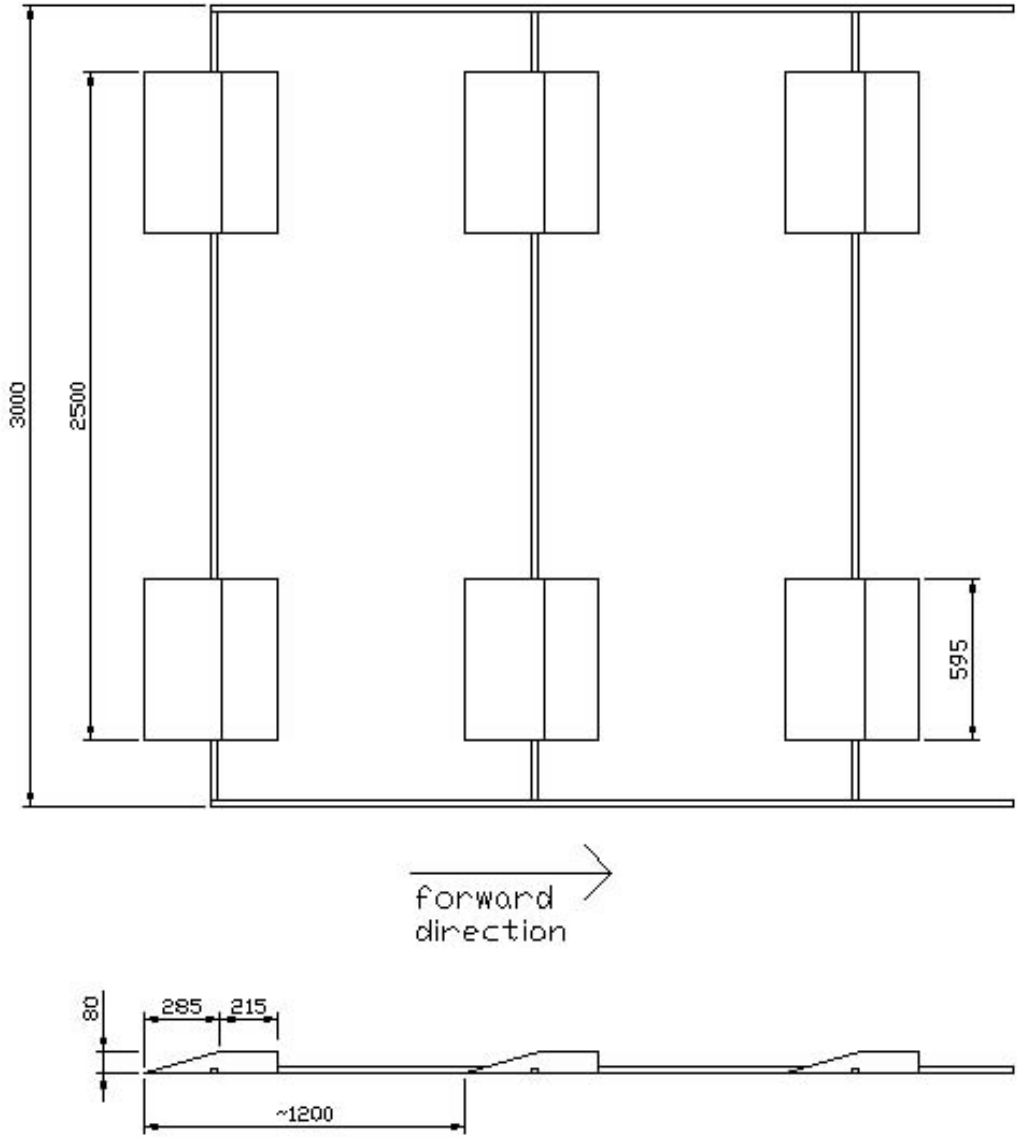

Figure 4.4: Orthogonal view of testing frame with bumps setup

As shown in Figure 4.4 the bumps are set in a frame like arrangement. Two parallel fixture bars are placed in the forward longitudinal direction with a spacing of 3 metres (1). The bumps are set in their approximate positions between the two fixture bars and stood upright. The steel bar cross members, each 3m in length, are then fed through the underside guides of two adjacent bumps, and the bumps laid onto the ground. The outer edges of the bumps should be 2.5m apart (see Figure 4.4). The vertical edge of the bumps should be facing uphill, and the sloping edge facing downhill, as required by the site. If the direction of uphill and downhill is not immediately known, the site should be surveyed so it can be determined. However, a long spirit level may be adequate. If the site is level, the bumps' direction is left to the discretion of the user.

The first pair of bumps in the series (the ones farthest downhill) are placed so that their crossbar's ends are perpendicular with the fixture bars' ends (2) (see Figure 4.5).

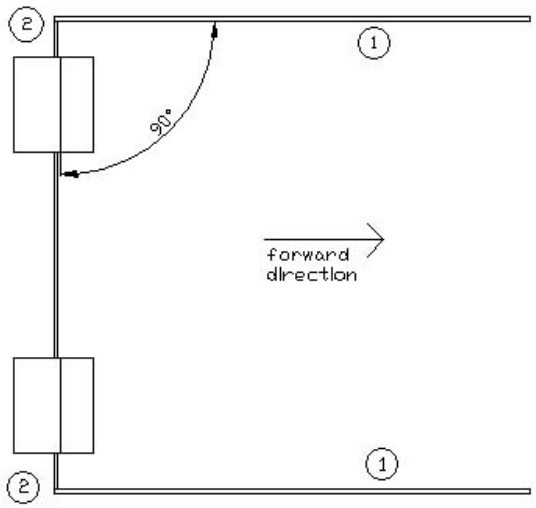

Figure 4.5: Stages 1 and 2 of testing arrangement setting up procedure

Once the first pair of bumps are in place, the crossbar and fixture bars should be affixed to the ground such that the crossbar and bumps are in a fixed position (3), and the fixture bars can pivot about their fixed ends (see Figure 4.6).

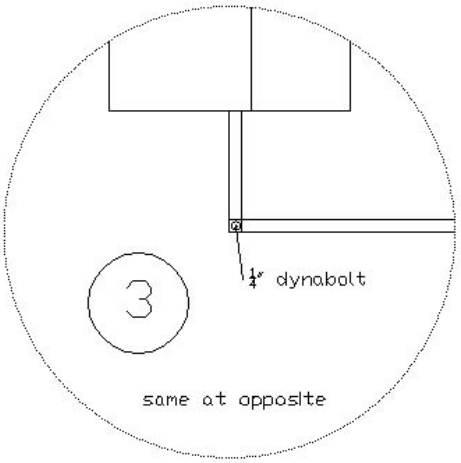

Figure 4.6: Stage 3 of testing arrangement setup highlighting corner fixture

Following the completion of stage 3, the second and third pairs of bumps are placed in position. The inter-axle spacing of the axle group to be tested is measured, and the second and third crossbars are attached to the fixture bars with ¼" bolts and wing nuts (see Figure 4.7).

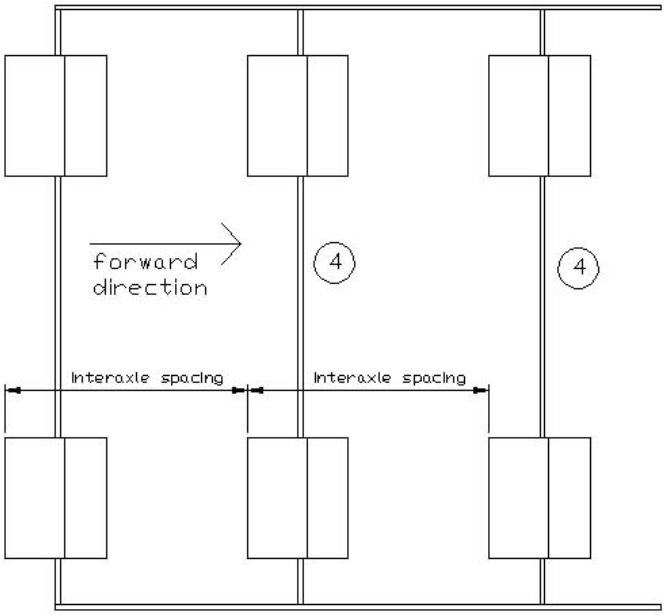

Figure 4.7: Stage 4 of testing arrangement setting up procedure

At this point, the testing setup is ready and the vehicle may roll into position, ready for data collection.

4.3 DATA RETRIEVAL USING AN ACCELEROMETER

Data is retrieved from a low-g (up to 50 m/s^2) accelerometer via a 6-core data cable fitted with British-Telecom connectors. The accelerometer is a force capacitor which is supplied a voltage. For different external forces acting upon the capacitor, the voltage changes, and the relative voltage is measured. Under the positive force of gravity (accelerometer positioned arrow downwards) the voltage is approximately 1.90V. Under the negative force of gravity (accelerometer positioned arrow upwards) the voltage is approximately 2.80V. These two values are taken as calibration points – the first as 0 m/s^2 and the second as 19.6 m/s^2 (2g). Following these calibration tests the accelerometer is positioned with its arrow pointing down. It then measures true acceleration, adjusted for the effects of gravity.

The accelerometer is mounted on a welding magnet, which does not interfere with its operation. A magnet was chosen as an attachment device because of an abundance of steel on most heavy vehicles, including the chassis, allowing for quick and easy placement and removal of the accelerometer. The accelerometer on its mounting magnet is shown in Figure 4.8.

Figure 4.8: Low-g accelerometer mounted on a welding magnet

The software provided with the Vernier Labpro data logger, Vernier Loggerpro 3, automatically interprets the signal coming from the data logger and provides an instantaneously updating acceleration plot (for sample rates up to 250Hz – see discussion in Chapter 5). From within Loggerpro 3, the calibration of the accelerometer is performed, and settings such as time-length of record and sample rate are chosen. Recordings are taken using Loggerpro 3, and saved as proprietary .xmbl files. .xmbl files contain time and acceleration data in an easily decipherable text format. This allows for relatively straightforward importing of information into data analysis

programs. However, if the user desires, Loggerpro 3 can save files in an even simpler .txt file. For use with the GUI, data should be saved in the .xmbl format.

As the voltage across the accelerometer is only a few volts, the precision of acceleration measurements is limited. Under static, zero-acceleration conditions, a constant bias of up to ±0.1 m/s^2 is usually noted. This miscalibration bias remains approximately constant for small time intervals, but changes after long durations due to factors such as atmospheric conditions, and also micro-effects on the accelerometer-capacitor after repeated use. Thus, it is necessary to recalibrate the accelerometer periodically to overcome any pronounced bias. For example, at one instant a bias of approximately –0.07 m/s^2 may be noted, yet 20 minutes later the bias may be approximately +0.05 m/s^2. For time records of the type used to collect truck bounce signals the bias does not vary significantly enough to warrant an assumption that the miscalibration bias is non-constant. As described later in Chapter 5.4, it is necessary to remove this bias using software in order to analyse the performance of the suspension.

For a time signal of 10 seconds (sample rate 200Hz) with constant bias of +0.1 m/s^2, under static conditions the acceleration-velocity-displacement plots in Figure 4.9 would be noted.

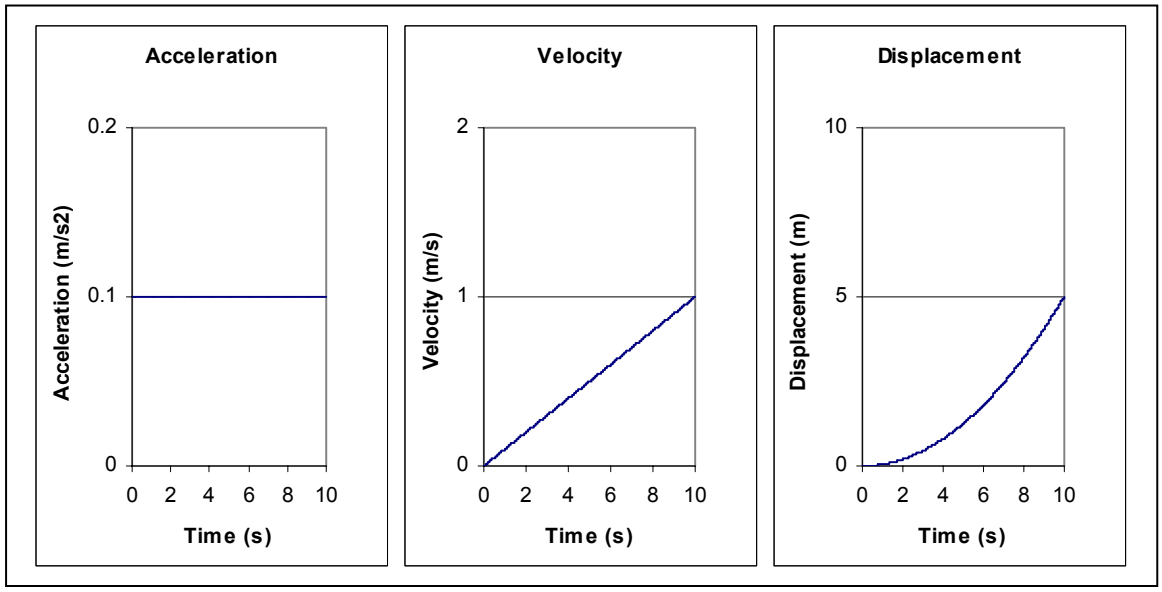

Figure 4.9: Acceleration, velocity and displacement plots for a constant acceleration of 0.1 m/s^2

From Figure 4.9 it is noted that even for a relatively small +0.1 m/s^2 miscalibration, the net effect on displacement after a period of 10 seconds is a significant 5m, and velocity is calculated at 1 m/s,

when it is in fact zero. For various miscalibrations, the effect on distorting velocity and displacement is tabulated in Table 4.1.

Acceleration miscalibration	Bias on true velocity after 10s	Bias on true displacement after 10s
±0.1 m/s^2	±1 m/s	±5 m
±0.05 m/s^2	±0.5 m/s	±2.5 m
±0.03 m/s^2	±0.3 m/s	±1.5 m
±0.01 m/s^2	±0.1 m/s	±0.5 m

Table 4.1: Affects of varying biases on true displacement figures

Miscalibration is especially troublesome considering the magnitude of displacement that a test of RFS incorporates is typically 80mm, and the resolution of the accelerometer is approximately 0.03 m/s^2. Such problems could be alleviated by the use of higher quality, better resolution accelerometers, or devices such as string gauges that measure displacement directly. However, given the limitations of the available equipment and a lack of suitable replacements, post-collection removal of bias is not a major problem and a relatively simple task. The simplicity of using an accelerometer more than offsets the problems associated with removing the miscalibration bias. Despite the problems of miscalibration bias, the accelerometer-Labpro combination is highly suitable to the purpose, as it provides data with a resolution fine enough to provide precise interpretation of results.

4.4 DATA COLLECTION DURING TESTING

Following accelerometer calibration, the accelerometer is attached to a vertical steel surface at approximately the midpoint of the suspension, at or above the chassis. It is not critical where the accelerometer is placed, so long as it is vertical and rigidly connected to the chassis. As extraneous vibration corrupts the acceleration data signal, it is important that the accelerometer is not affixed to any surfaces which may vibrate in a different manner to the chassis. Suitable surfaces include the web of a steel chassis I-beam and welded vertical load support beams. If no surface is available at the midpoint of the chassis, a point near to the middle is satisfactory, provided the accelerometer is approximately central to the horizontal plane of the suspension.

This procedure may be conducted prior to or at the point where the axle group is atop the set of bumps as in Figure 4.10.

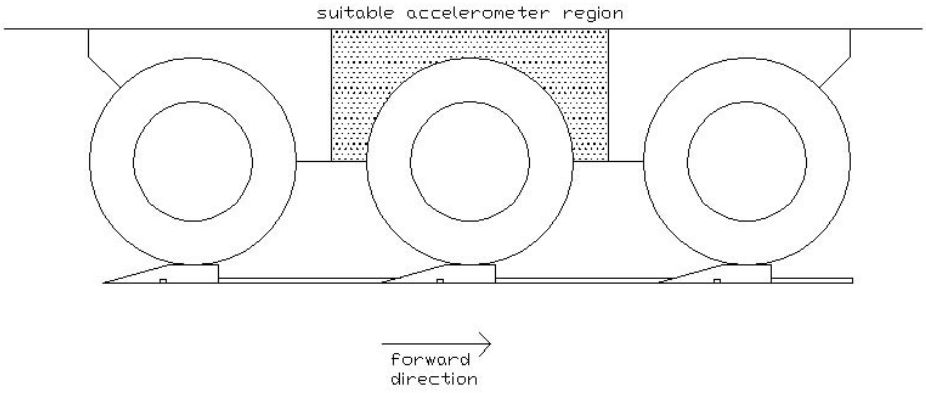

Figure 4.10: Axle grouping in bump-test-ready state

Data must be collected over a period of time sufficiently long to allow for a starting delay, collection of the useful signal, and an ending delay. Additionally, data with a higher sample rate is less prone to aliasing[2] type errors. However, hardware restrictions mean there is a compromise between sample rate and record time length. Experimental results with a sample rate of 250Hz and record time length of 15~20 seconds were found to be suitable for analysis purposes. As the frequencies of interest are much smaller than 250Hz, aliasing is avoided. Experiments were also taken at higher sample rates with lower record time lengths. However in such circumstances, the margins allowed to start and complete a recording are very fine, and given the nature of communications between data collection officer and vehicle operator are not recommended.

The technique found to be most successful involved the use of a countdown. Once the user is ready, he or she counts down from five to zero, at which point the heavy vehicle operator moves off the bumps. As the releasing of truck air brakes is not an instantaneous process, the countdown gives the heavy vehicle operator time to prepare the truck to move on zero. Countdowns can be performed orally, with hand signals or via UHF radio, depending on which is easiest in the circumstances. The user should begin recording data 2~3 seconds before the countdown finishes, or at the start of the countdown if desired. Enough time must be allowed for in the data signal length setting to capture the complete oscillation of the sprung mass.

◈ ◈ ◈ ◈

[2] Aliasing – 'If you've ever watched a western and seen the wheel of a rolling wagon appear to be going backwards, you've witnessed aliasing. The movie's frame rate isn't adequate to describe the rotational frequency of the wheel…' - *http://www.earlevel.com/Digital%20Audio/Aliasing.html*

5 GRAPHICAL USER INTERFACE (GUI)

To provide a relatively quick and instantaneous analysis of the truck bounce data signals, a graphical-user-interface (GUI) was developed. It was developed in 'Mathworks Matlab[3]', a computer programming environment suitable for integrating interactive and arithmetic programming functions. Matlab was ideal for the preliminary development of the RFS field test, but in the longer term, an all-in-one analyser should be developed to integrate the software and hardware needed to undertake testing.

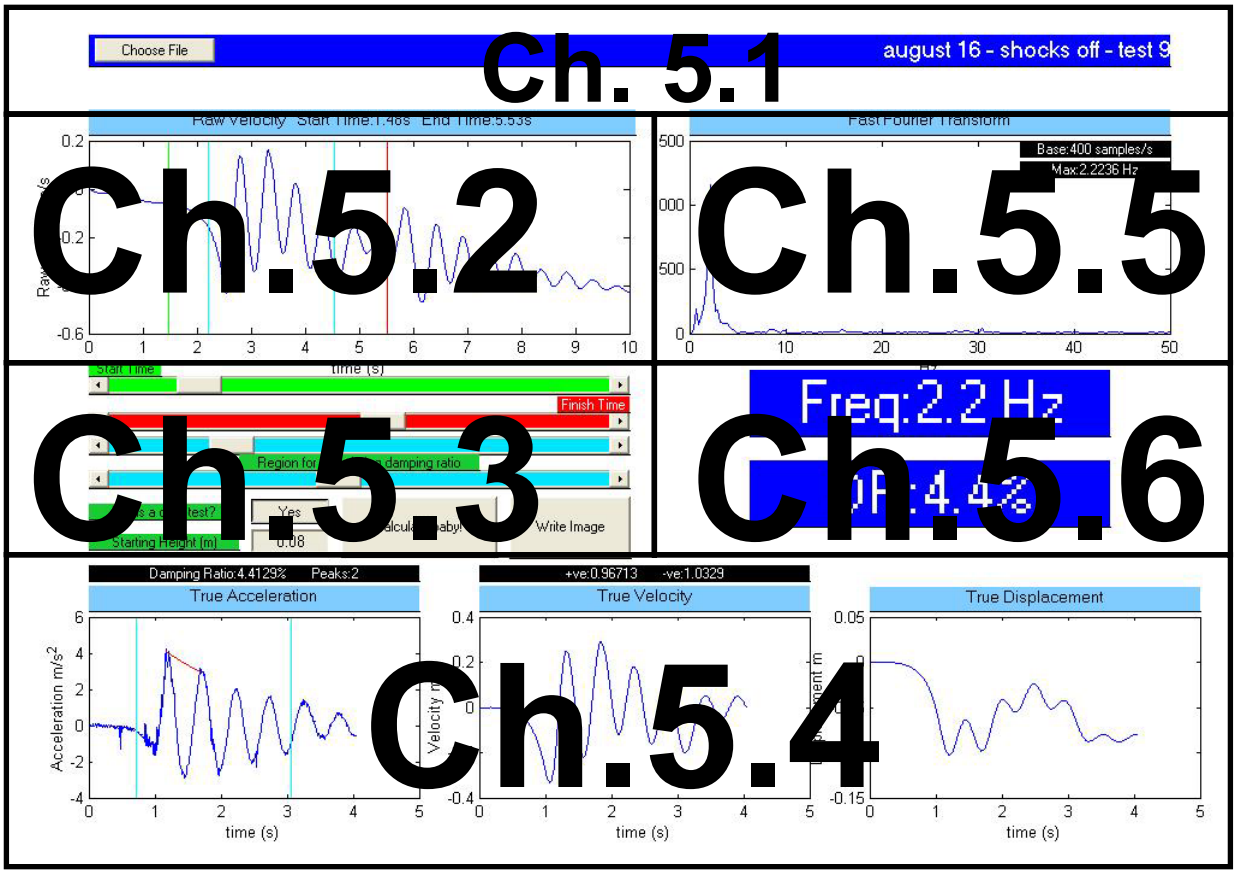

Figure 5.1: GUI Layout

The GUI was designed to be as stable as possible, providing the novice user with a relatively robust system. It was also designed to be straight forward to use with all its functions clearly explained. A detailed explanation of each operational area is provided to assist in understanding the GUI.

[3] "Matlab is a technical computing environment for high-performance numeric computation and visualization, produced by The MathWorks Inc" – *Massachusetts Institute of Technology*

The analysis process starts with a display of raw data. The user selects the region of useful raw data (between the green and red lines), which is then processed to remove experimental errors. Following processing, useful plots and data are displayed, allowing the user to understand the essential operational characteristics of a suspension.

5.1 LOADING BAR

The 'Choose File' button is the entry point into the GUI (see Figure 5.1). It is located at the top left corner of the GUI in the blue title bar, and is the only operable feature when the GUI is first started. When clicked, it opens a file dialogue which allows the user to select an .xmbl file to open and analyse. It will only accept .xmbl files as generated by the data collection software, Loggerpro 3, (explained in Chapter 4.3). This is because the GUI can only interpret .xmbl files generated by Loggerpro 3. However, other types of files can be analysed with minor reprogramming.

After a file is selected and opened, its name is shown in the blue title bar to indicate the .xmbl file being analysed. When the .xmbl file is saved in Loggerpro 3, it is important to give the file an accurate description of the test data that is stored within, for easy future reference.

5.2 INDICATIVE PLOT OF VELOCITY

After the loading of an .xmbl file is complete, a plot of sensor velocity is shown in the upper left corner of the GUI (see Figure 5.1). As the acceleration and time series data is a series of discrete time records and not continuous, a Simpson's rule mathematical approximation is used to integrate the sensor acceleration data to obtain velocity, and later to obtain displacement. However, sensor acceleration data contains some forms of bias, which are explained further in Chapter 5.4. This bias is later removed for the plots of true acceleration, velocity and displacement, but not for the first plot of velocity. The Simpson's rule integration technique used to determine velocity from acceleration (and similarly, displacement from velocity), for each discrete time acceleration data record n, is shown in Equation 5.1.

$$v_n = v_{n-1} + \frac{dt}{6} \cdot \left(a_{n-1} + 4 \cdot a_n + a_{n+1}\right)$$

$$v_1 = \frac{dt}{6} \cdot \left(4 \cdot a_1 + a_2\right)$$

$$v_N = v_{N-1} + \frac{dt}{6} \cdot \left(a_{N-1} + 4 \cdot a_N\right)$$

Equation 5.1: Simpson's rule for discrete data integration technique

Following the calculation of velocity values from raw acceleration data, a plot is shown to give a guide of the approximate movement pattern of the oscillating sensor. Velocity is plotted as it gives the best compromise between plot shape and plot smoothness. A plot of acceleration tends to be distractingly jagged and pointy, features which are removed by a first integration to velocity. A plot of displacement tends to have hard to distinguish features, as it is too smooth.

5.3 SLIDER BARS AND SETTINGS

After plotting the indicative plot of velocity, the slider bars and settings options become active on the middle left side of the GUI (see Figure 5.1). The slider bars are used to select the data regions of interest from the indicative plot of velocity. The upper two green and red slider bars are used to select the starting and ending times of the useful data. The green slider bar is used to select the starting time, and the red slider bar is used to select the ending time. The data either side of the selected curve region are not analysed. The excised curve at the beginning comes from the period when data starts being collected and when the heavy vehicle operator starts to move the vehicle. The excised curve at the end shows data after the truck has stopped rolling forward smoothly. The excised data has no value.

The two light-blue sliders immediately beneath the green and red sliders are used to select the region from which the damping ratio will be calculated. The region should generally bound the first few peaks of the plot. The bounded peaks are then used to calculate damping ratio using a log-decrement algorithm.

The first setting beneath the slider bars is a button to click if the analysis being performed is an analysis of a bump test. In some circumstances, the analysis will be performed on a signal which is not a bump test, and the algorithms used to analyse such data differ from the algorithms used to analyse bump test data. The second setting is a text box which is used to set the bump test height (only applicable when analysing bump tests). The default value is 0.08m which is the standard bump test height.

The largest button visible is clicked when all the settings are correct and the sliders adjusted as desired. This button starts the calculation process, which after completion results in the remainder of the GUI displaying various plots and results.

The fourth button is clicked when analysis is complete, and a record of the analysis is required for future reference. The record is saved in a picture .jpg file, in a location and with a name desired by the user. The default file name is the same as the analysis file name, differing only by its .jpg extension. Picture files are very easy to use for future data analysis purposes.

5.4 ADJUSTED ACCELERATION, VELOCITY AND DISPLACEMENT

The three plots at the bottom of the GUI are plots of adjusted acceleration, velocity and displacement (see Figure 5.1). They provide an accurate picture of the dynamics of a vehicle load undergoing a bump test, and exclude the data signal 'tails' as set by the user from the indicative plot of velocity. The 3 adjusted plots have miscalibration bias removed and have undergone some arithmetic offset manipulations to match the actual testing scenarios. Removal of miscalibration bias is achieved by a adding or subtracting a constant from the raw acceleration data. This is based upon an assumption that the underlying bias in the acceleration is constant. For data collection periods over small intervals, this is assumption is valid. The user should choose starting and ending times at which point the true velocity is zero. This is shown in Figure 5.2.

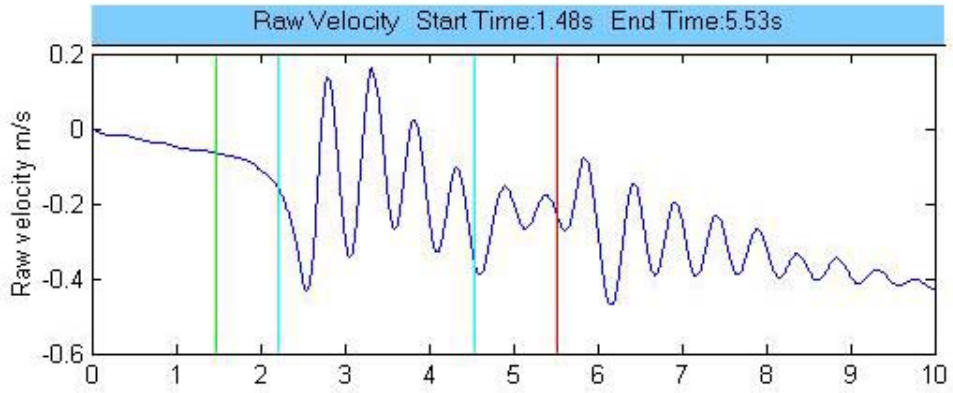

Figure 5.2: Indicative plot of velocity with starting and ending times set at points of zero velocity

For signals which are still oscillating and transient when useful data period finishes (as is the case in Figure 5.2, where a second external force was applied at approximately 5.7 seconds), the ending time is set at the point where velocity is halfway between peak and trough, and logically assumed to be zero. Were there no transient oscillating signal component, the constant acceleration bias would result in a straight line between the starting velocity and the ending velocity. The gradient of this

'mean velocity line' is related to the constant which is subtracted from the acceleration values by Equation 5.2.

$$\text{Adjustment } K = \frac{v_{\text{ending time}} - v_{\text{starting time}}}{t_{\text{ending time}} - t_{\text{starting time}}}$$

$$\text{For i} = \textit{starting time} \text{ to } \textit{ending time}, \; a_{i,\text{true}} = a_{i,\text{raw}} - K$$

Equation 5.2: Acceleration bias adjustment procedure

This adjustment is applied to the acceleration data, which is then plotted in the lower left corner of the GUI. The adjusted acceleration plot also includes the two light-blue lines corresponding to the damping ratio calculation (see Figure 5.3). It also has an exponential decay curve plotted, which corresponds to the calculated damping ratio. This curve is plotted to give the user a guide as to the appropriateness of the calculated damping ratio. The damping ratio calculation can at times be haphazard because of the lack of data used in its calculation. In some instances, it will give a misleading damping ratio figure. The best method to overcome this problem is to include more peaks in the damping ratio calculation region, giving more decrements over which to average. However, when there are very few peaks and this is not possible, the user should use the plotted exponential decay curve (which represents the upper boundary of the acceleration trace) to check that the acceleration trace would approximately fit with a curve representing the calculated damping ratio. The example in Figure 5.3 shows that the trace would fit approximately within the extended decay curve.

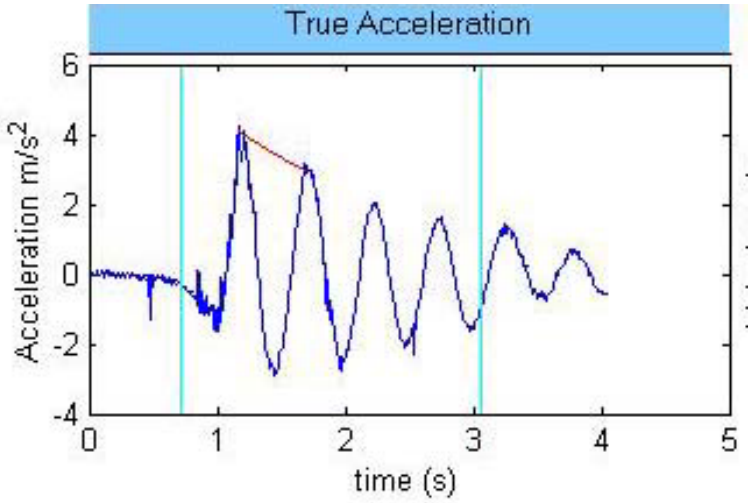

Figure 5.3: Adjusted plot of acceleration including light-blue damping-ratio-calculation boundary lines and partial exponential decay curve

A method referred to as ‘stretching’ is necessary to overcome the finite resolution of the data recording equipment, and the phenomenon of under and over-peaking that tends to occur. Under and over-peaking is a phenomenon in which the recorded acceleration peaks can be either too small or too large, such that when the acceleration data is double integrated, the resultant displacement plot does not match reality. Figure 5.4 helps to explain this phenomenon.

Following the removal of miscalibration bias from acceleration data, where the bump test was known to have been from a height 80mm, the double integration of acceleration shows a drop of 60mm (-0.06m on a displacement plot). This shows that the negative peaks are either too small, or the positive peaks are too high, or a combination of both. To offset this, positive and negative adjustment factors are applied to all the positive acceleration values and all the negative acceleration values.

Figure 5.4: Influence of under and over peaking on calculated displacement

The two factors applied to the acceleration values, α (positive values) and β (negative values) are related to each-other by Equation 5.3.

$$\alpha \cdot \beta = 1 \quad \text{or} \quad \alpha = {}^{1}\!/\!_{\beta}$$

Equation 5.3: Relationship of adjustment factors

Values of α and β below 0.95 and above 1.05 should be treated with some scepticism, and may indicate a possible user error or misunderstanding. Figure 5.5 shows the effect of the adjustment on an acceleration plot, with α and β factors of 1.01 and 0.99.

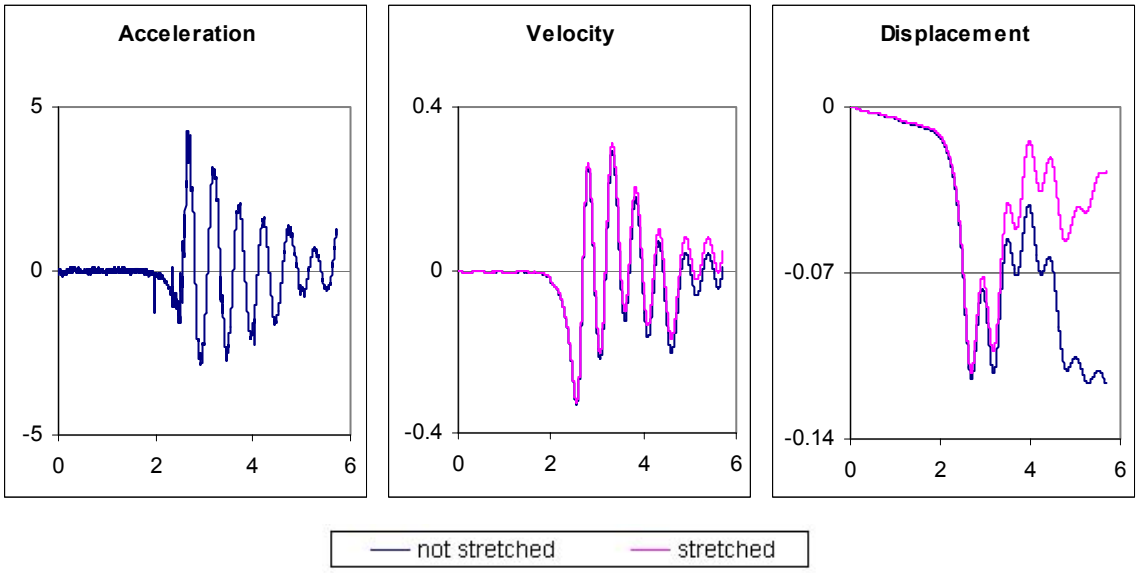

Figure 5.5: Effect of α and β on velocity and displacement after integrating

5.5 FOURIER PLOT

The upper right corner of the GUI (see Figure 5.1) shows the results of a Fourier transformation of the adjusted acceleration data. A Fourier transformation decomposes a signal into its frequency aspects. This type of transformation is well suited to oscillatory signals, such as are present with a bump test. The spikes on a Fourier transformation plot indicate the presence of a corresponding frequency in the data signal. In the case of bump testing, dominant spikes relating to natural suspension frequencies of approximately 1.5~4Hz should be noticed. In the case of testing ambient vibration signals with motors idling, spikes around 25~60Hz should also be noticed (refer to Figure 5.7 and Equation 5.4).

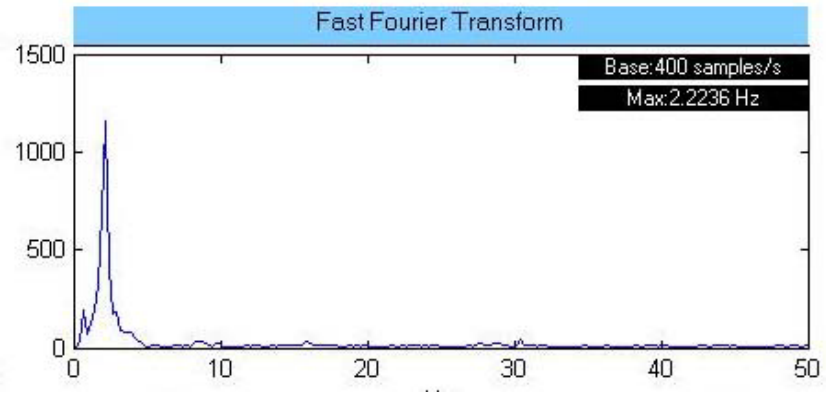

Figure 5.6: Fourier transform of airbag suspension bump test acceleration data. Peak at 2.2Hz

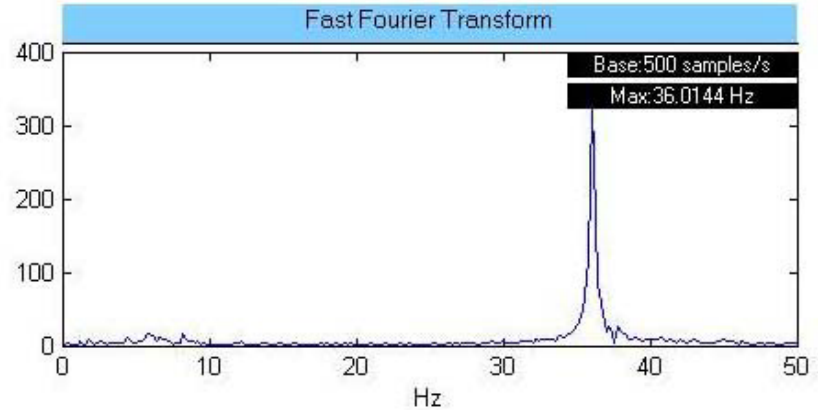

Figure 5.7: Fourier transformation of ~700rpm idling 6 cylinder engine signal, peak at 36Hz.

$$36\frac{\text{enginecombustions}}{\text{s}}\times\frac{1}{6}\frac{\text{cylinders}}{\text{engine}}\times 60\frac{\text{s}}{\text{min}}\times 2\frac{\text{revolutions}}{\text{cylindercombustion}}=720\text{rpm}$$

Equation 5.4: Equation relating Fourier peak to engine speed

In the case of bump testing, the dominant spike at around 1.5~4Hz (refer to Figure 5.6) is taken as the suspension natural frequency, which is then compared against standards that specify a RFS natural frequency of less than 2Hz.

It is important to note that the usefulness of a Fourier transformation is dependent on the sampling rate of its data signal. For the highest frequency of interest, sampling should be taken at twice that frequency. Using the Vernier Labpro with Loggerpro 3 at a sampling rate of 250 samples/second proved adequate for later Fourier analysis, as the frequencies of interest are well below 125Hz. However, for higher frequencies of interest, a higher sampling rate is necessary. The software limitations of Loggerpro 3 limit the sampling rate to 250Hz if dynamic feedback is desired. Without dynamic feedback, the user cannot see on the computer screen the data as it is being recorded. If the user cannot see the data as it is being recorded, it can lead to uncertainty, delay and confusion, particularly for traces of longer time duration. In those circumstances, the Loggerpro 3 screen may not update until data recording is complete, and this is quite disconcerting. Thus, a sampling rate maximum of 250Hz is recommended so that the user can enjoy the certainties of dynamic feedback.

5.6 IMPORTANT DATA

At the middle right of the GUI (see Figure 5.1) lie the two most important calculated data figures. These figures are those of the estimates of the suspension natural frequency and suspension damping ratio. They are displayed in a large font so that they are immediately clear when testing data is reviewed or stored.

The natural frequency is taken from the dominant spike on the Fourier transformation. The damping ratio is calculated using an arithmetic average log-decrement method. Using the region of the adjusted acceleration plot bounded by the two light-blue sliders, the values of the acceleration at the peaks within that region are determined. Then, Equation 5.5 is applied to determine the damping ratio, $\zeta_{average}$.

given acceleration values at each of n peaks, for $i = 1$ to $n-1$,

$$\delta_i = \ln\left(a_i / a_{i+1}\right)$$

$$\delta_{average} = \sum\left(\frac{\delta_i}{n-1}\right)$$

$$\zeta_{average} = \frac{\delta_{average}}{\sqrt{4\pi^2 + \delta_{average}^2}}$$

Equation 5.5: Average log-decrement calculation for damping ratio

A comparison of acceleration plots with high damping ratios and low damping ratios is shown in Figure 5.8 to demonstrate graphically the issues with using the log-decrement method with high damping ratios.

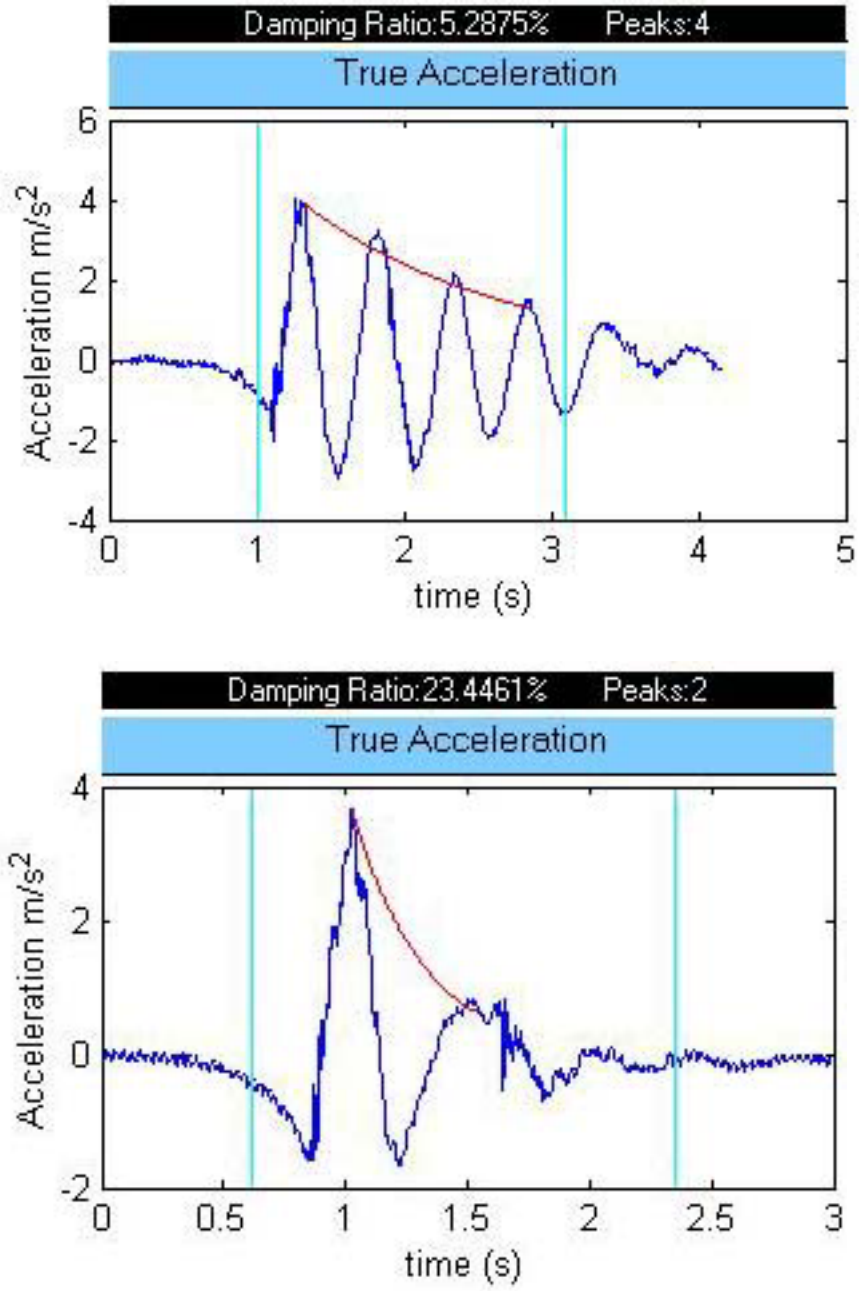

Figure 5.8: Low damping ratio versus high damping ratio, noting difference in number of available peaks with which to perform damping ratio calculation

6 FINDINGS

Four distinct testing sessions were conducted. The dates and specifics of each session are detailed in Table 6.1.

Date	Vehicle	Outcomes
July 12 2003	Prime mover with unladen air-suspension tandem axle trailer	• Usefulness of single-bump test rejected, i.e. dropping of one axle rather than all axles considered not useful • Familiarisation with data software • Side-effects of braking recognised
	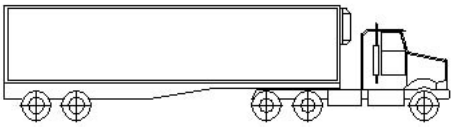	
July 18 2003	Semi-laden rigid truck with mechanical suspension	• Non-brake stopping mechanism employed • Rigid accelerometer attachment device proven
	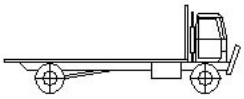	
August 16 2003	Prime mover with unladen air-suspension tandem axle trailer	• Use of multiple bumps in frame setup • Testing with and without dampers
	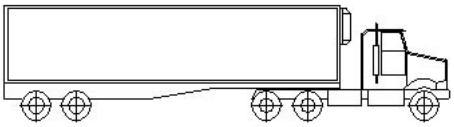	
October 1 2003	Prime mover with three laden air-suspension tri-axle trailers on tri-axle dollies	• Need for uphill site recognised • Use of synchronised user-driver communications
	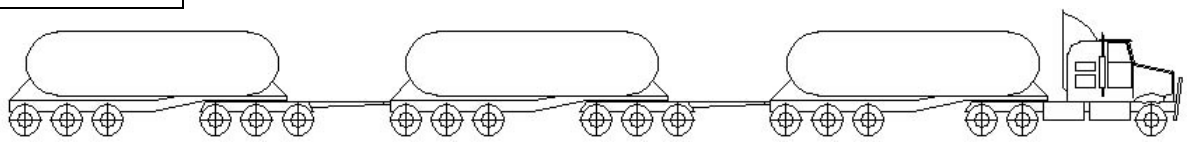	

Table 6.1: Testing dates, vehicles and key outcomes

Each testing session was approached with different aims and desired outcomes. These aims and desired outcomes were largely achieved, with some additional findings also made.

6.1 TESTING SESSION 1 – UNLADEN SEMI TRAILER

6.1.1 Testing Session 1 Summary

Testing session 1 was held on the morning of Saturday July 12 2003 in the yard of Sands Fridge Lines, Forrestfield. The heavy vehicle tested was a tandem-drive prime mover towing an unladen tandem-axle refrigerated trailer, equipped with a BPW air suspension. This vehicle would typically be used for the transport of refrigerated groceries to supermarkets in the Perth metropolitan area, and throughout Western Australia. The air-suspension trailer was the only part of the vehicle tested, and the prime mover was excluded. The vehicle was operated by Kevin Sands of Sands Fridge Lines, who was very kind in offering his services repeatedly throughout the duration of this investigation.

The testing setup consisted of two prototype bumps, attached to the ground by short chains. The two short chains were nailed into the asphalt surface at one end with roofing nails, and bolted onto the protruding reinforcement bar at the other. As such, the two bumps were not connected in any way, and alignment was conducted with a straight-edge. Re-alignment would prove necessary after each test, as the chains provided no rigid lateral support. When the vehicle reversed over the bumps, they would shift, necessitating realignment. This proved to be an inconvenience.

A personal computer was set on a table adjacent to the two bumps, and was powered from a nearby mains outlet.

The accelerometer was attached to the vehicle by the use of an adjustable clamp as this was an easy method of attachment. However, it was later found that the adjustable clamp would tend to vibrate at its own natural frequencies, adding unwanted noise to the acceleration data being collected from the trailer. The discovery of this oversight led to the attachment device being changed for future testing sessions.

An additional qualitative finding was the need for an extension cable for the accelerometer, as its standard length of 2.4m would prove too short and create a danger for the testing equipment.

6.1.2 Testing Session 1 Results and Conclusions

It was discovered that the usefulness of signals of data collected from vehicles rolling over bumps was limited, and that future testing would involve rolling off bumps. Its usefulness was limited due to the fact that such a rolling over test involves multiple external inputs rather than a distinct

external input, as is the case for a rolling off type test. The multiple external inputs mean that reasonably straightforward analysis of an exponential decay curve is not possible. To perform useful analysis of such curves was considered too difficult and would be too uncertain, and thus rolling-over type testing was rejected. The difference between the testing methods is shown in Figure 6.1 and Figure 6.2.

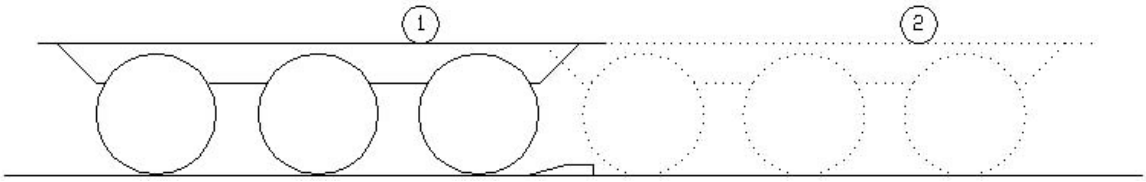

Figure 6.1: Starting and ending positions in a rolling-over type test

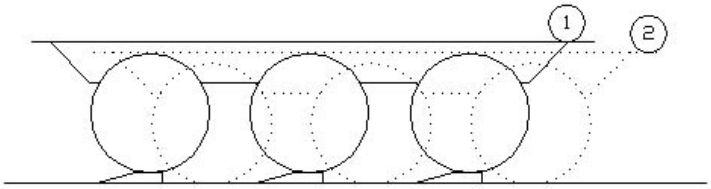

Figure 6.2: Starting and ending positions in a rolling-off type test

The use a non-rigid attachment device holding the accelerometer was found to be problematic. It was later discovered in later testing that this device exhibited strong natural frequencies, particularly at approximately 13Hz. The device's response to an impulse is shown in Figure 6.3 and Figure 6.4.

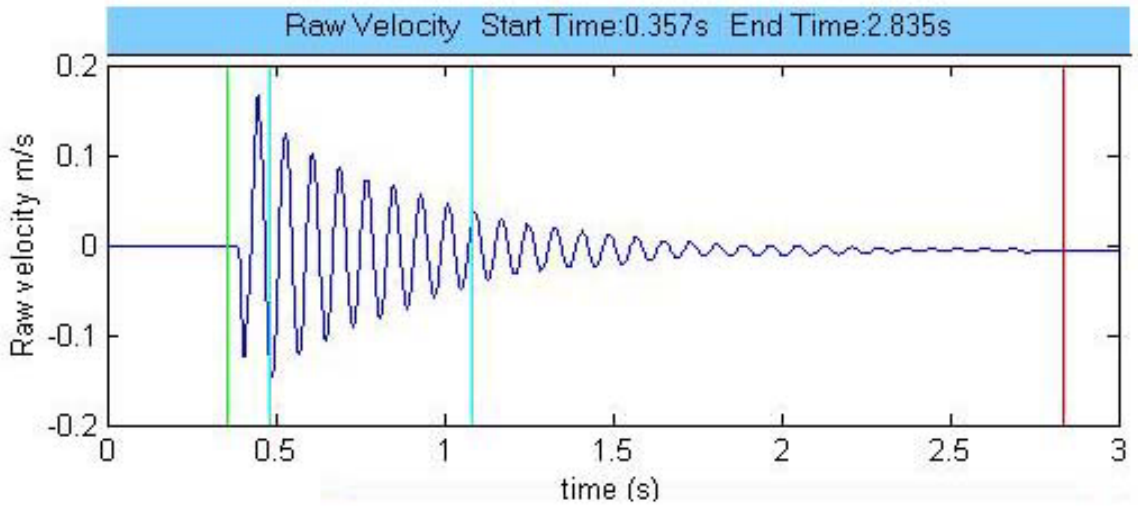

Figure 6.3: Attachment device transient velocity response to impulse input

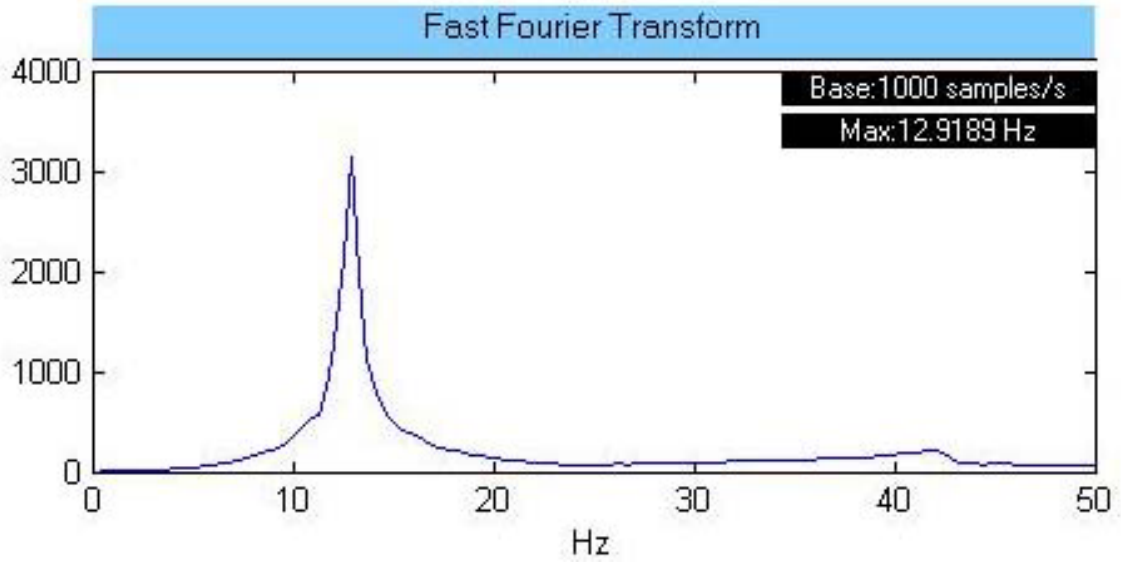

Figure 6.4: Fourier transform of attachment device impulse response

Five similar tests yielded similar results, with the attachment device showing an average dominant frequency of 13.0Hz. There is also a smaller peak at approximately 44Hz.

When working with the vehicle bump test, these natural frequencies tend to influence the acquired data. The 13.0Hz natural frequency and the 44Hz natural frequency both have a strong influence of on the Fourier transformations, as shown in Figure 6.5.

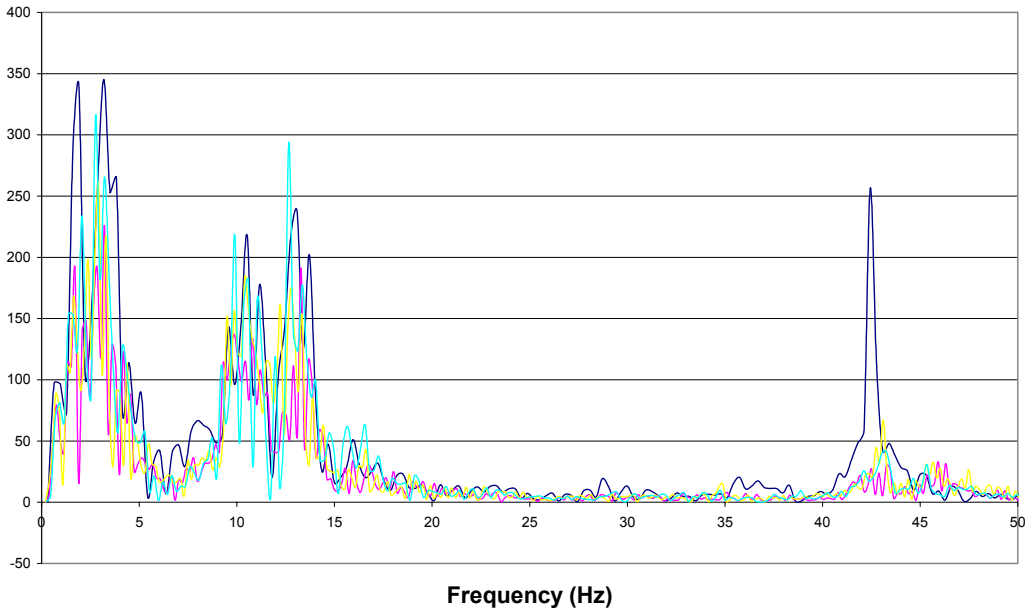

Figure 6.5: Fourier transformations of acceleration data from testing session 1

It can be seen from each of the Fourier transforms of the vehicle bump test acceleration data in Figure 6.5, that there are no distinct peaks. Each shows a series of peaks between 0-5Hz, a further set of peaks between 9-15Hz, and a further less dominant set of peaks around 44Hz. The peaks between 9-15Hz and around 44Hz correspond to the natural frequencies of the attachment device, and have the effect of adding vibrations to the recorded data signal that are not of interest, and not vibrations related to the suspension. Thus, the need to change the attachment device from a clamp to a rigid connection was recognised.

Due to these additional frequencies, and the lack of a 'clean drop' impulse input, the plots of velocity and displacement show a lack of clear decay curves, which is due to the nature of rolling-over tests.

6.2 TESTING SESSION 2 – SEMI-LADEN RIGID TRUCK

6.2.1 Testing Session 2 Summary

Testing session 2 was held on the afternoon of Friday July 18 2003 in the parking area of Baden Powell Reserve, Ardross. The vehicle tested was a single-drive rigid tray-back Mitsubishi truck, equipped with mechanical-leaf suspension. This vehicle would typically be used for the transport of tools, equipment, fuel and water to road construction worksites throughout Western Australia. The rear axle was the only part of the vehicle tested, and the steer axle was excluded. The vehicle was partially loaded with equipment, but was however not weighed. The vehicle was operated by Mark Peters and the vehicle was loaned from Western Stabilisers Pty Ltd.

The testing setup was the same as in testing session 1, with the exception of the accelerometer being attached to the vehicle with electrical tape. Additionally, rolling-off type testing was performed instead of rolling-over type testing. Testing of the influence of motor-induced vibrations was performed to discover their effect on bump-test data. Methods of stopping other than via the application of brakes were trialled.

6.2.2 Testing Session 1 Results and Conclusions

Useful data was gained with regards to the damping ratio and natural frequency of the mechanical suspension. These results are demonstrated in Table 6.2.

Test Number	Natural Frequency	Damping Ratio
13	3.4Hz	7.3%
14	3.7Hz	5.3%
15	3.6Hz	9.3%
16	3.8Hz	4.5%
Average	3.6Hz	6.6%

Table 6.2: Results of testing semi-laden mechanically-sprung rigid truck

A typical velocity response is shown in Figure 6.6.

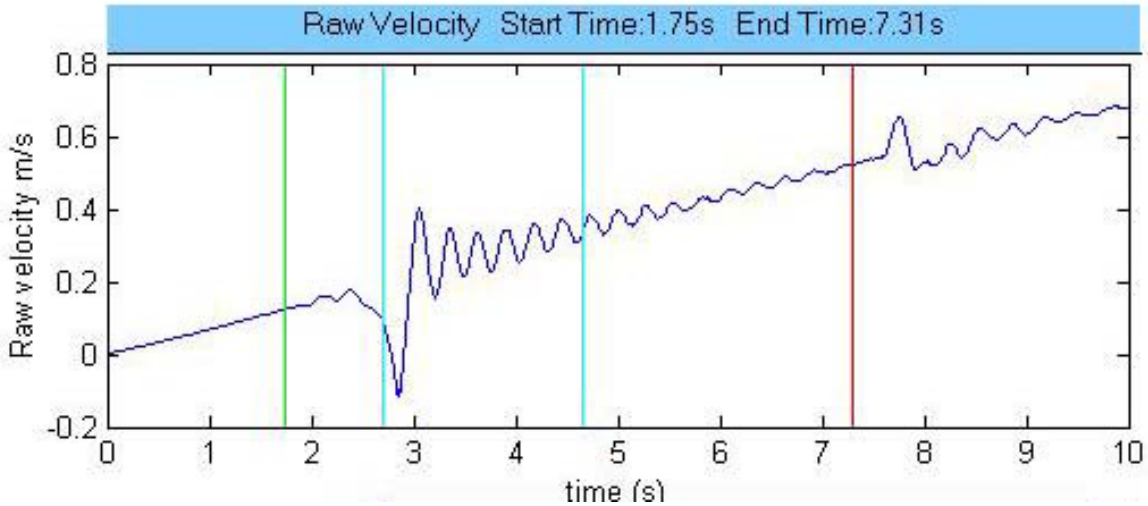

Figure 6.6: Unadjusted velocity response of rigid truck mechanically-sprung rear axle

It is noted from Figure 6.6 that the response is very similar to a sinusoidal decay curve, which proves useful for analysis. In Figure 6.6 at approximately 7.5s, a second response related to stopping is noticed. Also a positive miscalibration bias of approximately $+0.07 m/s^2$ is noted.

6.3 TESTING SESSION 3 – UNLADEN SEMI TRAILER

6.3.1 Testing Session 3 Summary

Testing session 3 was held on the morning of Saturday August 16 2003 in the yard of Sands Fridge Lines, Forrestfield. The heavy vehicle tested was essentially the same as that used in testing session 1, a tandem-drive prime mover towing an unladen tandem-axle refrigerated trailer, equipped with a BPW air suspension. The air-suspension trailer was the only part of the vehicle tested, and the prime mover was excluded. The vehicle was again operated by Kevin Sands.

The qualitative findings from testing sessions 1 and 2 were applied so as to gain maximum useful results from testing session 3. Major changes and improvements were the following:

- Four extra bumps were constructed, and those used in the first two sessions were modified.
- The frame components were purchased and customized.
- An extension lead for the accelerometer was purchased.
- The GUI was made completely functional.
- The accelerometer was mounted on a welding magnet.

Bump-testing was conducted with shock absorbers attached and shock absorbers removed. Results under both scenarios were ascertained for comparison. Stopping was accomplished by the rear wheels rolling up the incline of the next bump in the series.

6.3.2 Testing Session 2 Results and Conclusions

Testing with attached dampers

Dampers Attached		
Test Number	Natural Frequency	Damping Ratio
1	2.2Hz	24.5%
2	2.1Hz	15.3%
3	2.3Hz	23.4%
6	2.0Hz	26.7%
7	2.1Hz	28.9%
8	2.2Hz	22.8%
Average	2.2Hz	23.6%

Table 6.3: Results of bump testing unladen air-suspension trailer with dampers attached

Table 6.3 shows that the average damping ratio for the unladen trailer with dampers attached was 23.6%. This is better than the 20% standard required for suspensions to meet road friendliness. However, the trailer was unladen, which does alter its sprung characteristics.

In terms of repeatability of the test, it is noted that test 2 displayed a damping ratio of 15.3%. However, the data for this test was corrupted, as the driver applied the vehicle's brakes, rather than allowing the vehicle to roll. Thus, results from tests where brake application occurs, should be treated as outliers, and discarded as they are not useful.

If the results of test 2 are discarded from the sample, the average damping ratio increases to 25.3% and the average natural frequency stays at 2.2Hz. The measured damping ratio ranges from 22.8% to 28.9%, and the natural frequency from 2.0Hz up to 2.3Hz. The results are reasonably consistent, with the damping ratio meeting the road friendly criteria, but the natural frequency failing the road friendly criteria.

The variation in the damping ratio results can be partially contributed to the log-decrement method used for its calculation. Damped data signals usually have only two useful peaks, and the lack of being able to average across several peaks can lead to variable individual results. This is demonstrated in the adjusted acceleration traces shown in Figure 6.7.

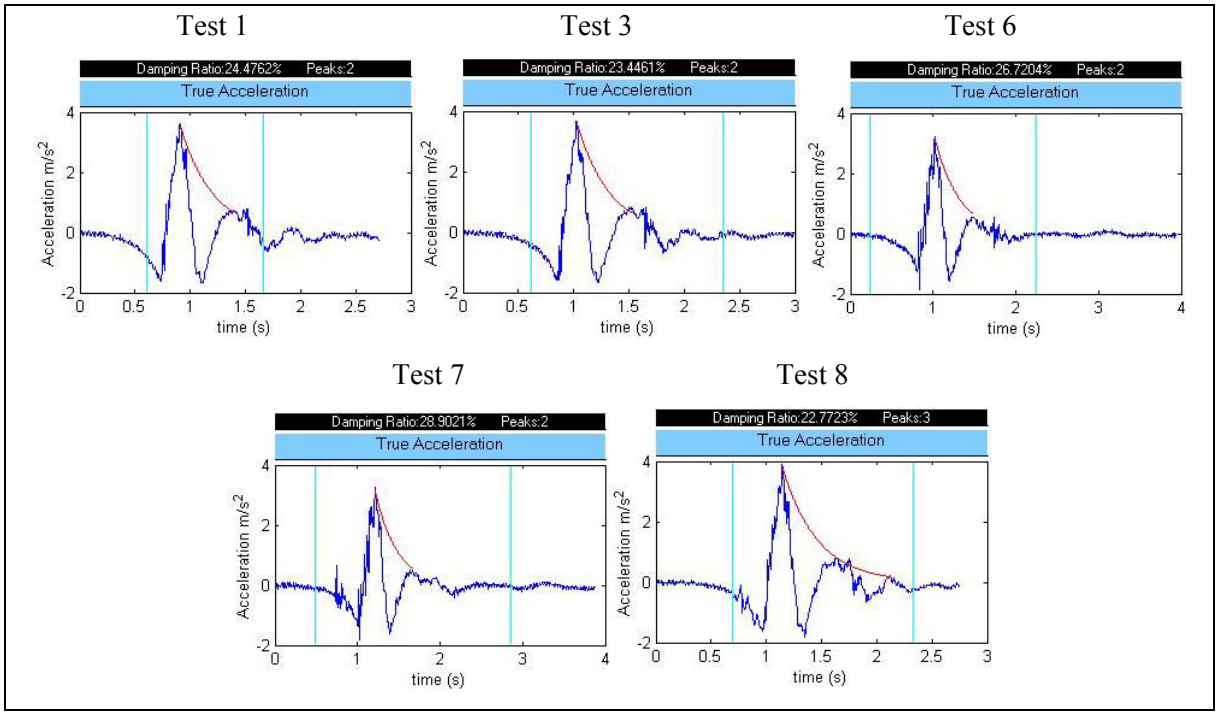

Figure 6.7: Adjusted acceleration plots of unladen trailer with dampers attached

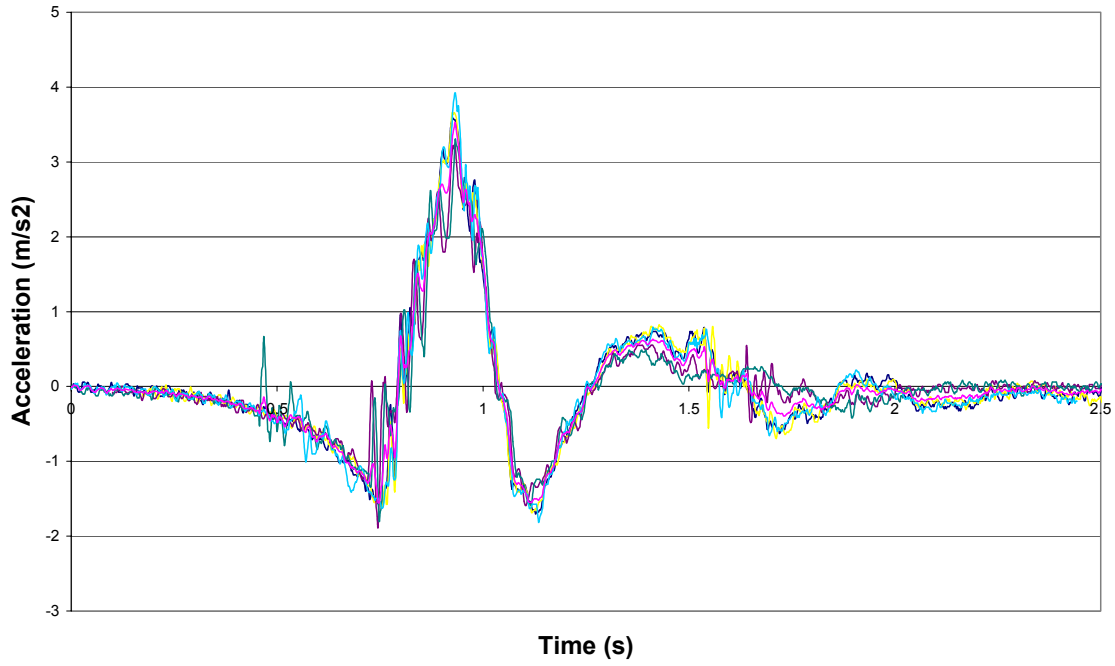

Figure 6.8: Multiple adjusted acceleration plots for trailer with attached dampers

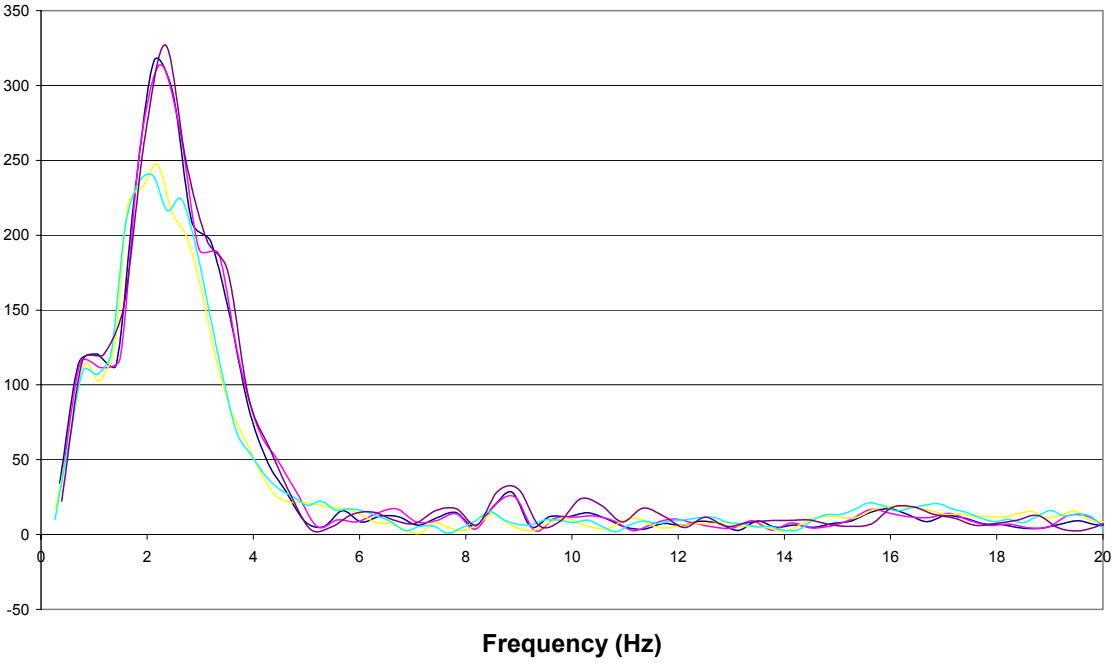

Figure 6.9: Multiple Fourier transformations of adjusted acceleration for trailer with attached dampers

As can be seen from Figure 6.8 and Figure 6.9, the shapes of the individual acceleration plots and Fourier transformations are similar. For the acceleration plots, the first two peaks of each plot are almost identical in terms of magnitude and spacing. As it these two peaks that dominate the damping ratio calculation, it can be seen that the test is repeatable. Likewise, the similar nature of the individual Fourier transformations suggests that testing a suspension with dampers attached is repeatable.

However, the unladen nature of the vehicle does not allow for direct comparison to road friendliness. An increase in the sprung mass by a large factor would lead to a decrease in the natural frequency. In this instance, the sprung mass would be only a few tonnes, yet fully loaded it could be around twenty tonnes. Allowing for this magnitude increase in mass, it is likely that this suspension would meet both frequency and damping ratio road friendliness requirements, if tested loaded.

Testing with removed dampers

Dampers Removed		
Test Number	Natural Frequency	Damping Ratio
9	2.1Hz	5.0%
10	2.1Hz	6.5%
11	2.2Hz	5.4%
12	2.1Hz	5.5%
13	2.2Hz	5.3%
14	2.2Hz	5.9%
15	2.2Hz	4.7%
16	2.1Hz	6.1%
Average	2.2Hz	5.5%

Table 6.4: Results of bump testing unladen air-suspension trailer with dampers removed

Table 6.4 shows the average damping ratio for the trailer with its dampers removed is 5.5%, which is considerably lower than the average damping ratio for dampers attached. It is also well below the RFS requirement of 20%. The results vary between 4.7% and 6.5%, which is less variation than was seen in the case of dampers attached. This can be attributed to the log-decrement damping ratio calculation, which can be averaged across more peaks when the damping ratio is lower.

Multiple acceleration data and Fourier transform plots are shown in Figure 6.10 and Figure 6.11.

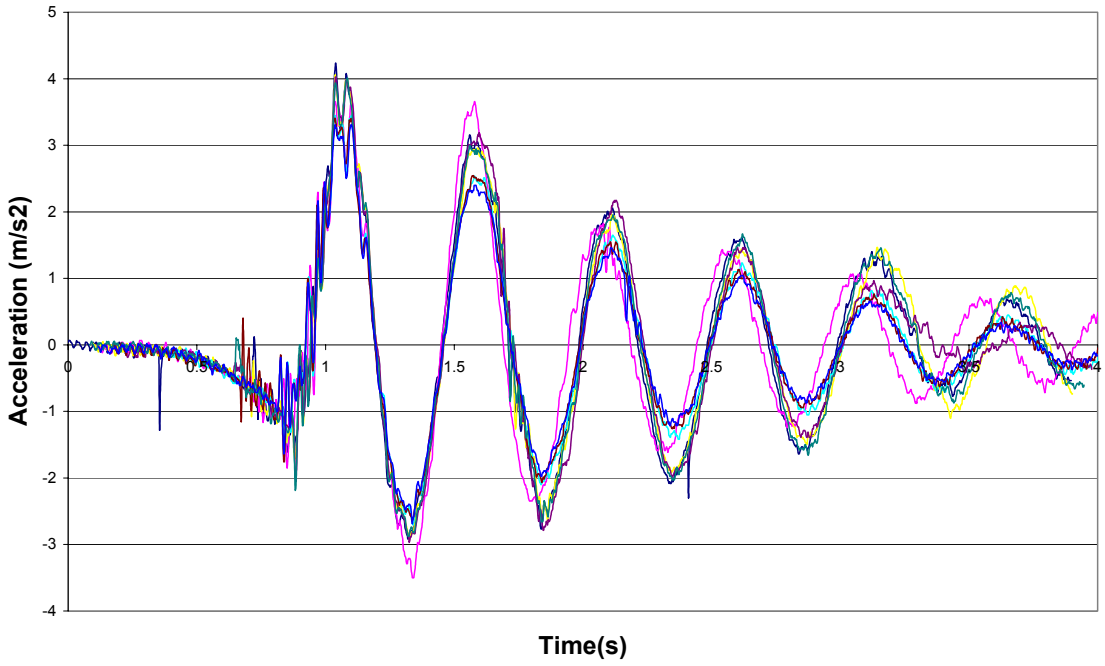

Figure 6.10: Multiple adjusted acceleration plots for trailer with removed dampers

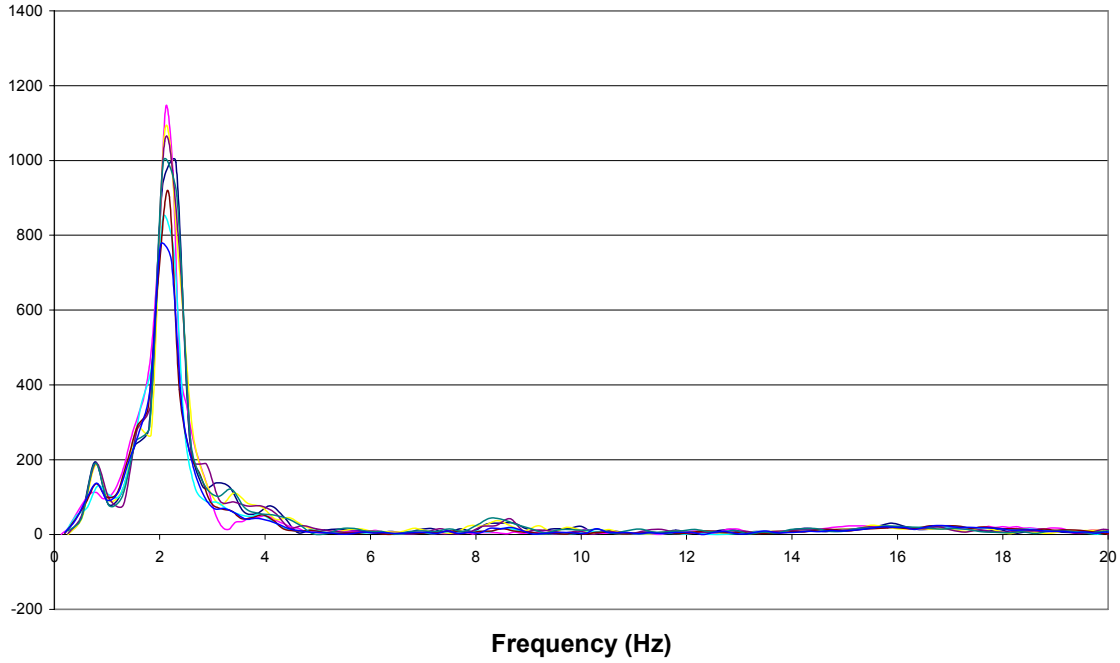

Figure 6.11: Multiple Fourier transformations of adjusted acceleration for trailer with removed dampers

It can be seen from Figure 6.10 that the general shape of the acceleration plots from different tests on an undamped trailer are very similar, and thus the test on an undamped vehicle is repeatable. It is also seen from the Fourier transformation in Figure 6.11 that the peaks are at approximately the same value, as noted earlier in Table 6.4.

The repeatability of tests, shown up by the similarity in acceleration plots and Fourier transformations, for both damped and undamped trailers is an indication that the test is suitable in that it provides repeatable results.

It is noted that there is a small peak at approximately 8.5Hz in both Fourier transformations in Figure 6.9 and Figure 6.11. These peaks relate to tyre bounce frequencies, which were a concern expressed in some literature, such as Cebon [06]. However, it can be seen by the relative magnitudes on the Fourier plots that the tyre bounce frequencies have little influence on the transient response of an unloaded trailer.

6.4 TESTING SESSION 4 - LADEN TRIPLE ROAD TRAIN

6.4.1 Testing Session 4 Summary

Testing session 4 was held on the afternoon of Wednesday October 1 2003, on a gravel access road at the Paddington Gold Mine, north of Kalgoorlie-Boulder. The heavy vehicle tested was a Kenworth tandem-drive prime mover towing three laden trailers. Each trailer was a tri-axle, and the two dollies were tri-axles, all running Hendrickson air suspensions. The whole vehicle was tested, with each axle grouping tested only once.

Methods and procedures were the same as used in testing session 3. However, the road surface used was compacted gravel. The vehicle was weighed at the weights shown in Table 6.5. It can be seen that the vehicle was marginally above statutory mass limits on most of its axle groups.

Group	Mass
Steer	6.1t
Tandem drive	17.4t
Trailer 1 tri-axle	20.1t
Dolly 1 tri-axle	20.0t
Trailer 2 tri-axle	21.8t
Dolly 2 tri-axle	20.5t
Trailer 3 tri-axle	20.8t

Table 6.5: Masses of axle groups on triple road train

6.4.2 Testing Session 4 Results and Conclusions

Testing session 4 was did not yield useful results about the sprung response of a loaded air suspension. Unusually inclement weather hampered proceedings, and as was later discovered, the testing apparatus had been set on a slight downhill grade. At the time of setup grade had not been considered an issue. However, given the mass of the heavy vehicle, and nature of the momentums involved, it was soon discovered that stopping the vehicle without the use of vehicular braking would not occur. As a consequence, when braking was not applied, each tri-axle group would continue to roll forwards until all three axles were past the set of bumps, similar to the situation shown in Figure 6.1. As a consequence, a uniform input was not applied to the suspension, but instead three distinct inputs. The first input was as all three axles dropped from each of their bumps, as designed. However, the second input occurred as axles two and three rolled over bumps

one and two, and then the third input as axle three rolled over bump one. This yielded displacement plots such as in Figure 6.12.

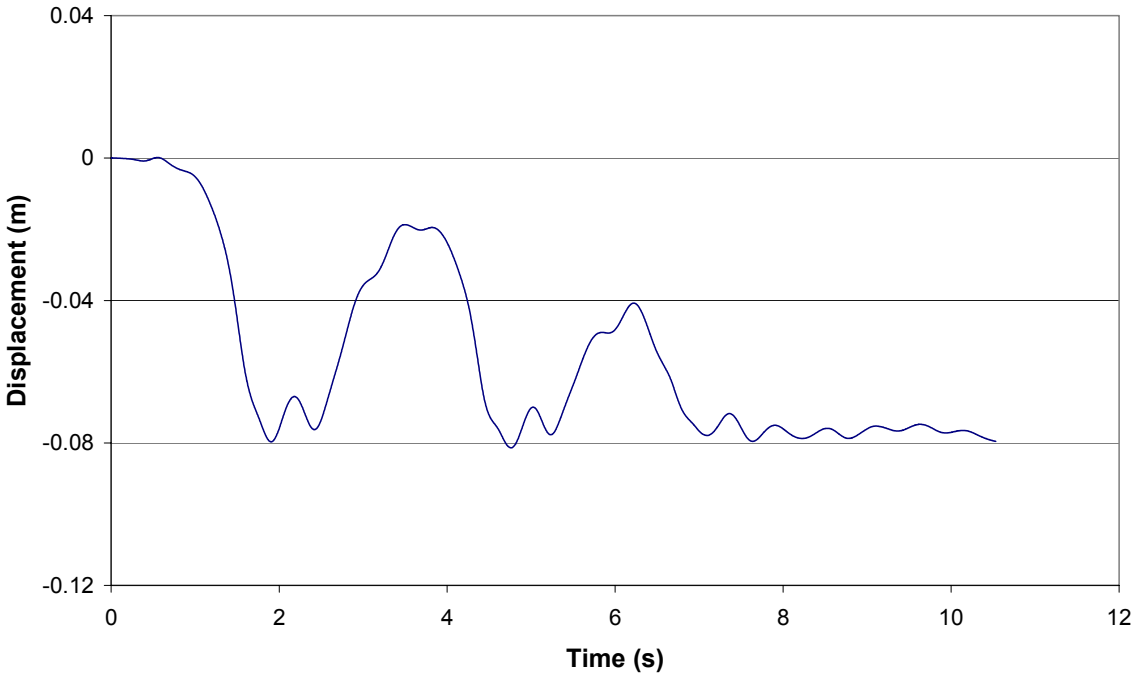

Figure 6.12: Displacement plot from trailer 3 axle group

As can be seen, the plot resembles three bumps. The magnitude of each decreases, because for peak two, only two axles are raised, and for peak three only one axle is raised, and the suspension self levels.

However, such plots are not useful for determining natural frequency or damping ratio of a suspension, due to the lack of a clean impulse input. The lack of a clear natural frequency is shown in Figure 6.13.

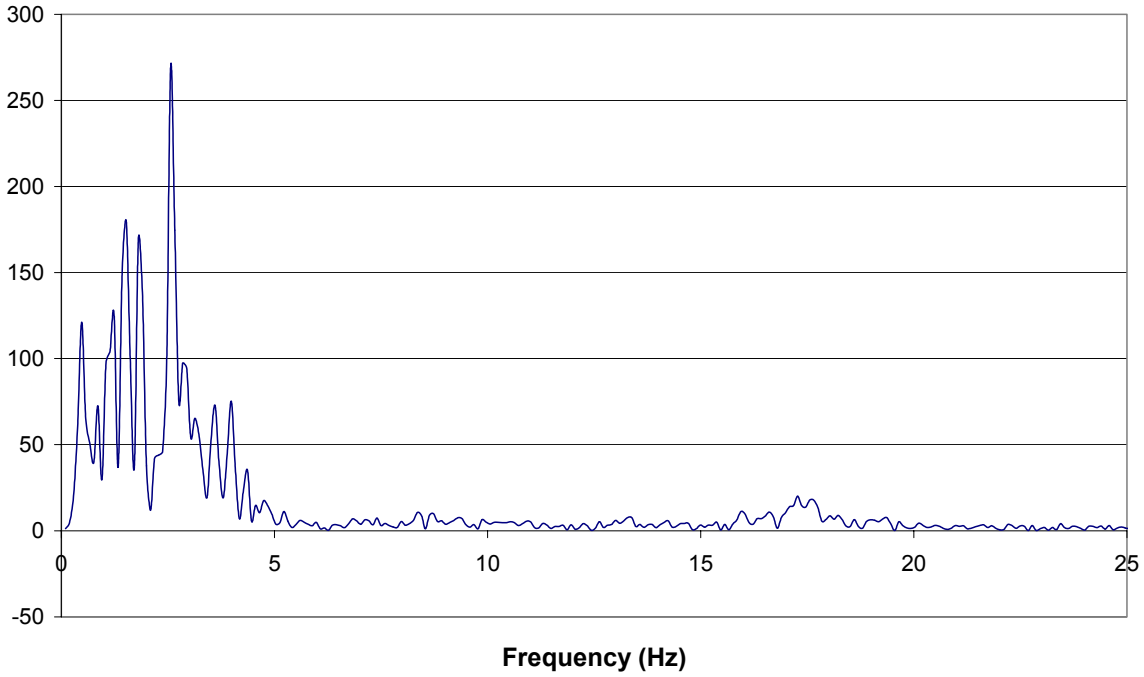

Figure 6.13: Fourier transformation corresponding to displacement plot in Figure 6.12

It can be seen that there is the lack of a distinct peak. However, there is very little response in the 8Hz region, indicating that on loaded vehicles, the influence of tyre bounce frequencies is negligible. This is an important quantitative finding, and was demonstrated repeatedly during testing session 4.

Thus, few useful numerical results were gained from testing. Qualitative gains however were substantial, such as refinements in user-driver communications, operations from portable computers in unsatisfactory climatic conditions, and a 'feel' for general field operability.

The lack of testing under loaded conditions useful for determining natural frequency and damping ratio does constitute a general research shortcoming. However, it is believed that the results from the qualitative results gained in testing session 4 indicate that successful quantitative field testing would occur, given suitable site grade and climate conditions.

7 CONCLUSIONS

The bump test that has been developed in this investigation is designed to identify two key performance characteristics of heavy vehicle suspensions. These characteristics – the suspension's sprung natural frequency and damping ratio – are the important performance parameters in determining whether a suspension meets road friendly performance criteria.

Key achievements included:

- the building of a set of bumps and a frame in which to place them, such that repeatable and reliable suspension testing may be performed
- the development of a comprehensive analysis GUI, allowing for on-the-spot interpretation of testing signals
- use of a magnet-mounted accelerometer for measuring suspension sprung mass acceleration
- the development of sophisticated data correcting algorithms
- the organising and completion of four individual testing sessions, with each achieving specific goals and outcomes

Ultimately, as shown in Chapter 6, the test developed is repeatable and determines the suspension natural frequency and damping ratio successfully.

Key findings included:

- typical suspension testing yields one dominant natural frequency, and tyre bounce frequencies have no significant influence on sprung mass response loaded or unloaded
- the damping ratio of an unloaded suspension changes from >20% to approximately 5% when shock absorbers are detached
- the natural frequency of an air suspension is not largely influenced by damping, but may be influenced by load
- the natural frequency of a mechanical suspension is approximately 3.8Hz, and significantly different from an airbag suspension natural frequency
- the damping ratio of a mechanical leaf-spring suspension is approximately 5%

Further development of the testing procedure developed in this investigation is warranted, as the testing procedure presented is still in a beta development phase. Potential exists for the systems wide integration of the data collection and processing equipment into a single unit. Potential also

exists for testing equipment (frame and bumps) to be manufactured for user friendliness and robustness.

8 REFERENCES

[01] Organisation for Economic Co-operation and Development. 1997, *Dynamic Interaction Between Vehicles and Infrastructure Experiment (DIVINE) – Proceedings*, OECD Publications, France.

[02] Anon. *Council Directive 92/7/EEC*. 1992, The Council of European Communities.

[03] MM Starrs Pty Ltd. 2000, ARRB Pty Ltd, Ian Wright and Associates, *Economic Evaluation to Confirm the In-service Performance of Road Friendly Suspensions*, NRTC, Canberra.

[04] Prem, H., George, R., McLean, J. 1998, 'Methods for Evaluating the Dynamic-Wheel-Load Performance of Heavy Commercial Vehicle Suspensions' in *5th International Symposium on Heavy Vehicle Weights and Dimensions*, Maroochydore, Queensland, pp. 252-278

[05] Sweatman, P., McFarlane, S., Komadina, J., Cebon, D. 2000, *In-Service Assessment of Road-Friendly Suspensions*, NRTC, Canberra.

[06] Cebon, D. 1999, *Handbook of Vehicle-Road Interaction*, Swets & Zeitlinger, The Netherlands.

[07] Federal Office of Road Safety. 1999, *Certification of Road-Friendly Suspension Systems*, DOTARS, Canberra.

[08] Travaglini, D. 2000, *Effects of shock absorber deterioration on the road friendly behaviour of a heavy vehicle,* Honours Thesis, University of Western Australia.

[09] National Road Transport Commission. 1997, *Increase Mass Limits: Compliance and Enforcement Issues – Discussion Paper*, NRTC, Canberra.

[10] Roberts, W., Prem, H., Heywood, R., Boully, G. 2002, 'Dynamic Interaction of Vehicles and Bridges' in *7th International Symposium on Heavy Vehicle Weights and Dimensions*, Delft, The Netherlands, pp. 423-432

APPENDIX A

MATLAB MODELLING FILE

The following Matlab file was used for the purposes of modelling, as detailed in Chapter 3. The listed shock absorber parameters were adjusted for testing in an undamped situation. It outputs the data of the type seen in Figure 3.6 and Figure 3.7, which are plots of vertical displacements at the key points of the suspension.

File: modelling.m

```
clc
clear all

% suspension variables to be defined

dspringo=.300;              % (m) spring bore - this is also the
          diameter of the upper spring piston
M=4000;                   % (kg) sprung trailer mass
m=400;                    % (kg) axle mass
mtyre=100;                 % kg


Rsloaded=0.4;
Rtfree=0.425;

g=9.81;                   % (m/s^2) gravity

ktyre=850000;             % N/m
ctyre=85000;              % Ns/m

Cfr2=0;                     % 2nd order damping coefficient for fast
          rebound zone
Cfr1=7063;                  % 1st order damping coefficient for fast
          rebound zone
Cfrc=-691;                   % Constant damping coefficient for fast
          rebound zone
R4lima=-0.042;            % Rebound zone limit which delineates fast
          from slow rebound
Csr2=405770;               % 2nd order damping coefficient for slow
          rebound zone
Csr1=44416;                % 1st order damping coefficient for slow
          rebound zone
Csrc=0;                     % Constant damping coefficient for slow
          rebound zone
R4limb=0.039;                % Middle limit which delineates slow
          rebound from slow bounce
Csb2=-261341;              % 2nd order damping coefficient for slow
          bounce zone
Csb1=96511;                % 1st order damping coefficient for slow
          bounce zone
Csbc=-885.6;                % Constant damping coefficient for slow
          bounce zone
R4limc=0.148;              % Bounce zone limit which delineates slow
          from fast bounce
Cfb2=0;                     % 2nd order damping coefficient for fast
          bounce zone
```

```
Cfb1=30653;                % 1st order damping coefficient for fast
           bounce zone
Cfbc=3263.5;               % Constant damping coefficieent for fast
           bounce zone

polytropcoeff=1.4;          % ratio of specific heats for air -
           related to spring equation


Vspring(1)=(Rsloaded*pi*(dspringo^2)/4);
Fspring(1)=M*g;
Pspring(1)=Fspring(1)/(pi*(dspringo^2)/4);
idealgasconst=Pspring(1)*(Vspring(1)^polytropcoeff);
defltyre(1)=-(M+m)*g/ktyre;
deflspring(1)=0;

y1(1)=0;
y2(1)=Rtfree+defltyre(1);
y3(1)=y2(1)+Rsloaded;

y1dot(1)=0;
y2dot(1)=0;
y3dot(1)=0;

y1dotdot(1)=0;
y2dotdot(1)=0;
y3dotdot(1)=0;

Fg=(M+m+mtyre)*g;

R4dot(1)=y3dot(1)-y2dot(1);


% Damping Curve

for n=2:50000

    fprintf('%5.0f\n',n);
    t(n)=(n-1)/10000;

    if y1(n-1) > -0.08
        Fg(n)=0;
    else
        Fg(n)=(mtyre*y1dotdot(n-1))+(mtyre*g)+(ctyre*(y1dot(n-1)-
           y2dot(n-1)))+(ktyre*(y1(n-1)-y2(n-1)));
        y1dot(n-1)=-y1dot(n-1);
        y1(n-1)=-0.08;
    end

    y1dotdot(n)=(Fg(n)-(mtyre*g)+(ctyre*(y2dot(n-1)-y1dot(n-
           1)))+(ktyre*(y2(n-1)-y1(n-1)-Rtfree)))/mtyre;
    y1dot(n)=y1dot(n-1)+((y1dotdot(n)+y1dotdot(n-1))*(t(n)-t(n-
           1))/2);
    y1(n)=y1(n-1)+((y1dot(n)+y1dot(n-1))*(t(n)-t(n-1))/2);
```

```
    if R4dot(n-1) < R4lima
        Fdamper(n-1)=(Cfr2*R4dot(n-1)*R4dot(n-1))+(Cfr1*R4dot(n-
           1))+Cfrc;
        dcurve(n-1)=1;
    elseif R4dot(n-1) < R4limb
        Fdamper(n-1)=(Csr2*R4dot(n-1)*R4dot(n-1))+(Csr1*R4dot(n-
           1))+Csrc;
        dcurve(n-1)=2;
    elseif R4dot(n-1) < R4limc
        Fdamper(n-1)=(Csb2*R4dot(n-1)*R4dot(n-1))+(Csb1*R4dot(n-
           1))+Csbc;
        dcurve(n-1)=3;
    else
        Fdamper(n-1)=(Cfb2*R4dot(n-1)*R4dot(n-1))+(Cfb1*R4dot(n-
           1))+Cfbc;
        dcurve(n-1)=4;
    end


    y2dotdot(n)=((-m*g)-(ctyre*(y2dot(n-1)-y1dot(n-1)))-
           (ktyre*(y2(n-1)-y1(n-1)-Rtfree))+Fdamper(n-1)-Fspring(n-
           1))/m;
    y2dot(n)=y2dot(n-1)+((y2dotdot(n)+y2dotdot(n-1))*(t(n)-t(n-
           1))/2);
    y2(n)=y2(n-1)+((y2dot(n)+y2dot(n-1))*(t(n)-t(n-1))/2);

    y3dotdot(n)=((-M*g)-Fdamper(n-1)+Fspring(n-1))/M;
    y3dot(n)=y3dot(n-1)+((y3dotdot(n)+y3dotdot(n-1))*(t(n)-t(n-
           1))/2);
    y3(n)=y3(n-1)+((y3dot(n)+y3dot(n-1))*(t(n)-t(n-1))/2);

    R4dot(n)=y3dot(n)-y2dot(n);

    Vspring(n)=((y3(n)-y2(n))*pi*(dspringo^2)/4);
    Pspring(n)=idealgasconst/(Vspring(n)^polytropcoeff);
    Fspring(n)=Pspring(n)*(pi*(dspringo^2)/4);

end

subplot(2,2,1), plot(y1)
title('y1')
subplot(2,2,2), plot(y2)
title('y2')
subplot(2,2,3), plot(y3)
title('y3')
subplot(2,2,4), plot(Fspring)
title('Fspring')
```

APPENDIX B

GUI ANALYSES

Testing session 1 analyses

Testing session 1

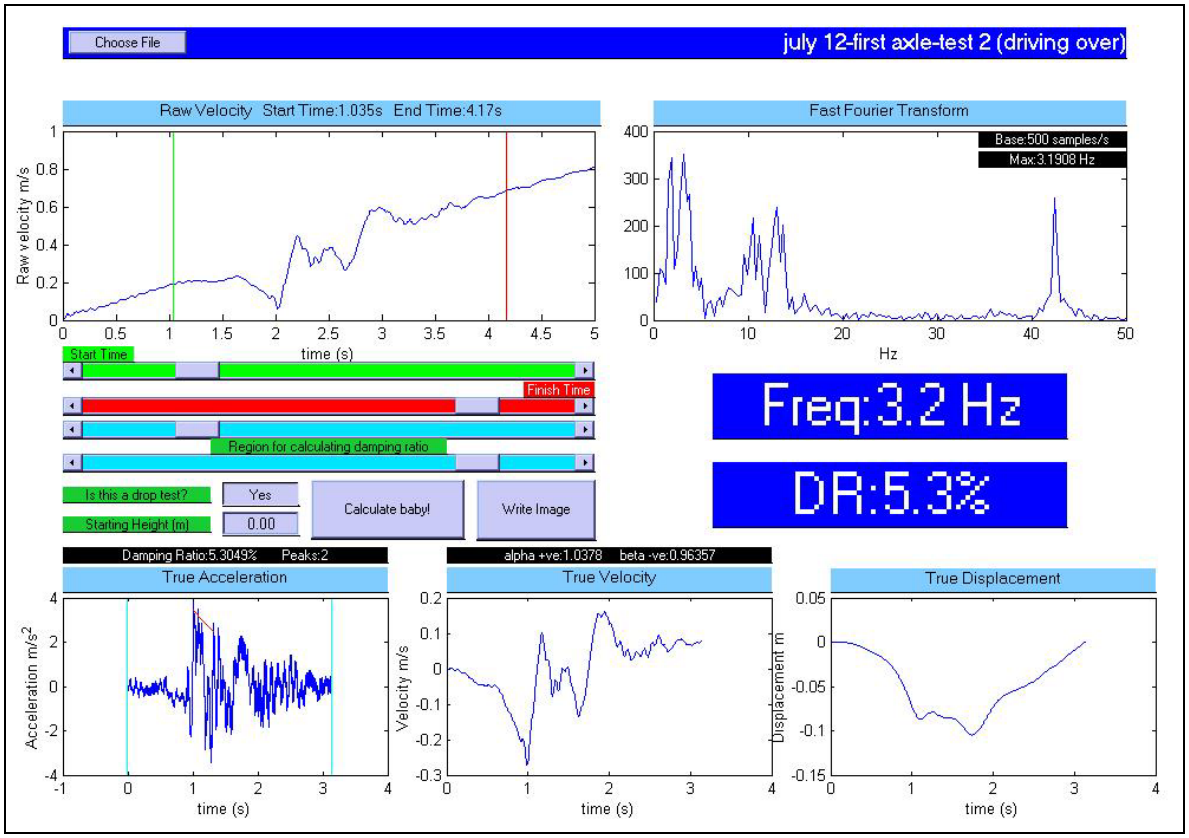

Testing session 1

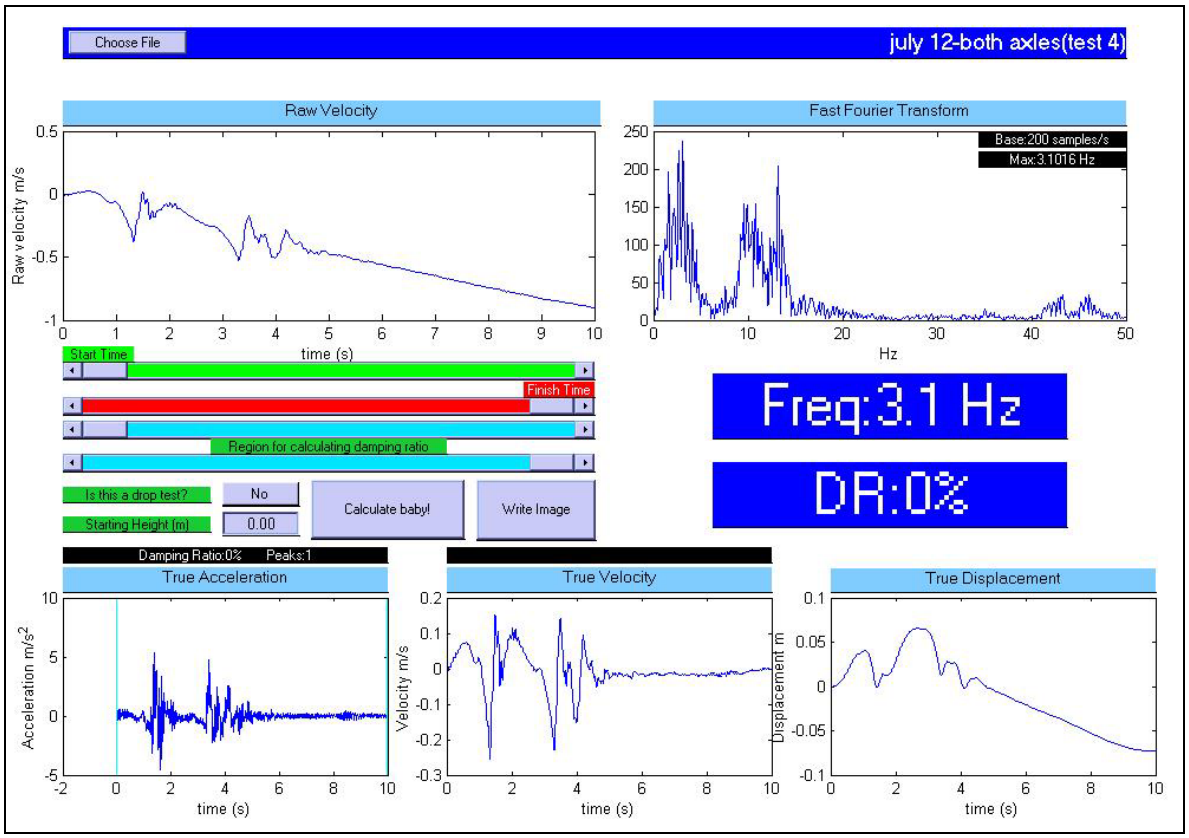

Testing session 1

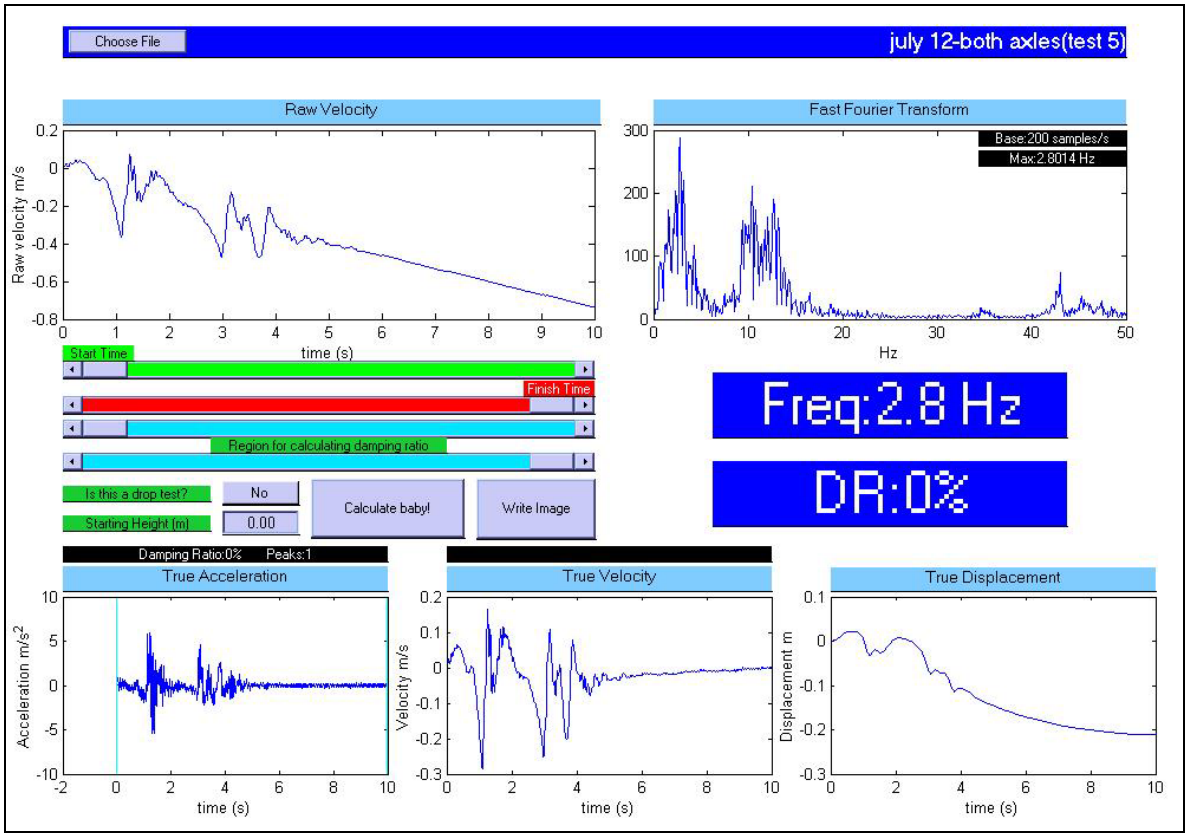

Testing session 1

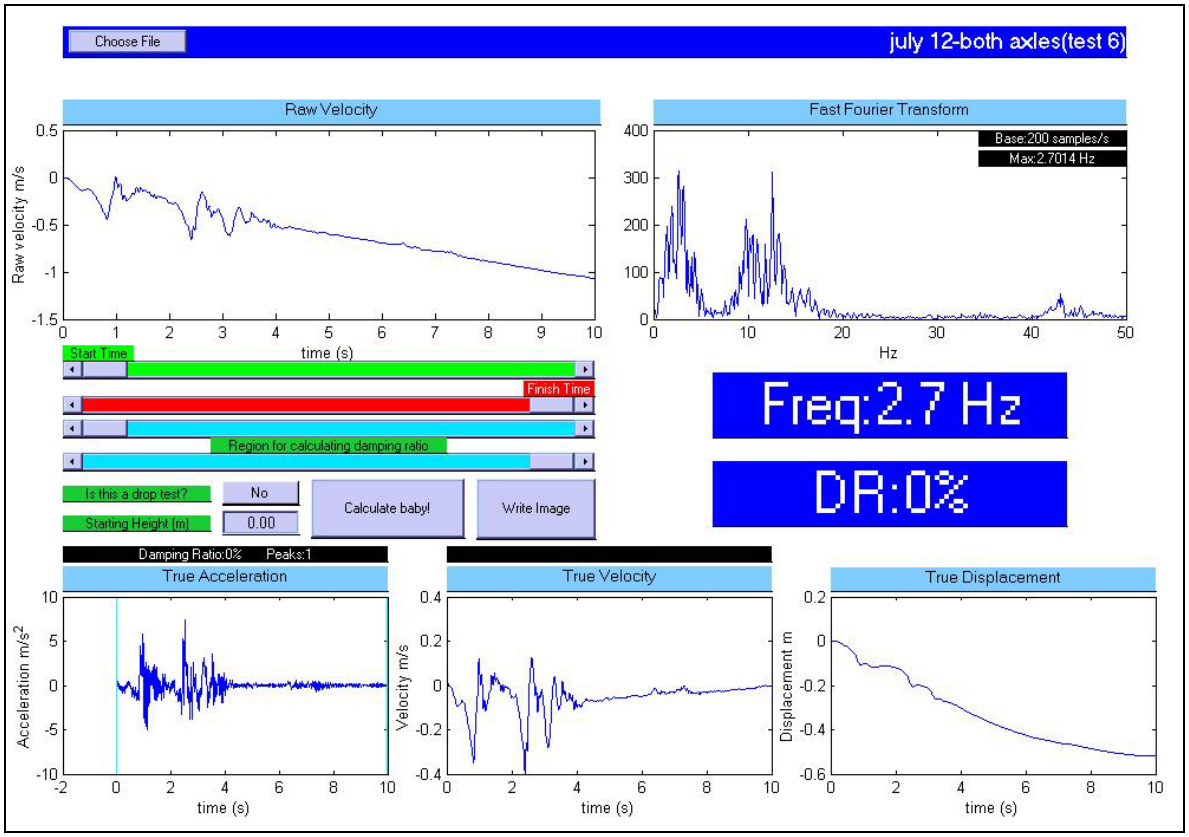

Testing session 1

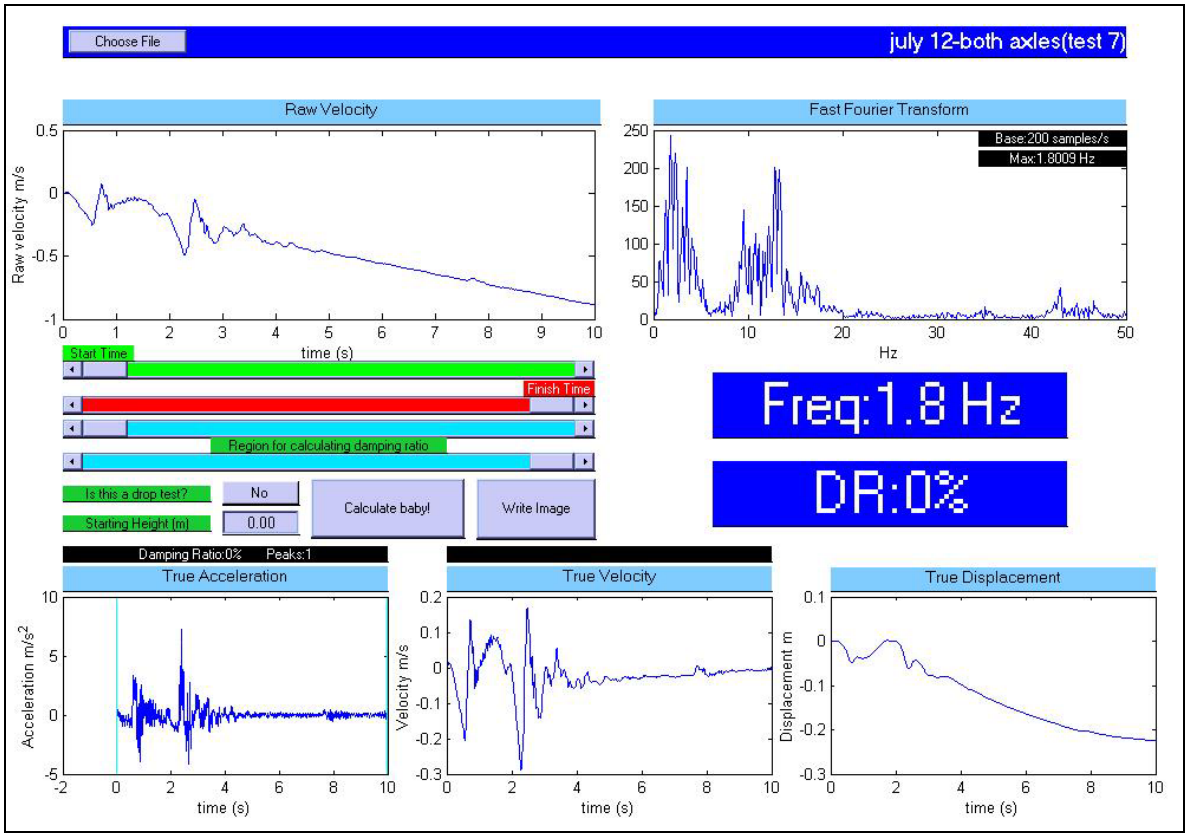

Testing session 1

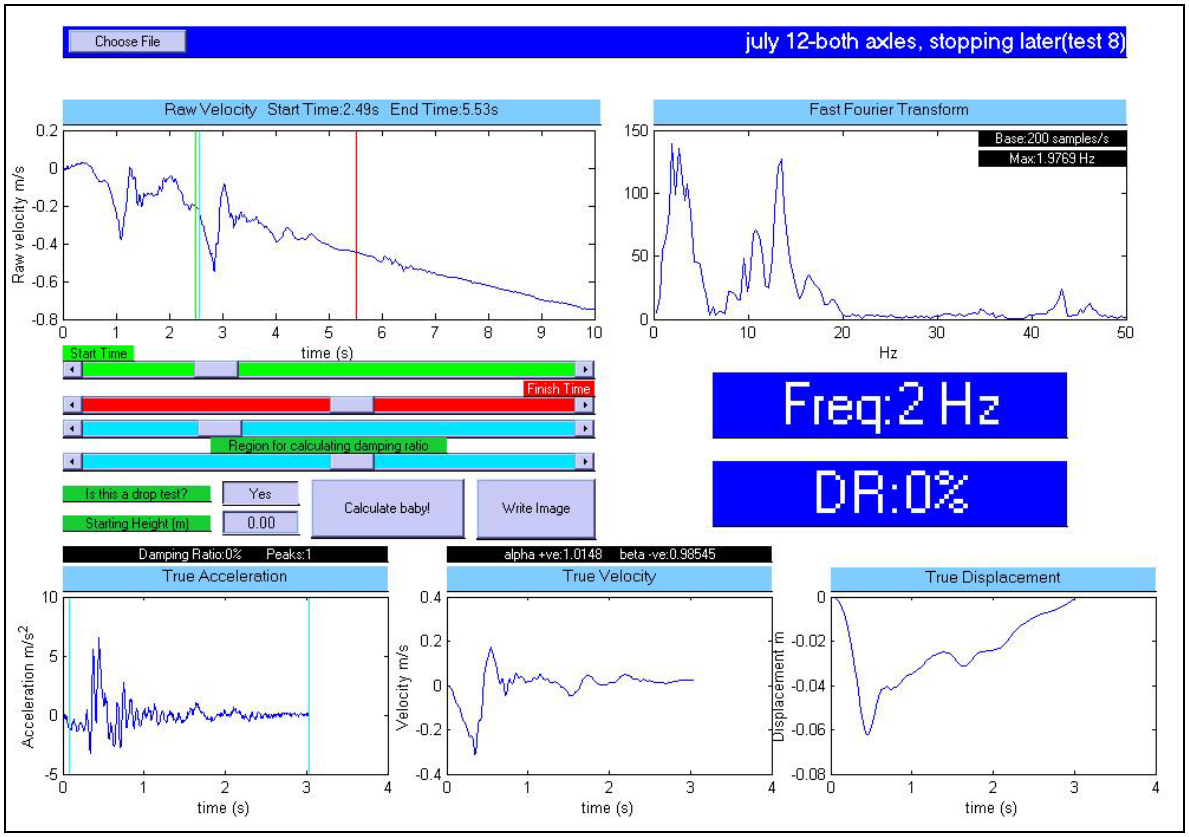

Testing session 1

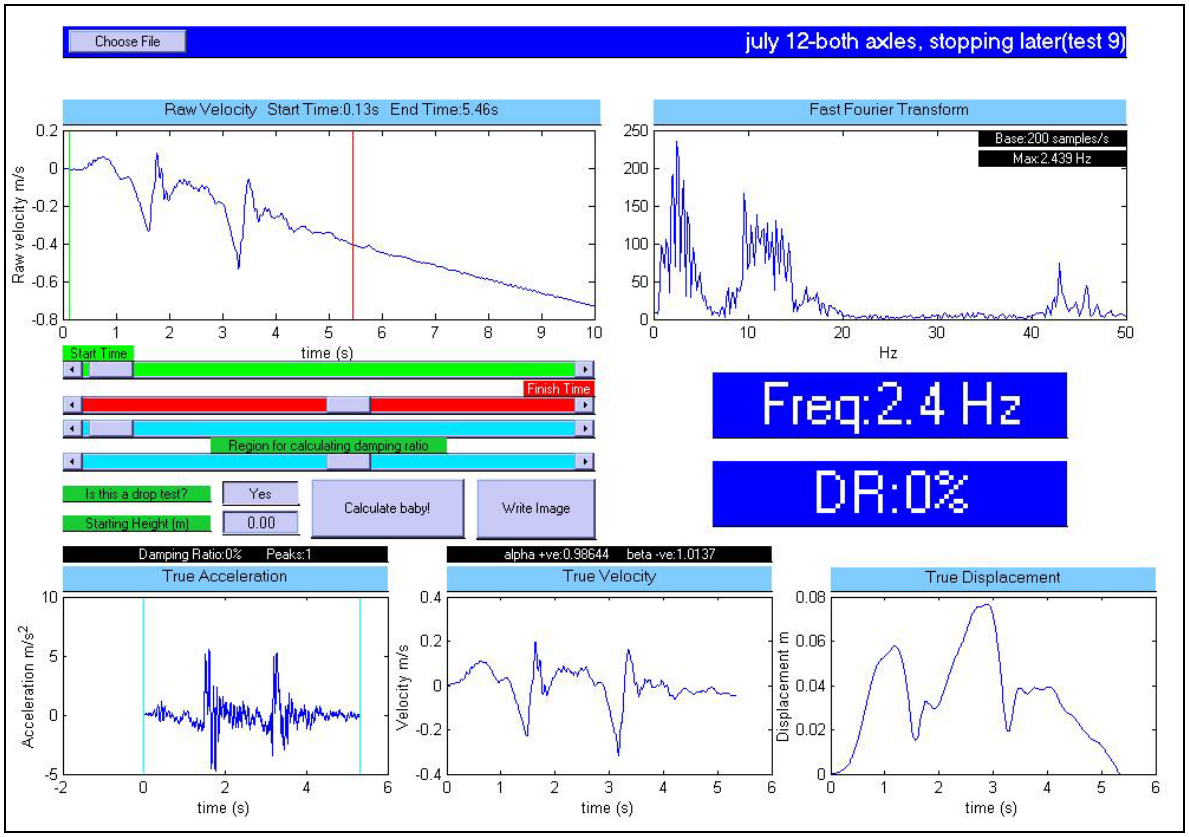

Testing session 1

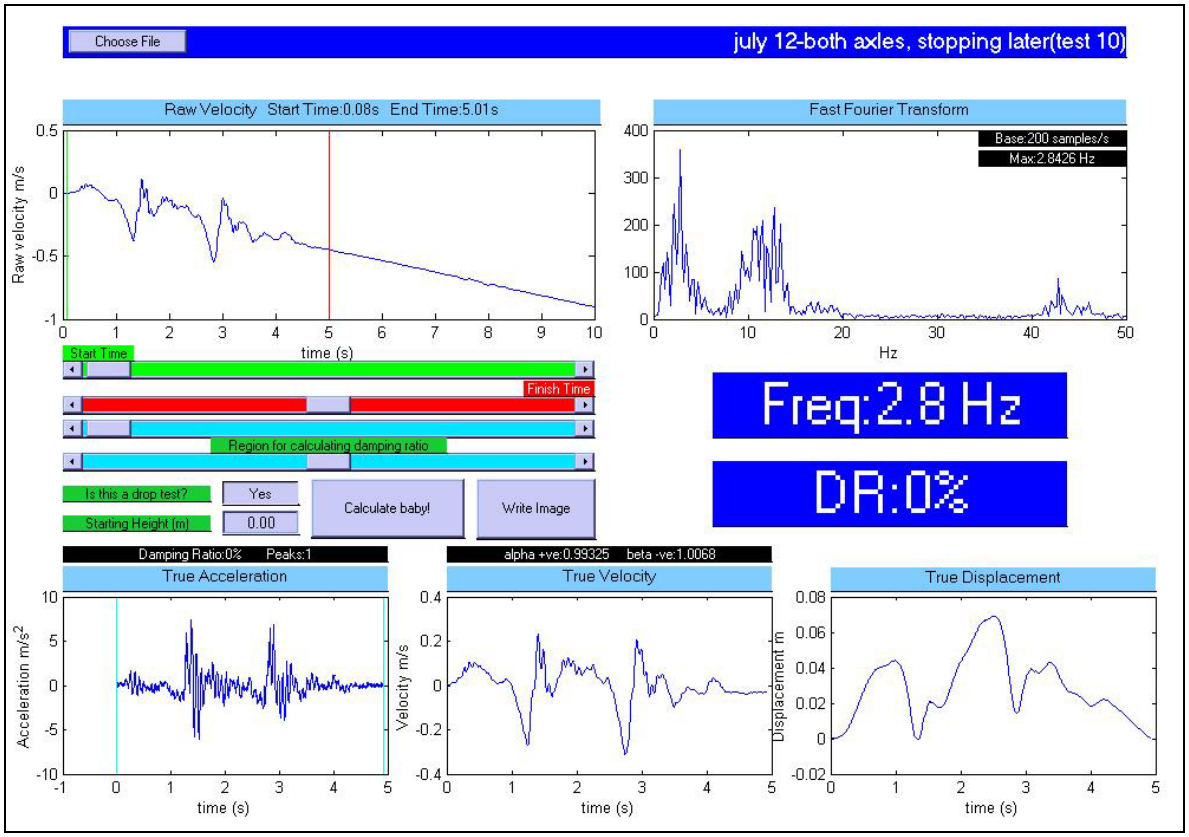

Testing session 1

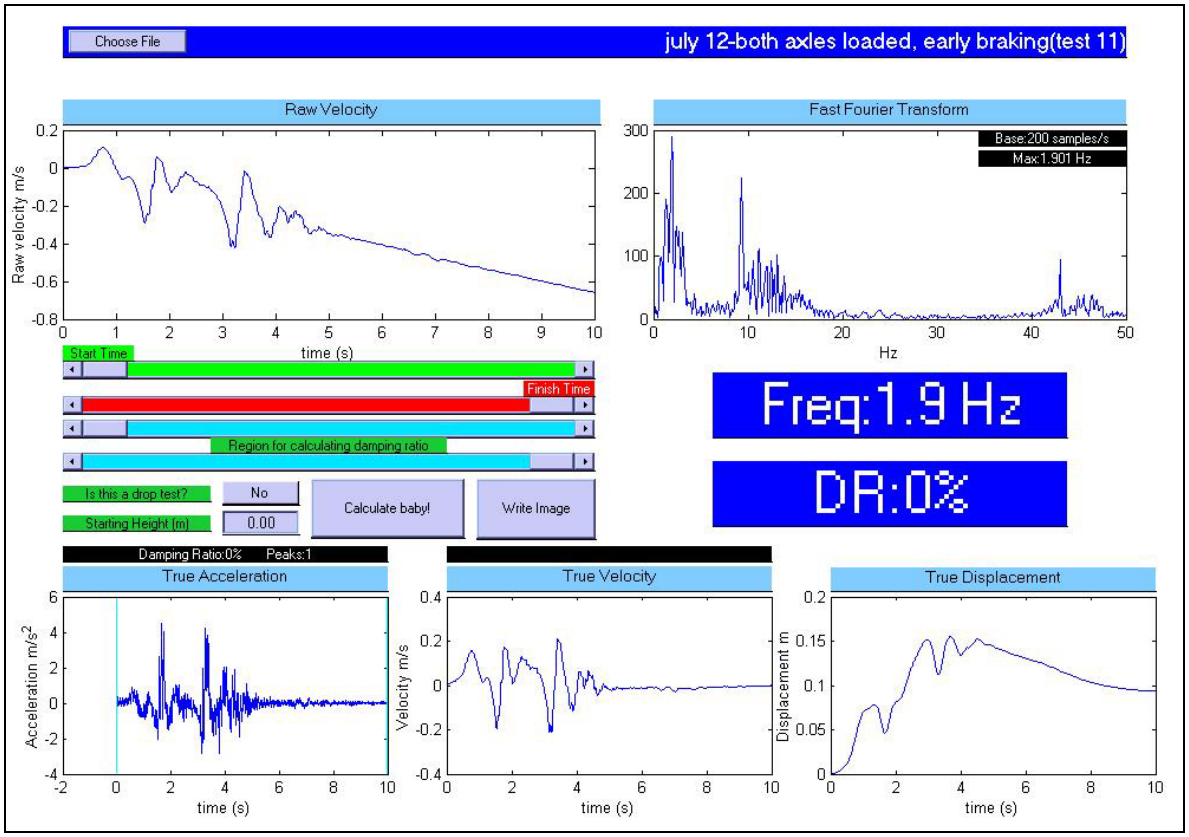

Testing session 1

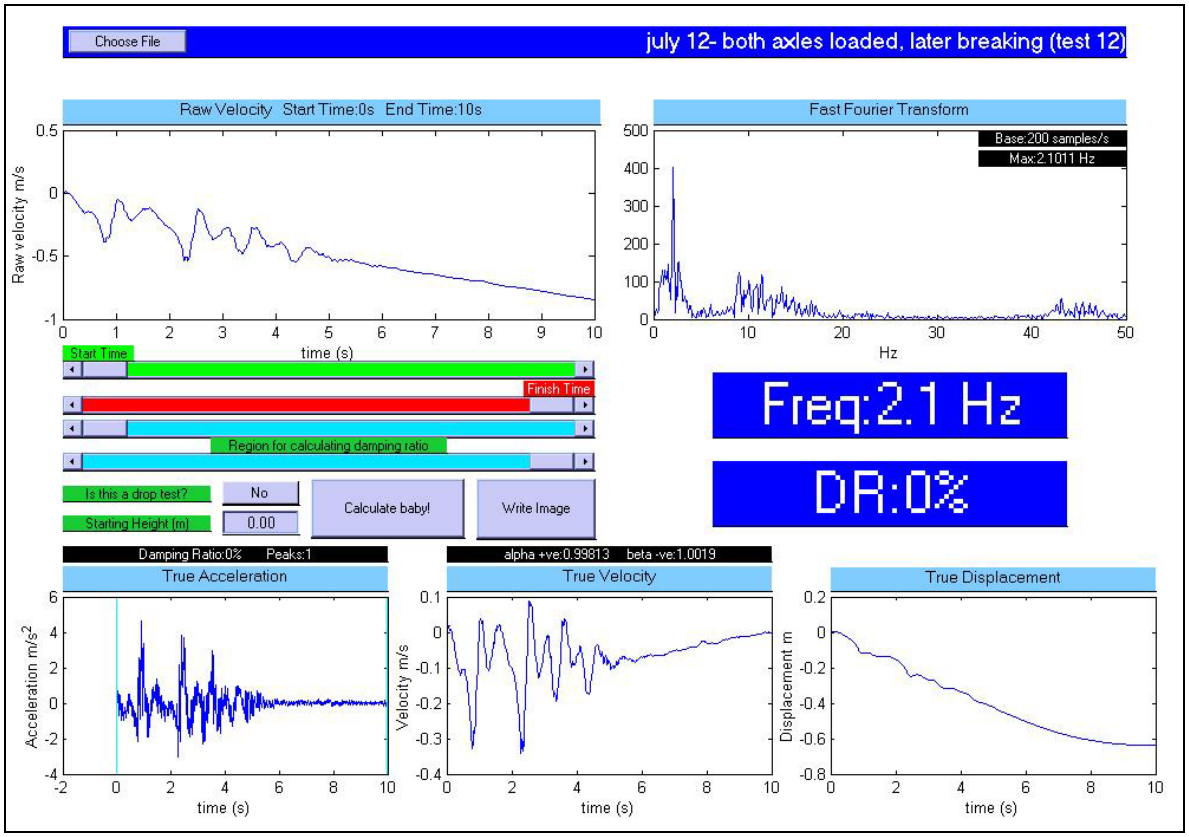

Testing session 1

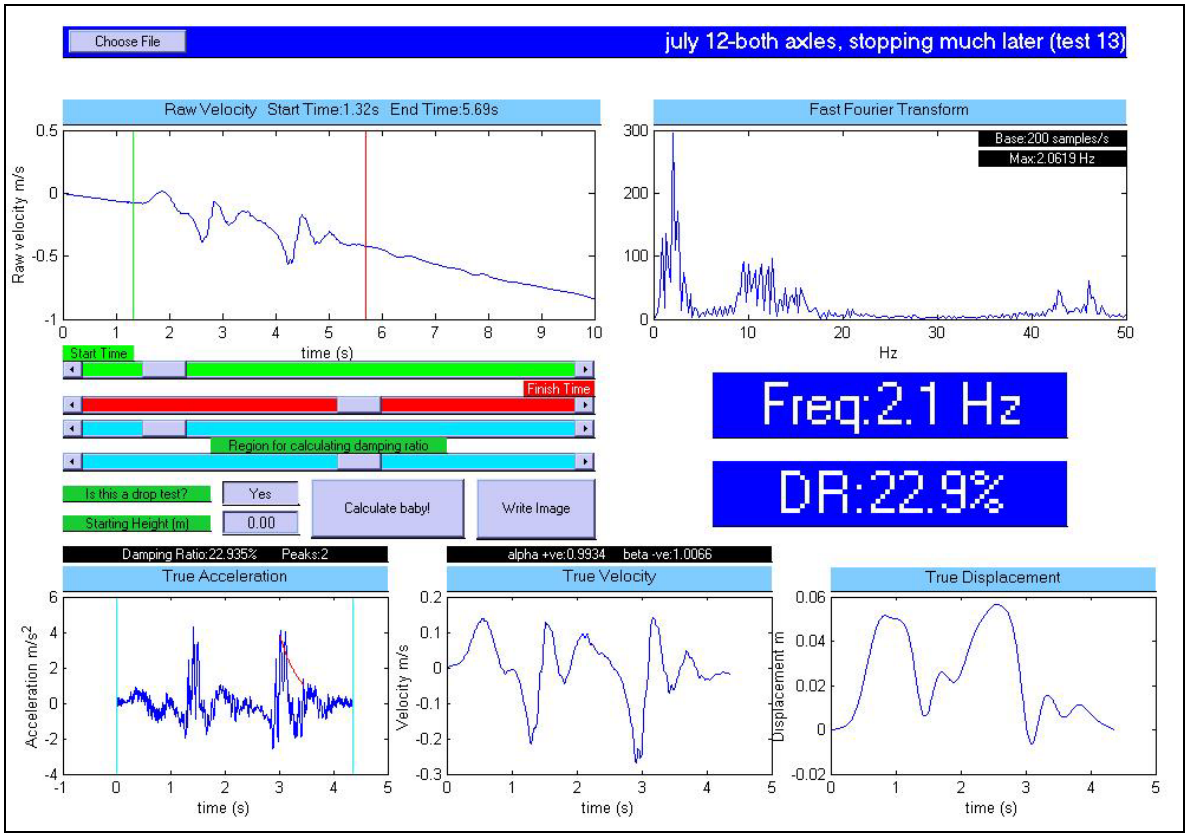

Testing session 1

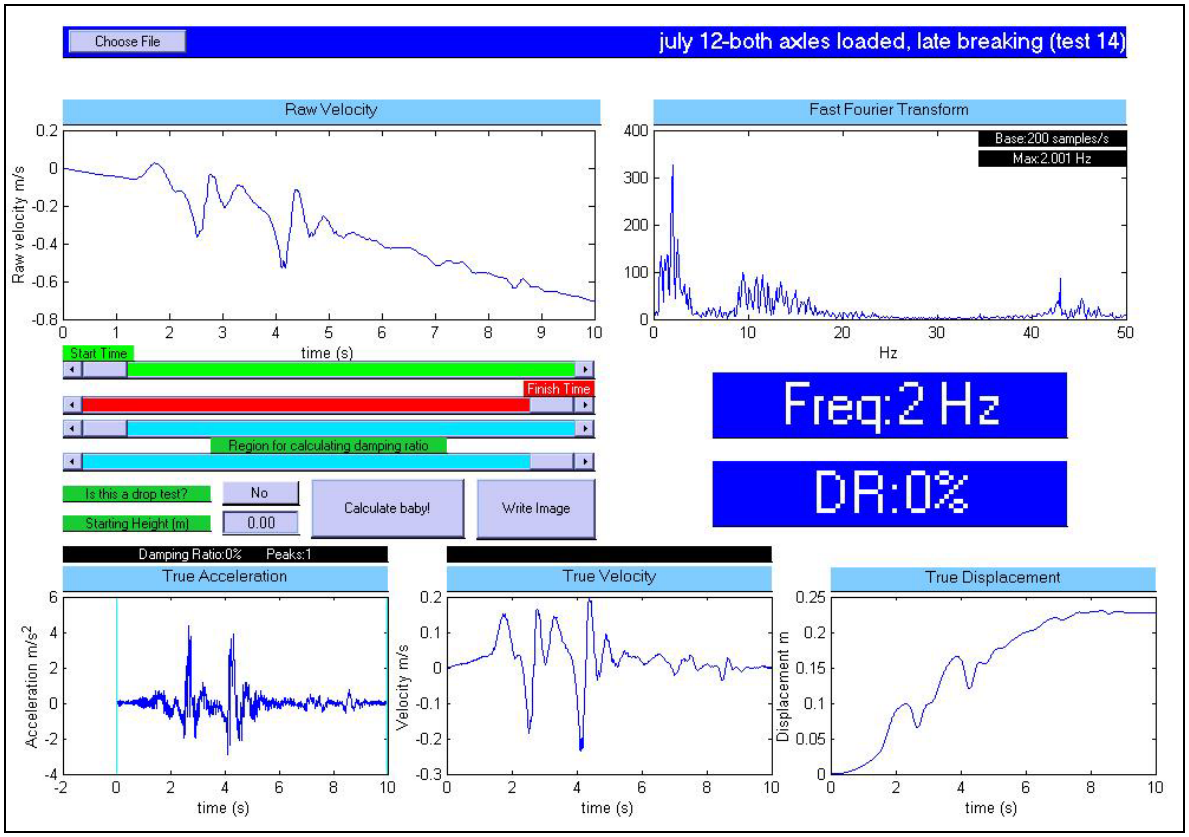

Testing session 1

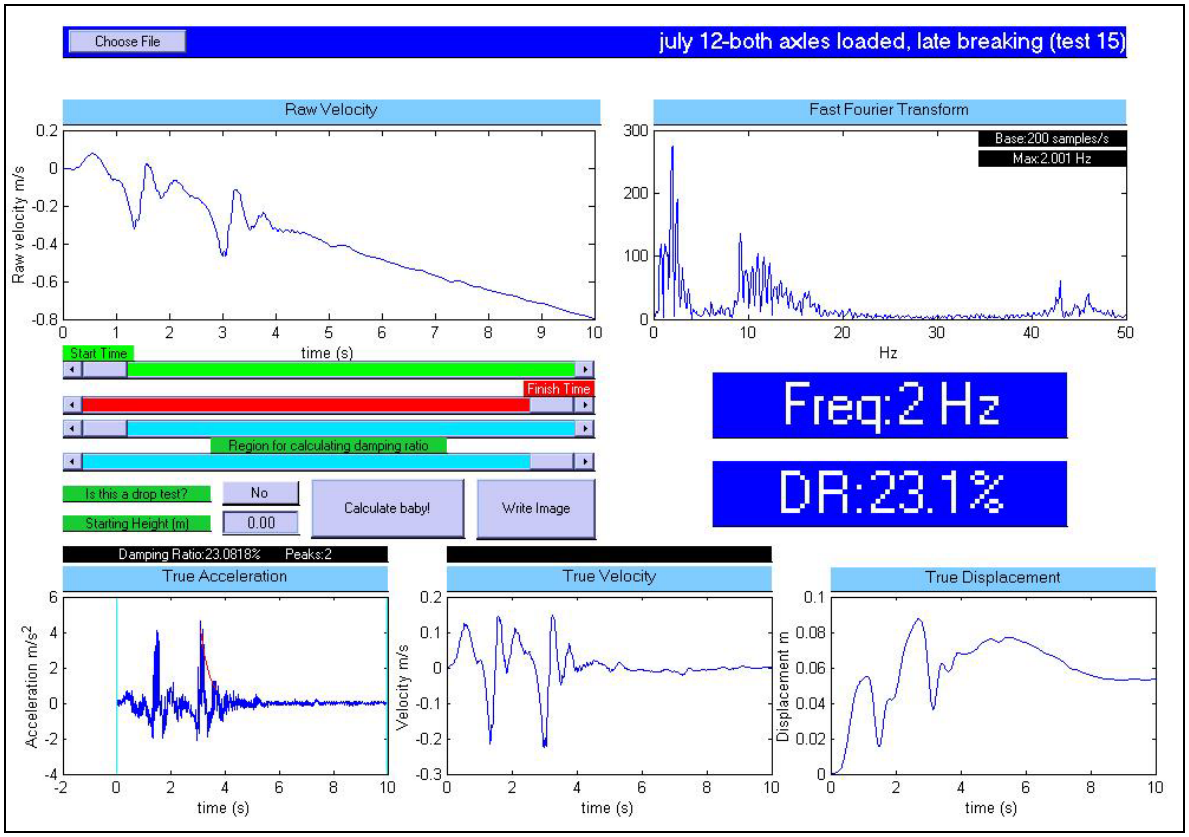

Testing session 1

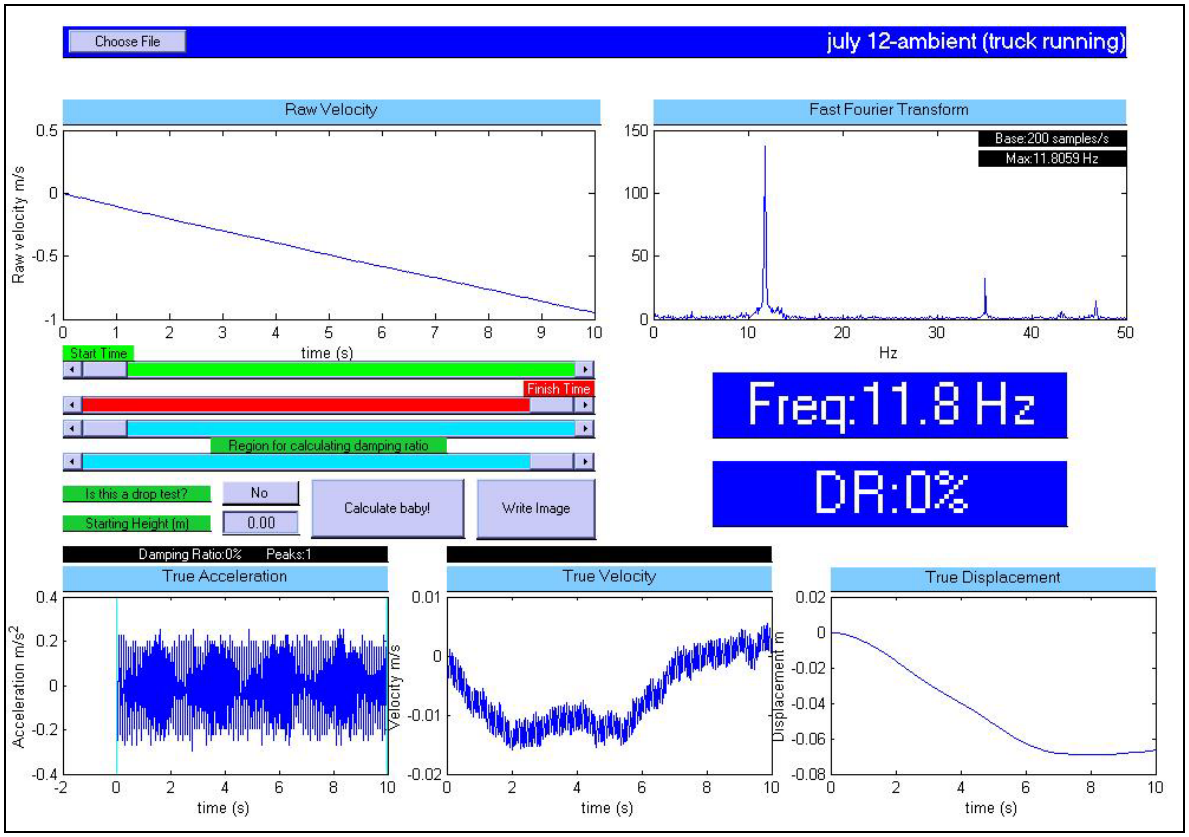

Testing session 1

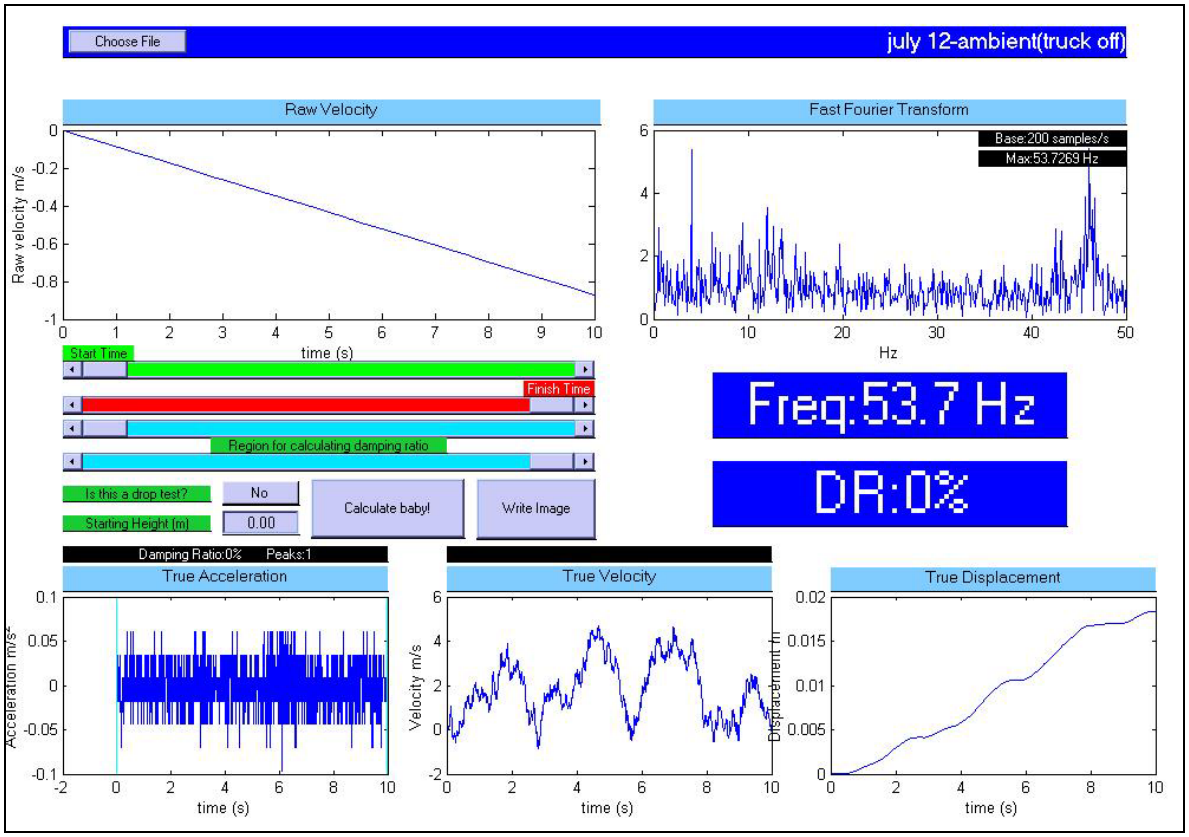

Testing session 1

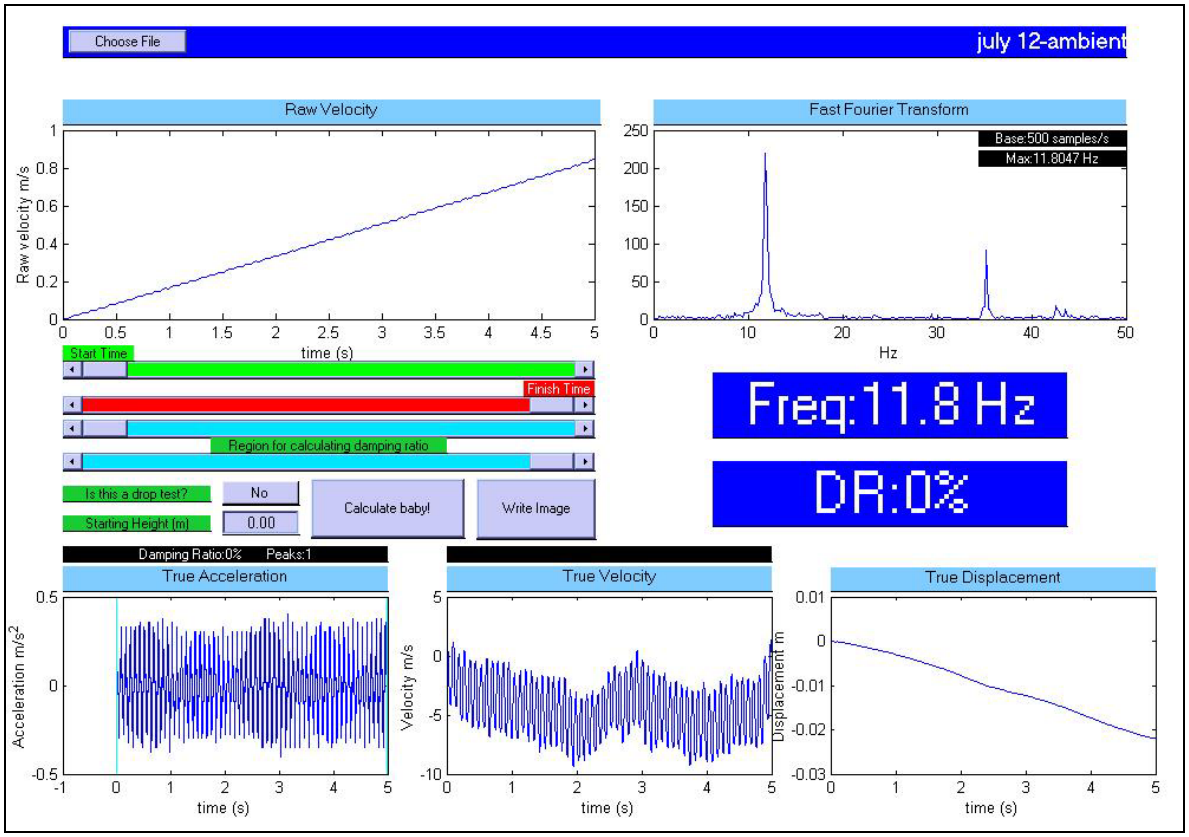

Testing of the non-rigid attachment device with an impulse input

Attachment device testing

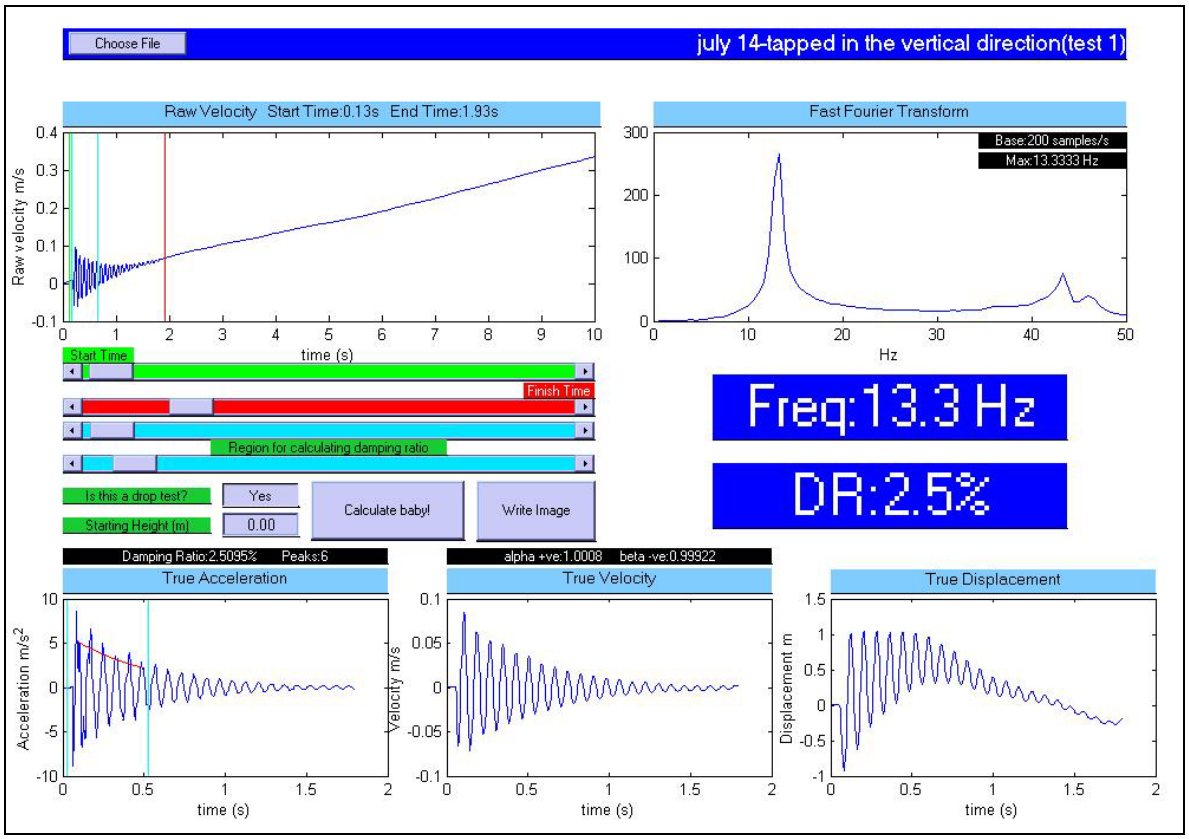

Attachment device testing

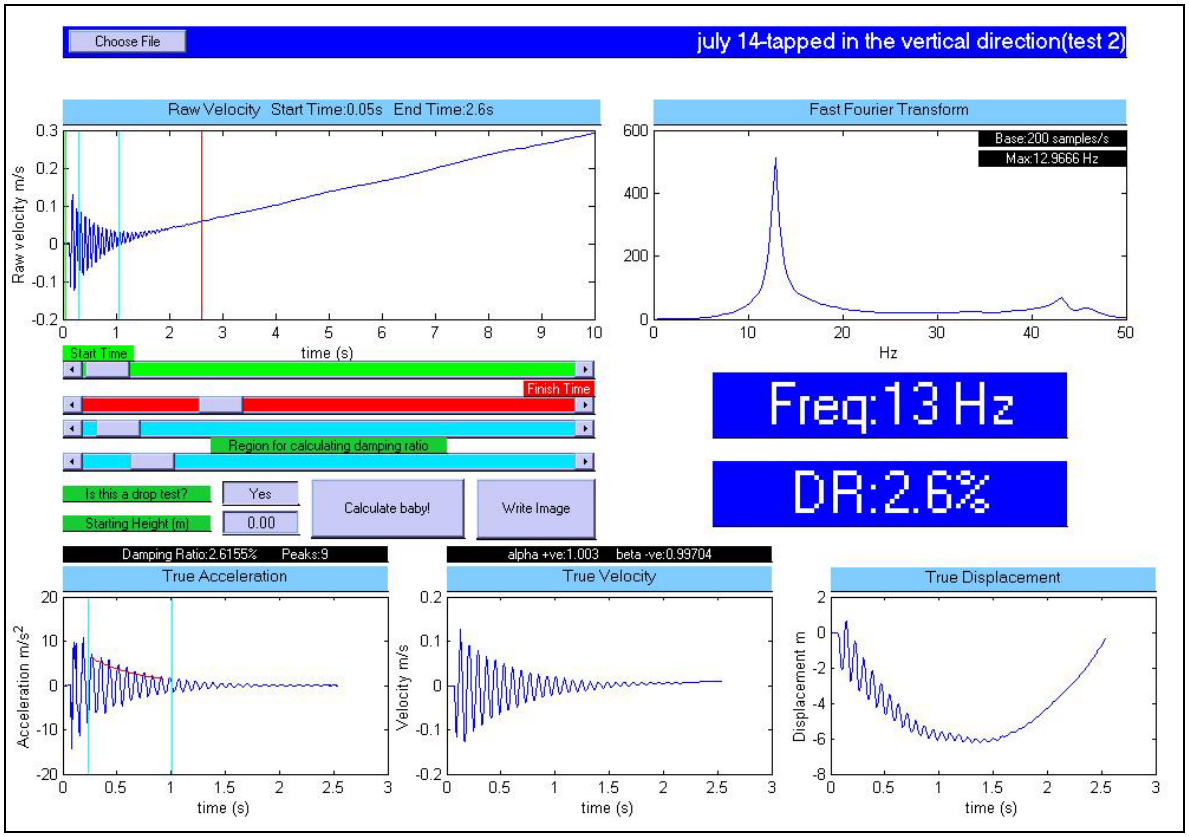

Attachment device testing

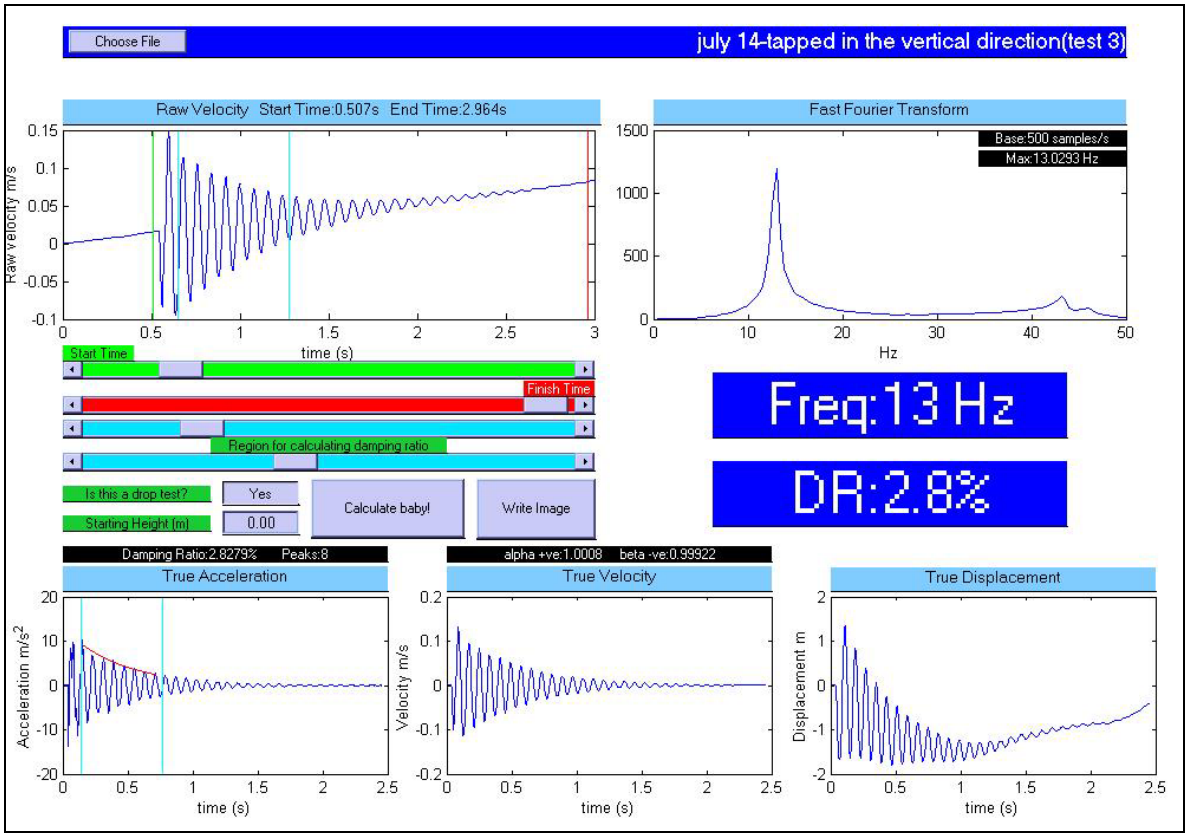

Attachment device testing

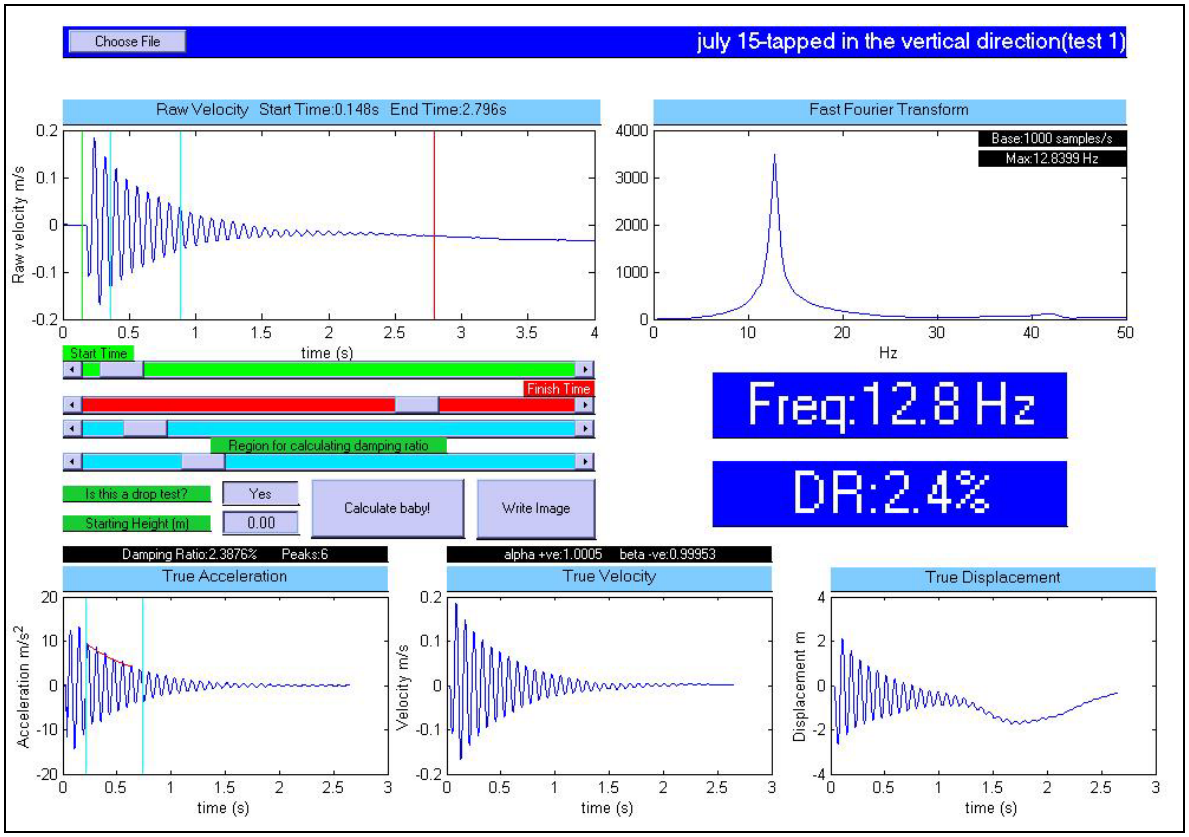

Attachment device testing

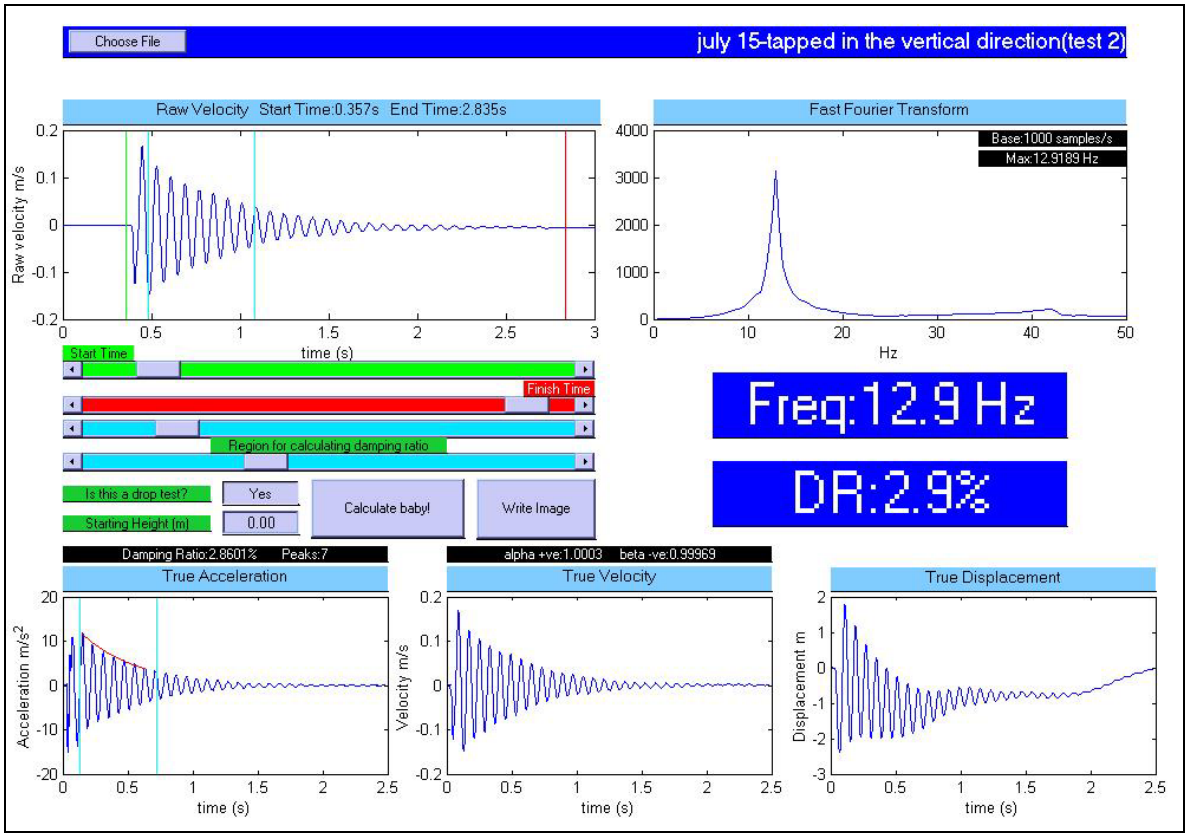

Testing session 2

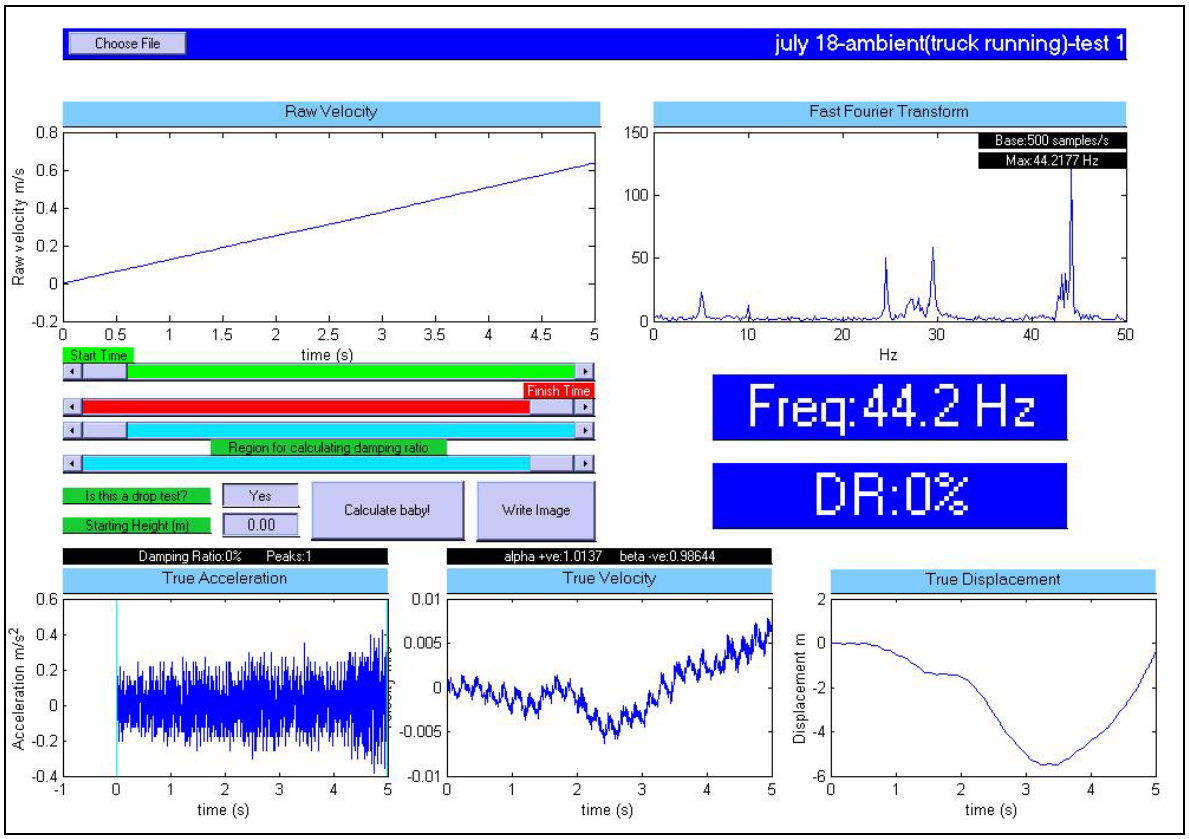

Testing session 2

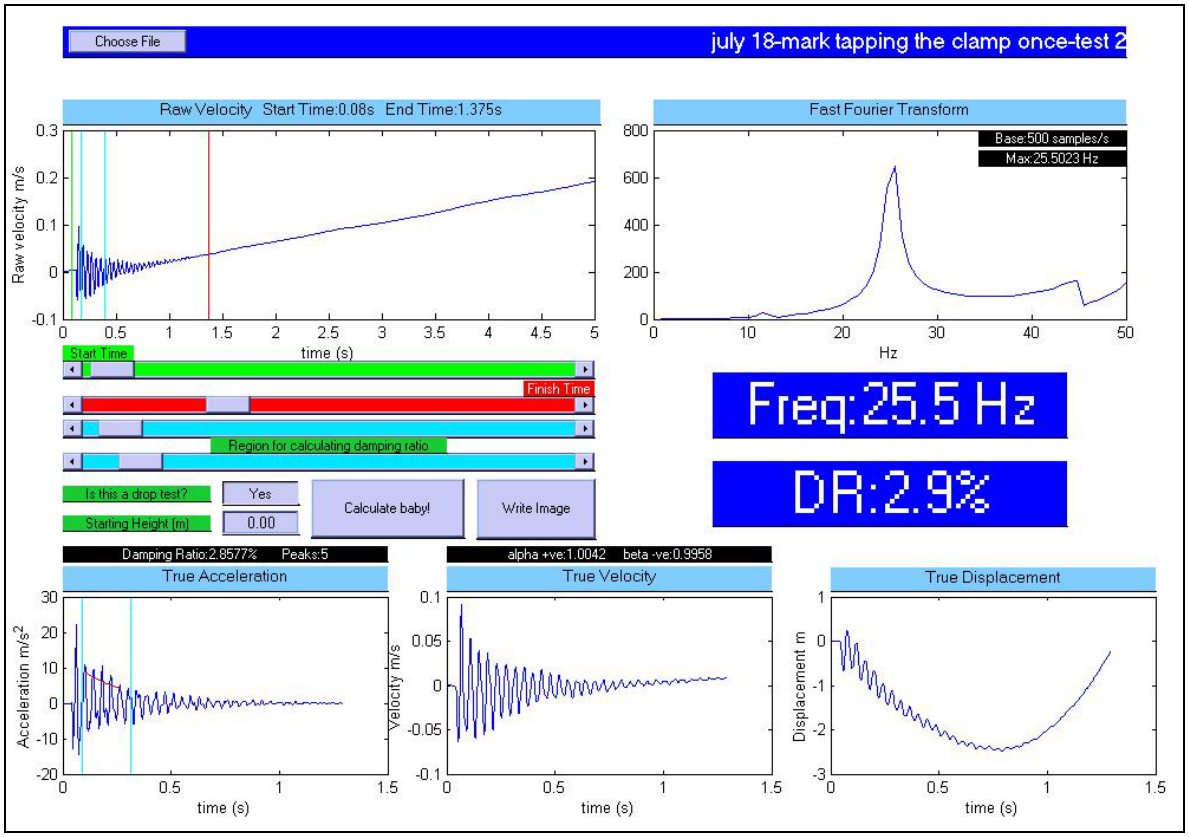

Testing session 2

Testing session 2

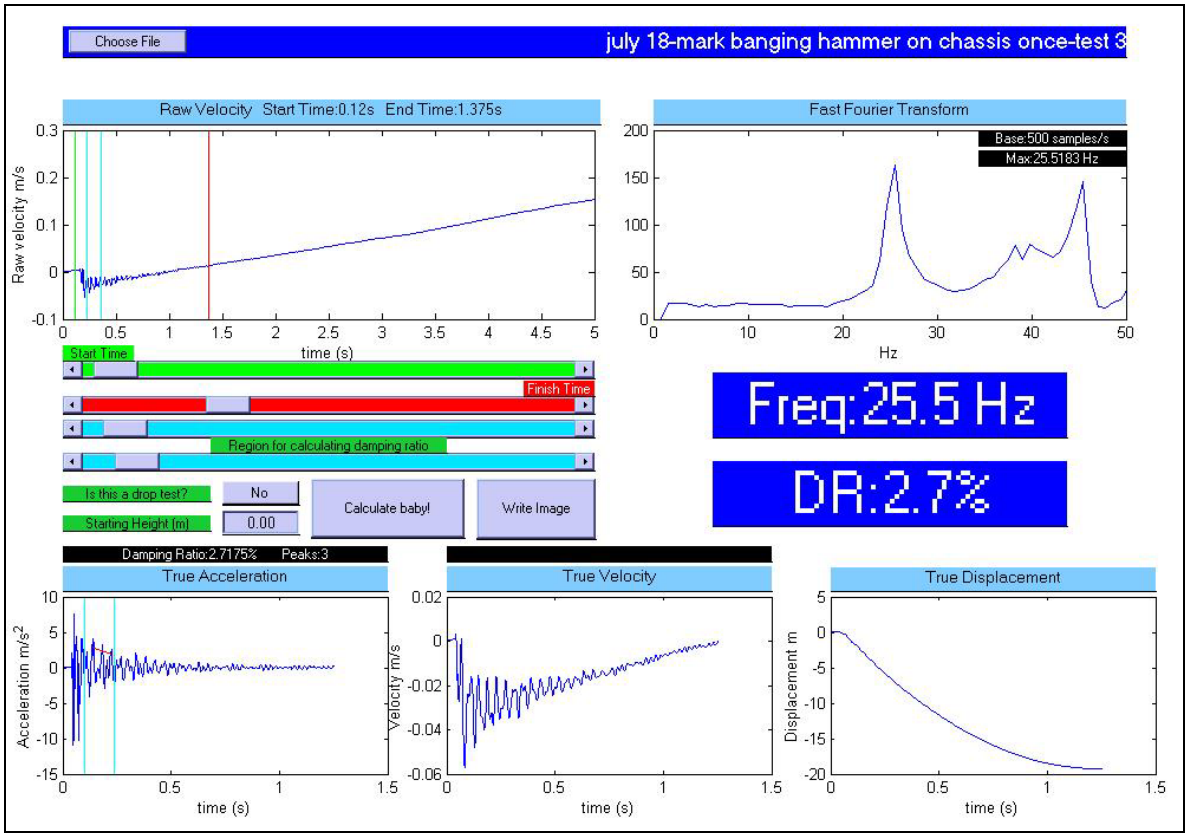

Testing session 2

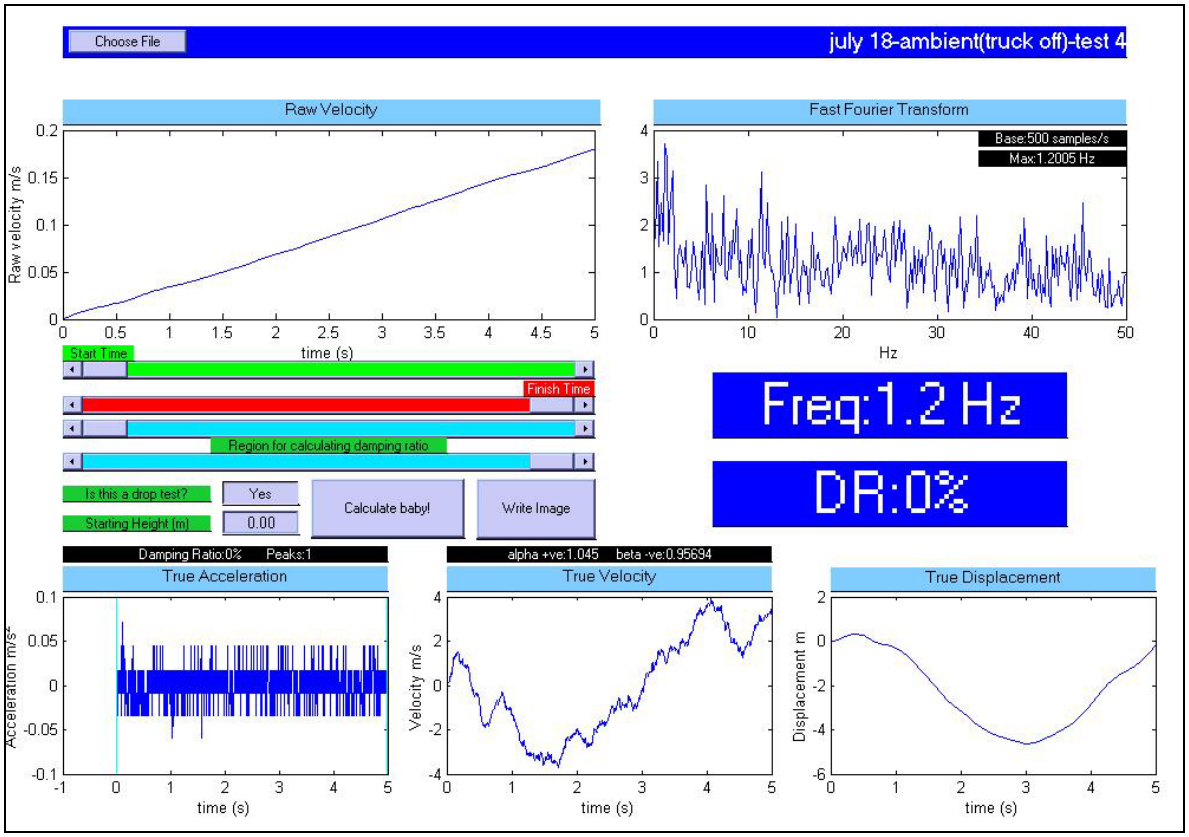

Testing session 2

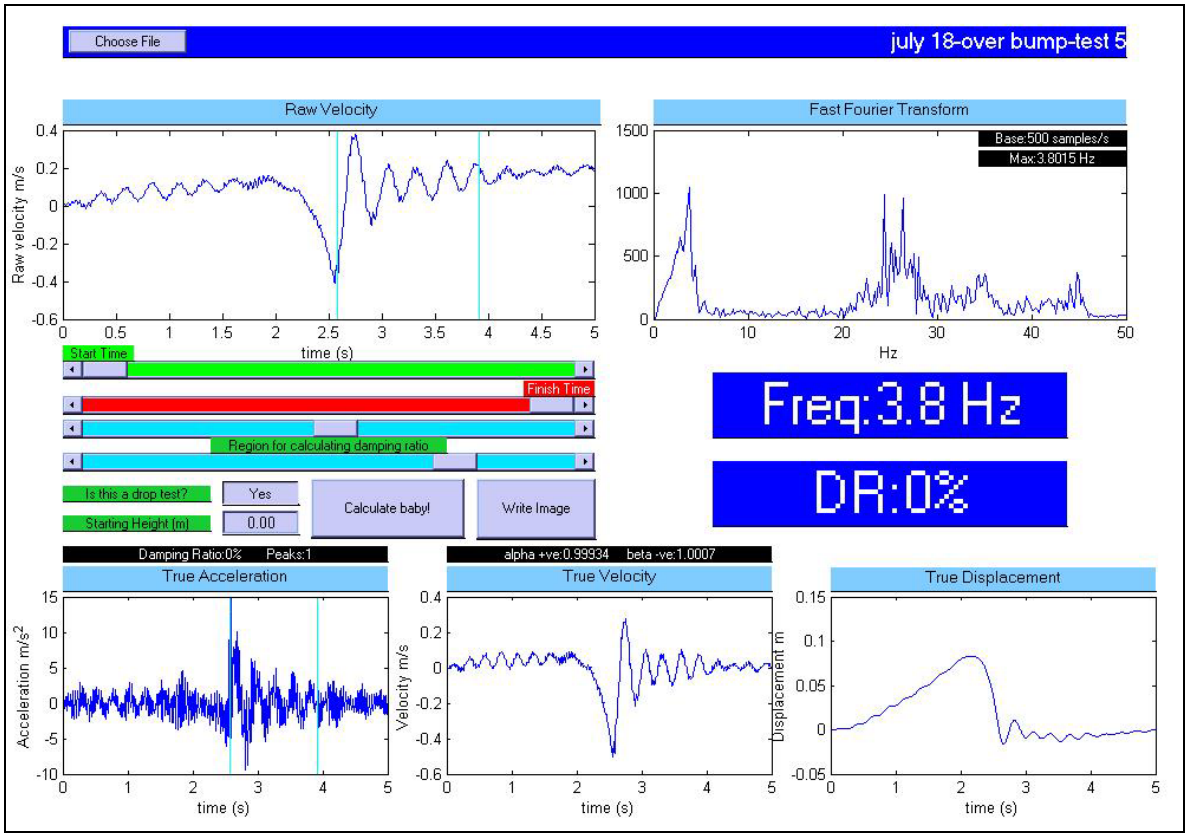

Testing session 2

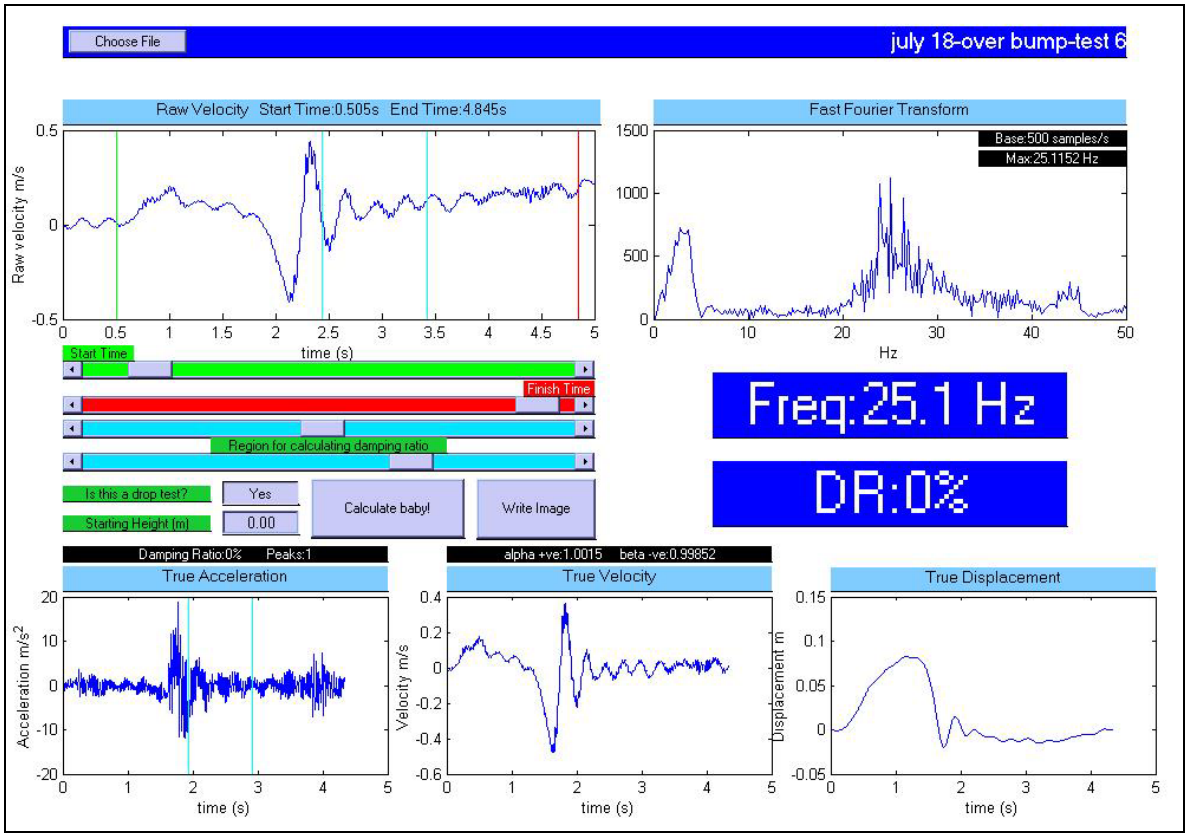

Testing session 2

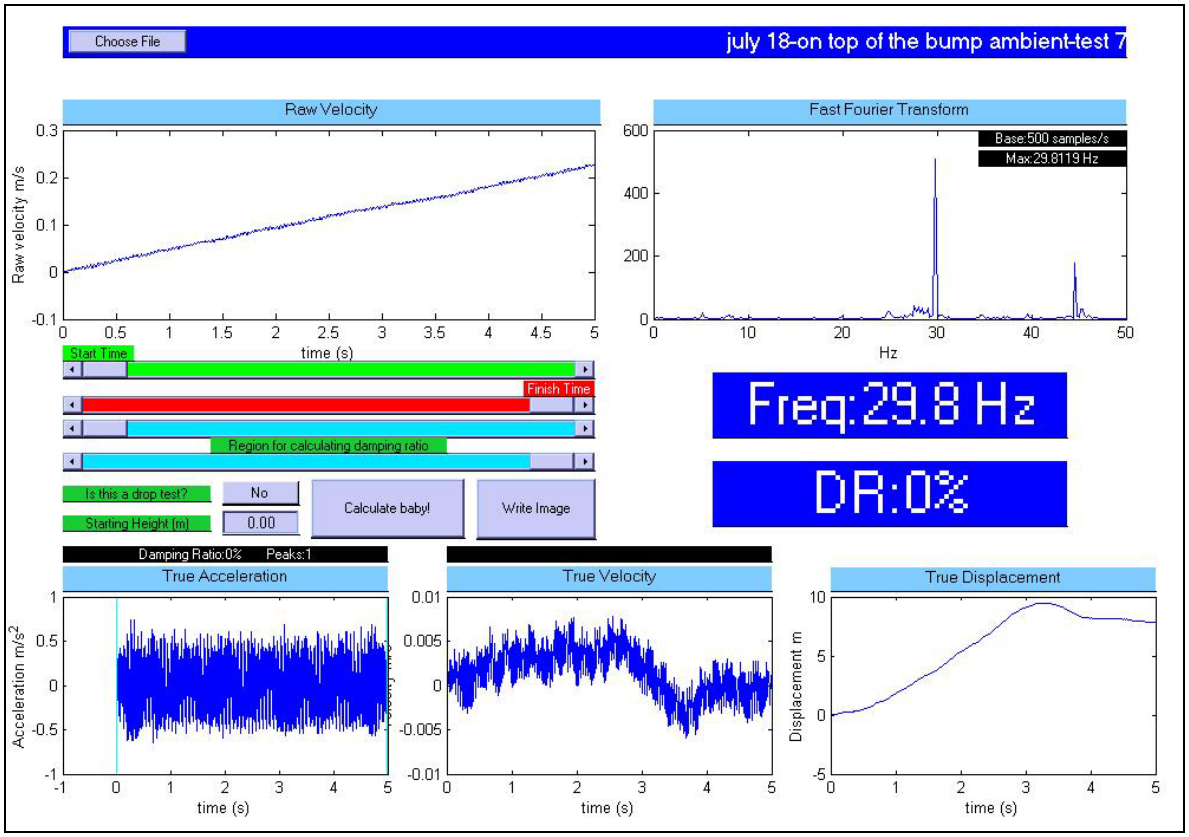

Testing session 2

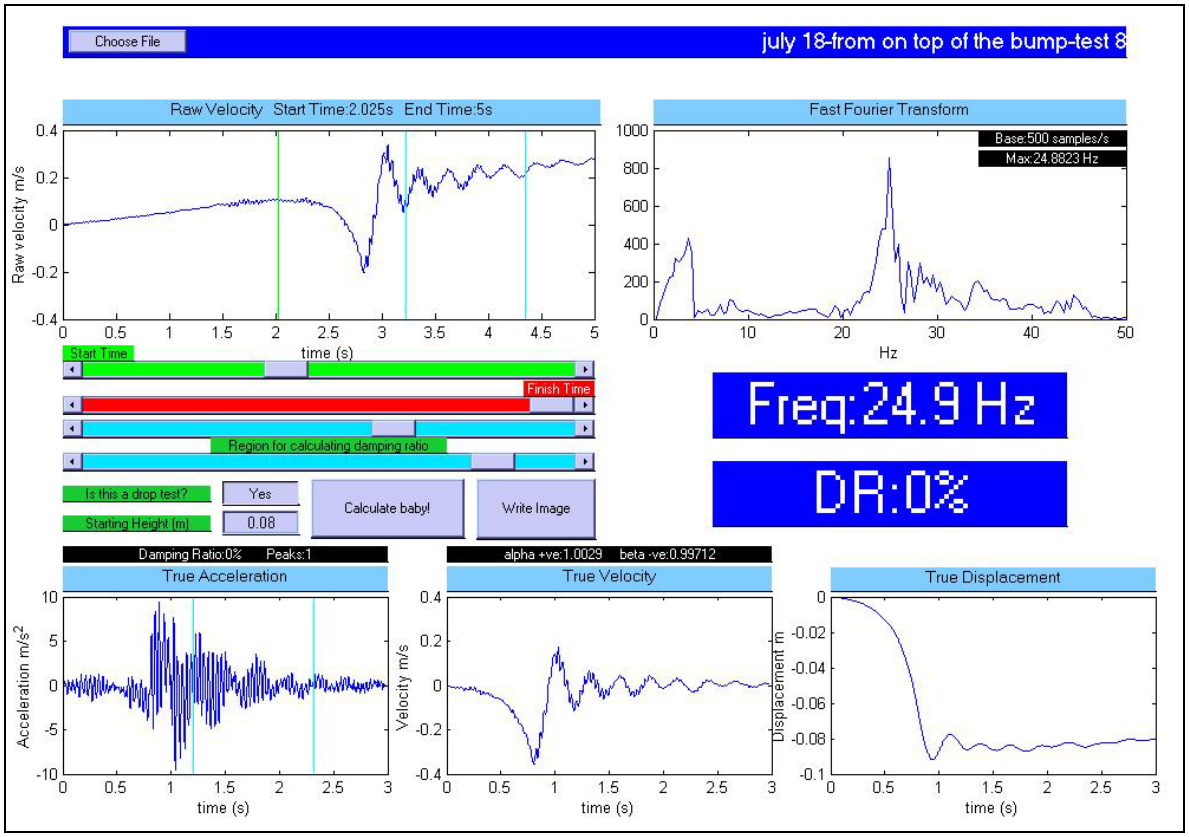

Testing session 2

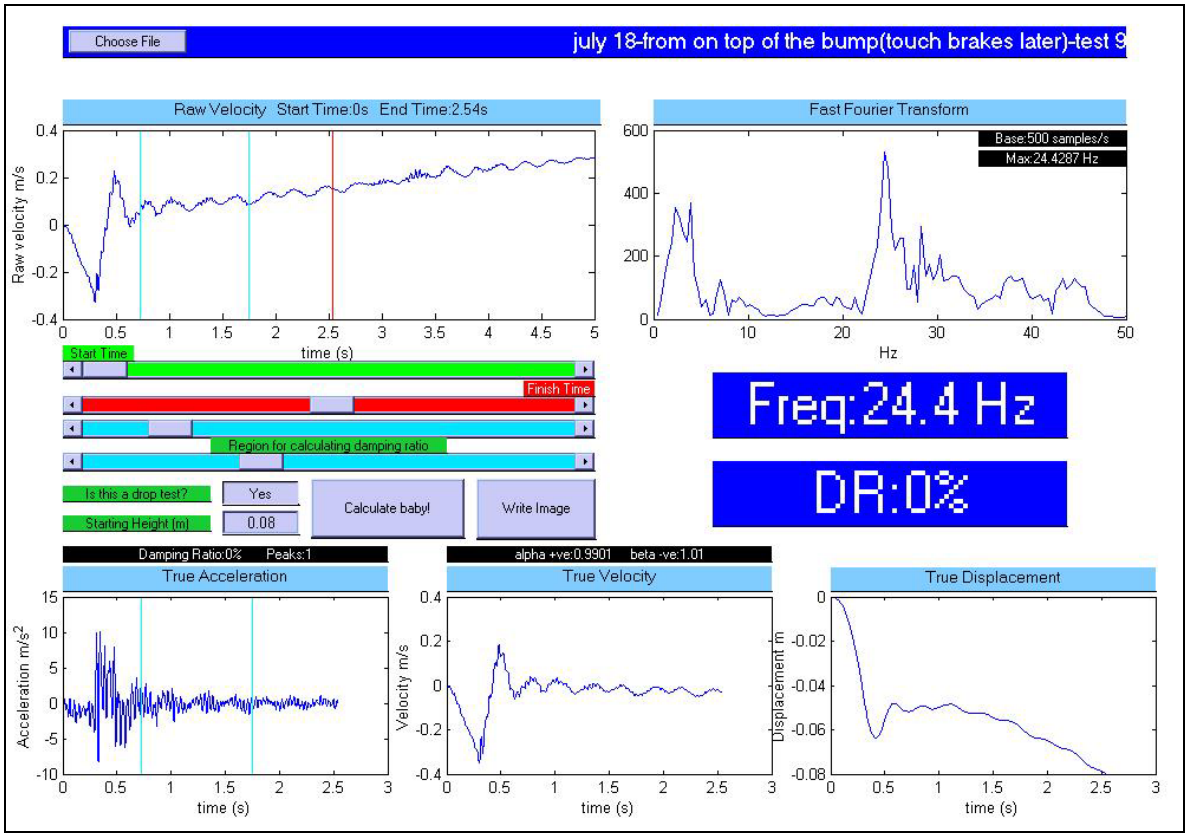

Testing session 2

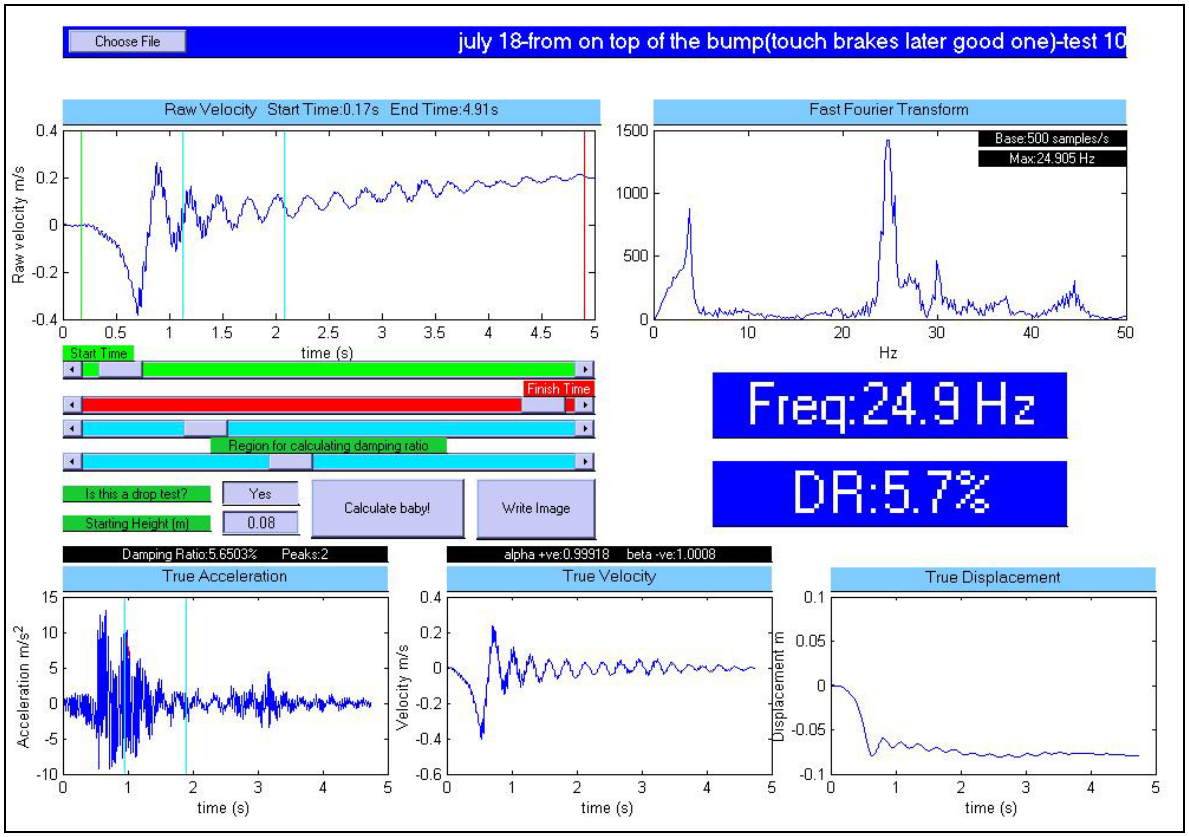

Testing session 2

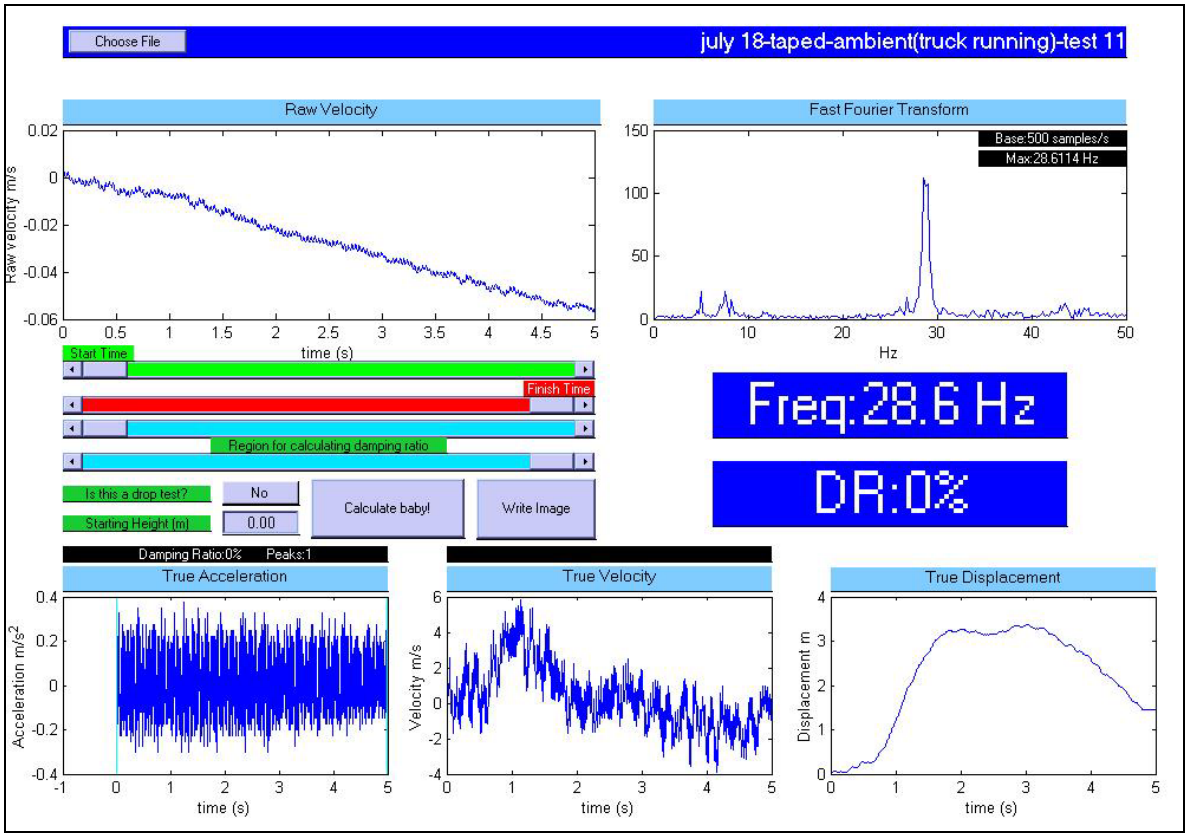

Testing session 2

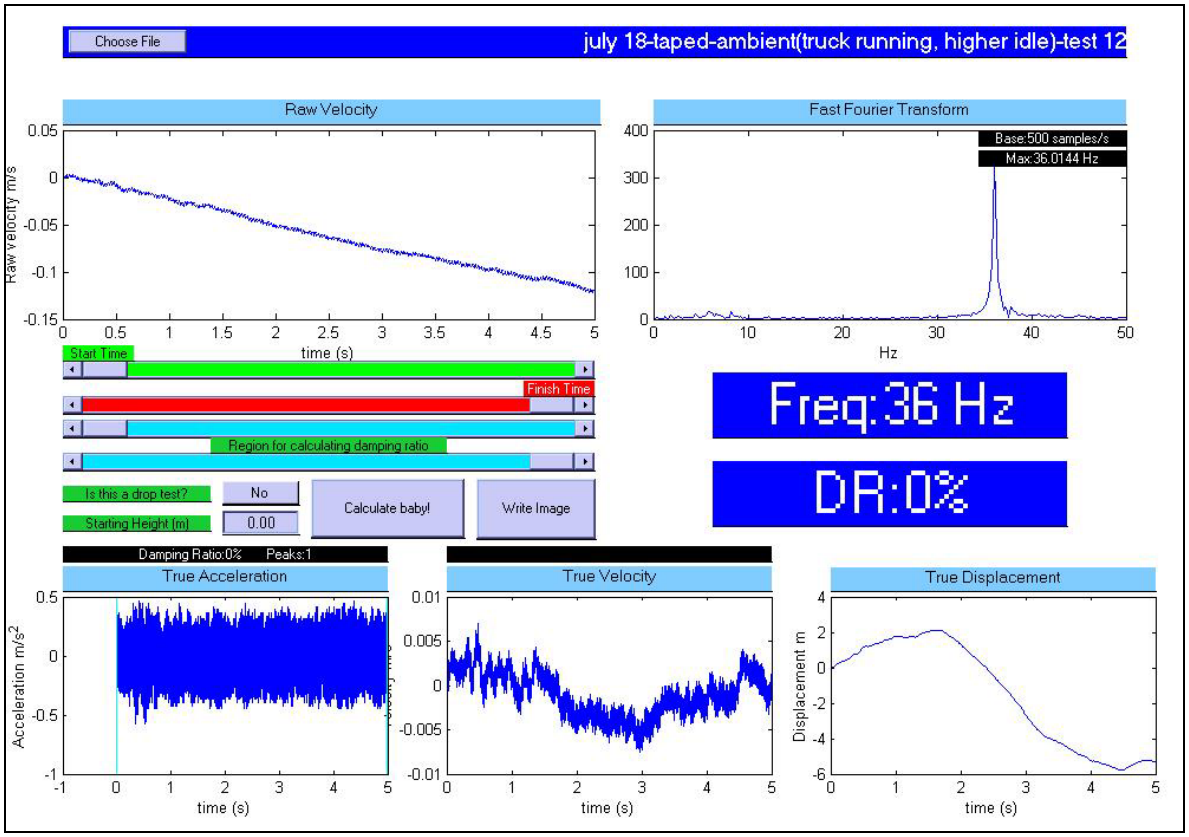

Testing session 2

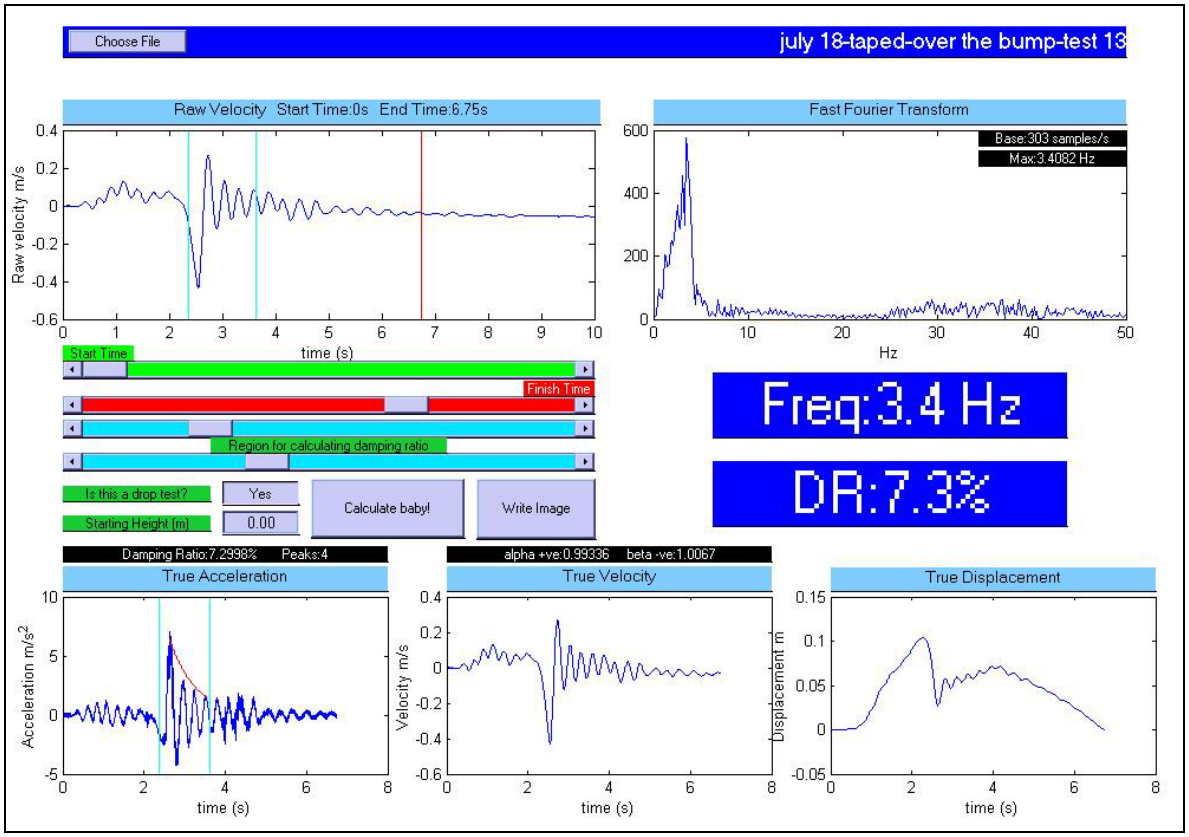

Testing session 2

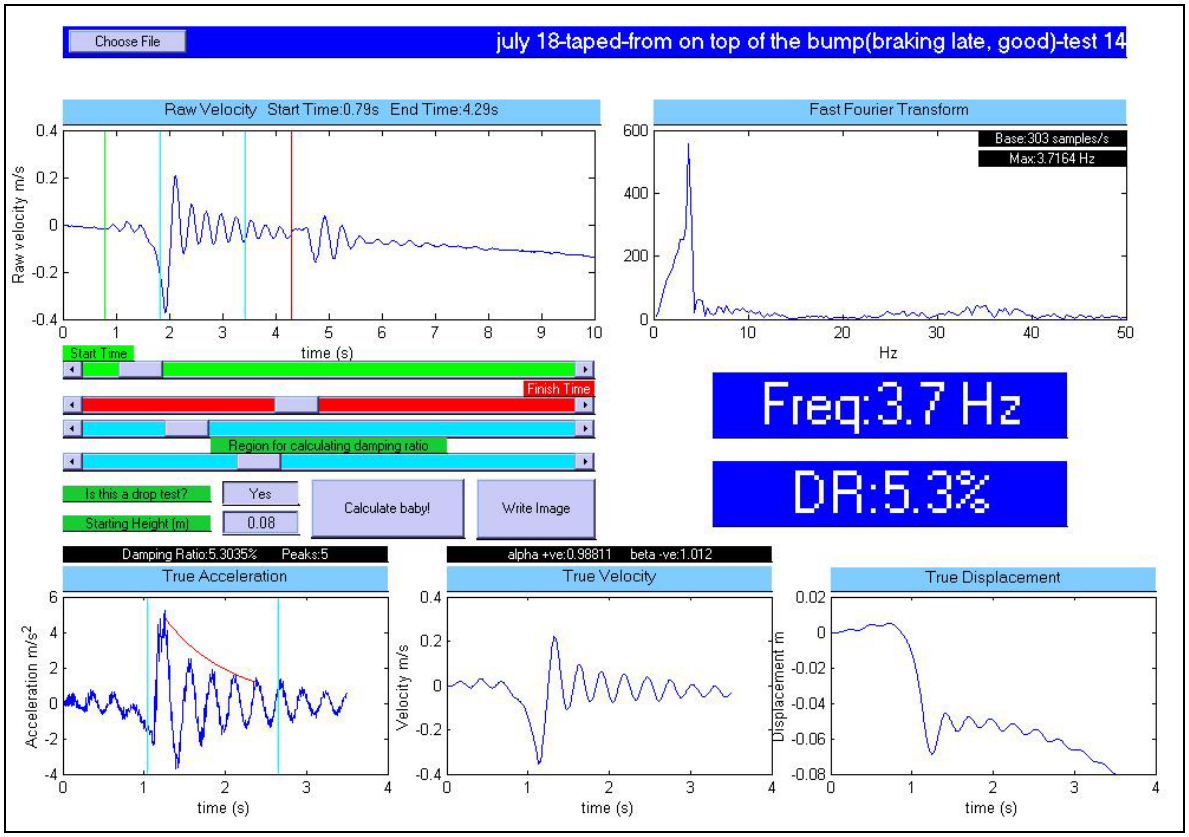

Testing session 2

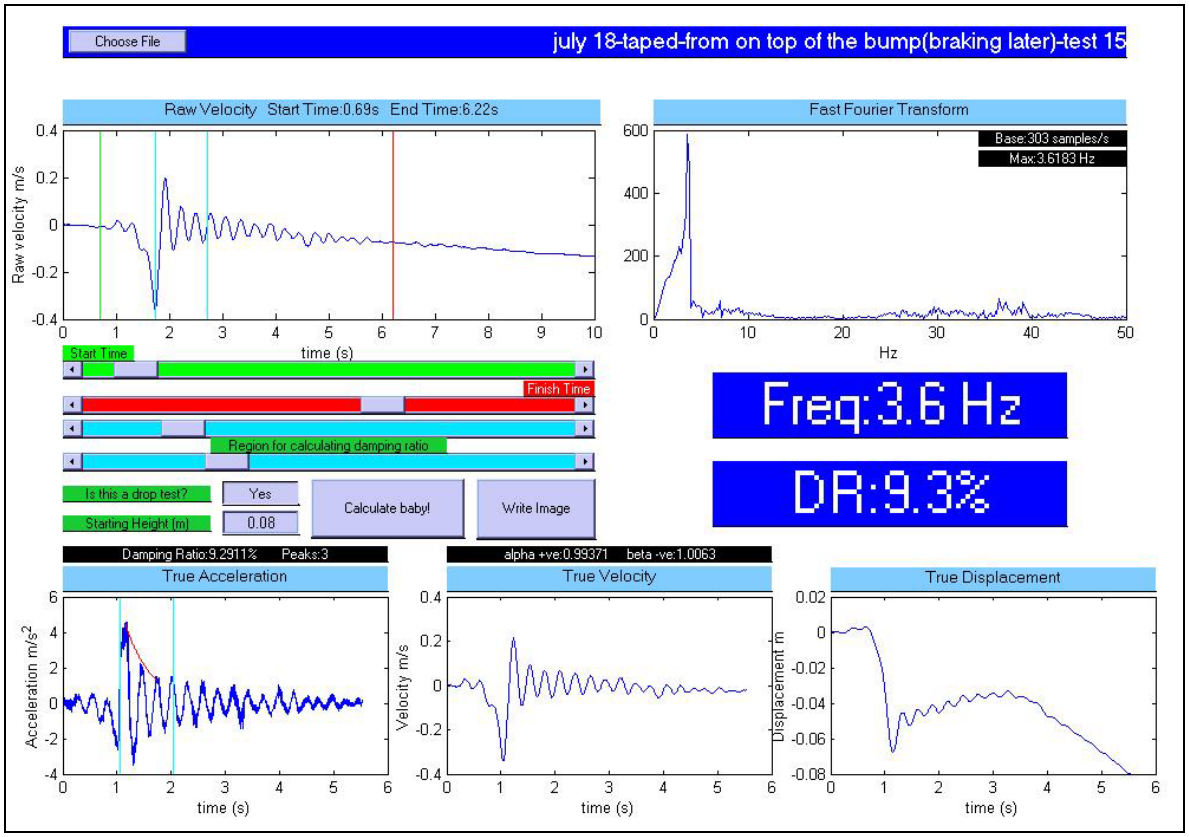

Testing session 2

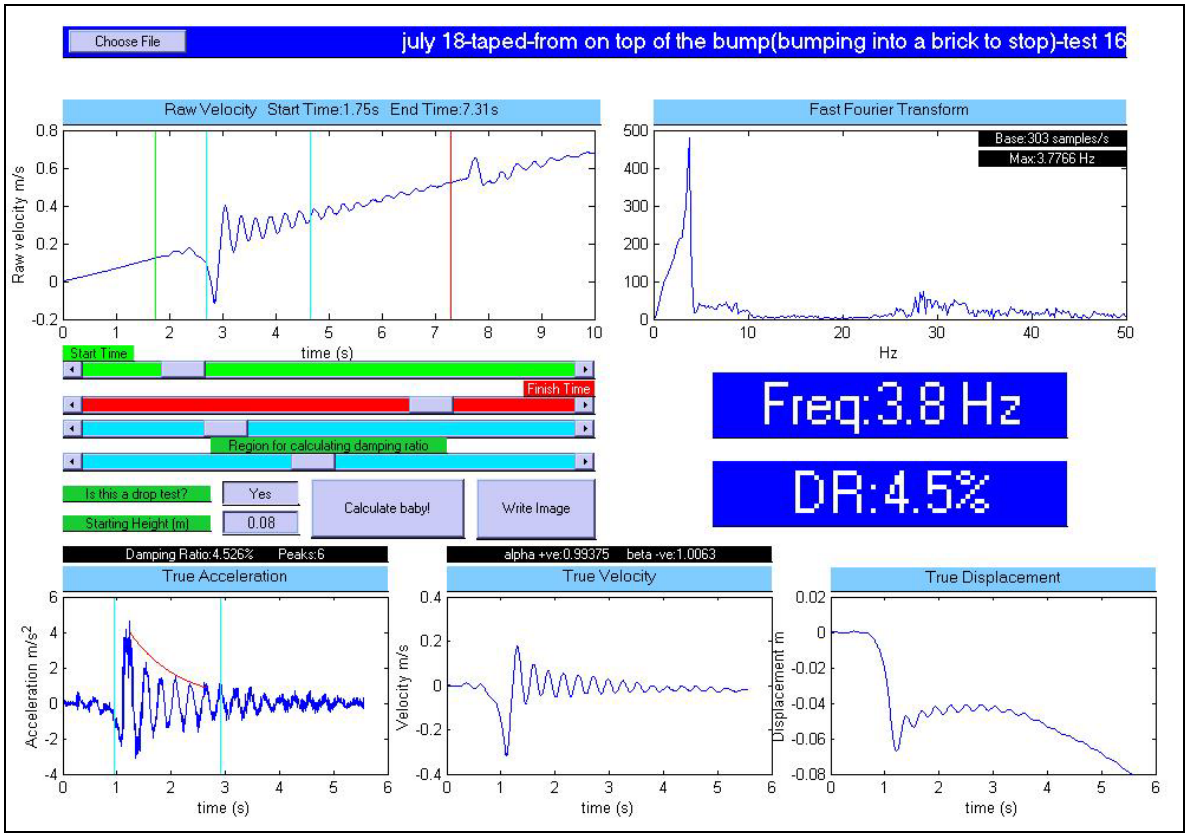

Testing session 3

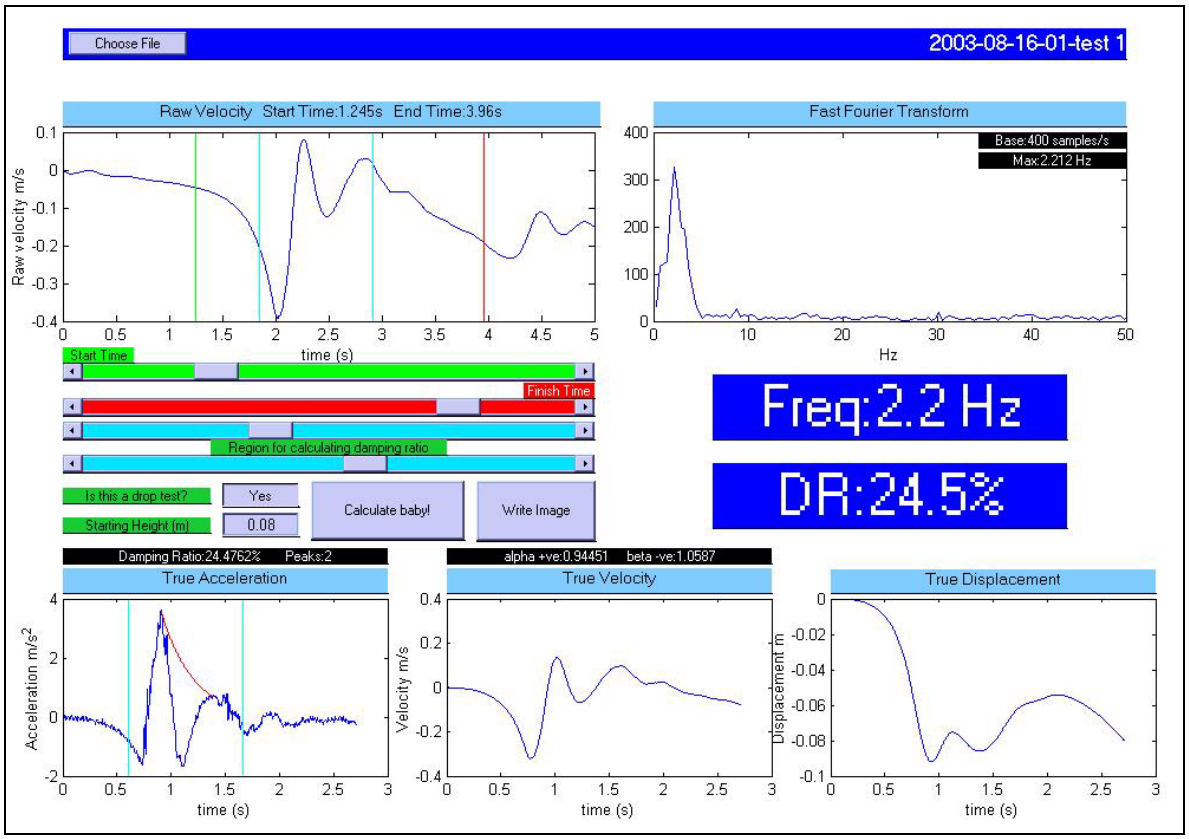

Testing session 3

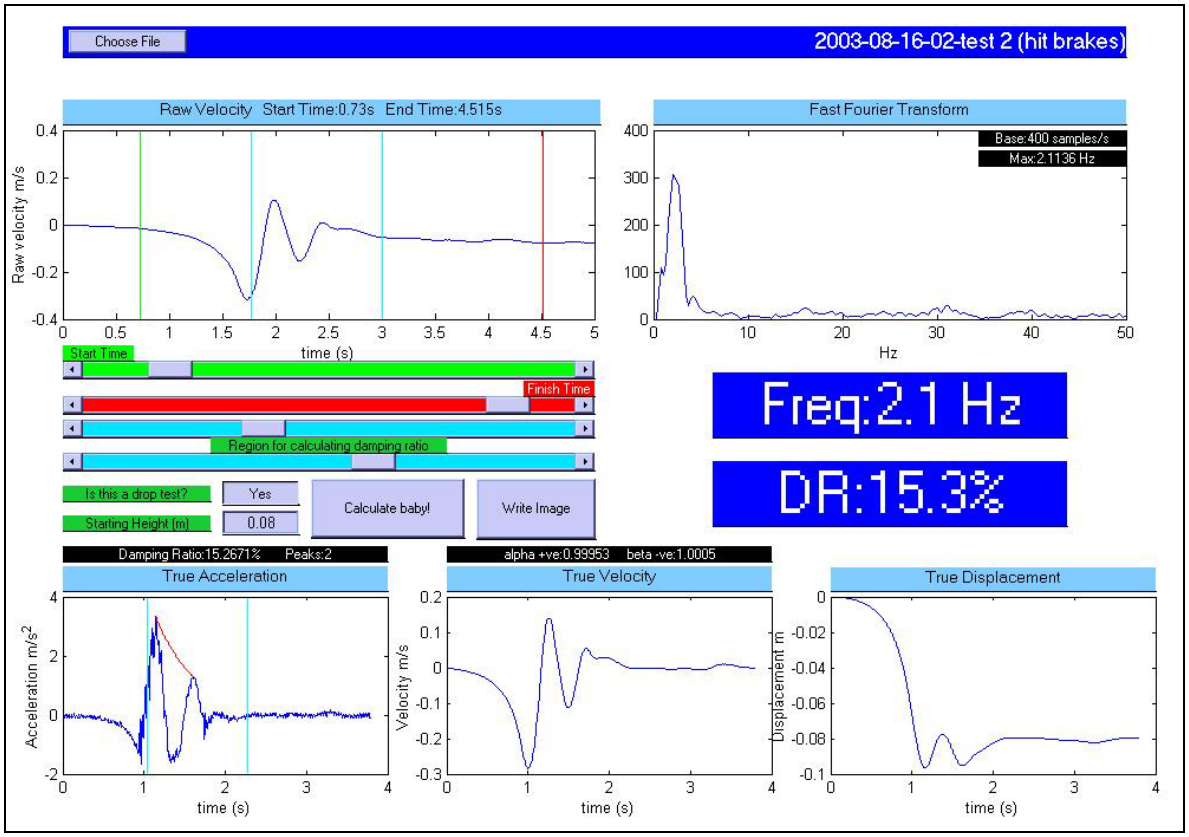

Testing session 3

Testing session 3

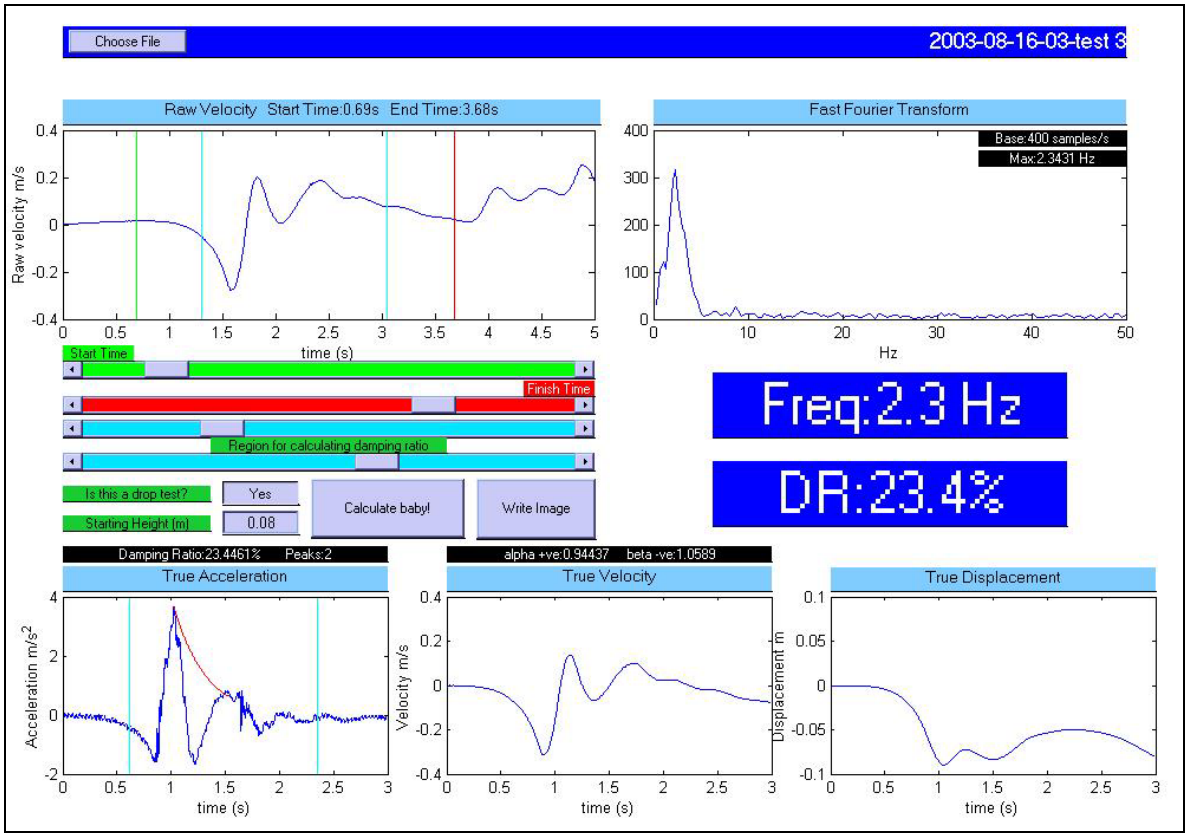

Testing session 3

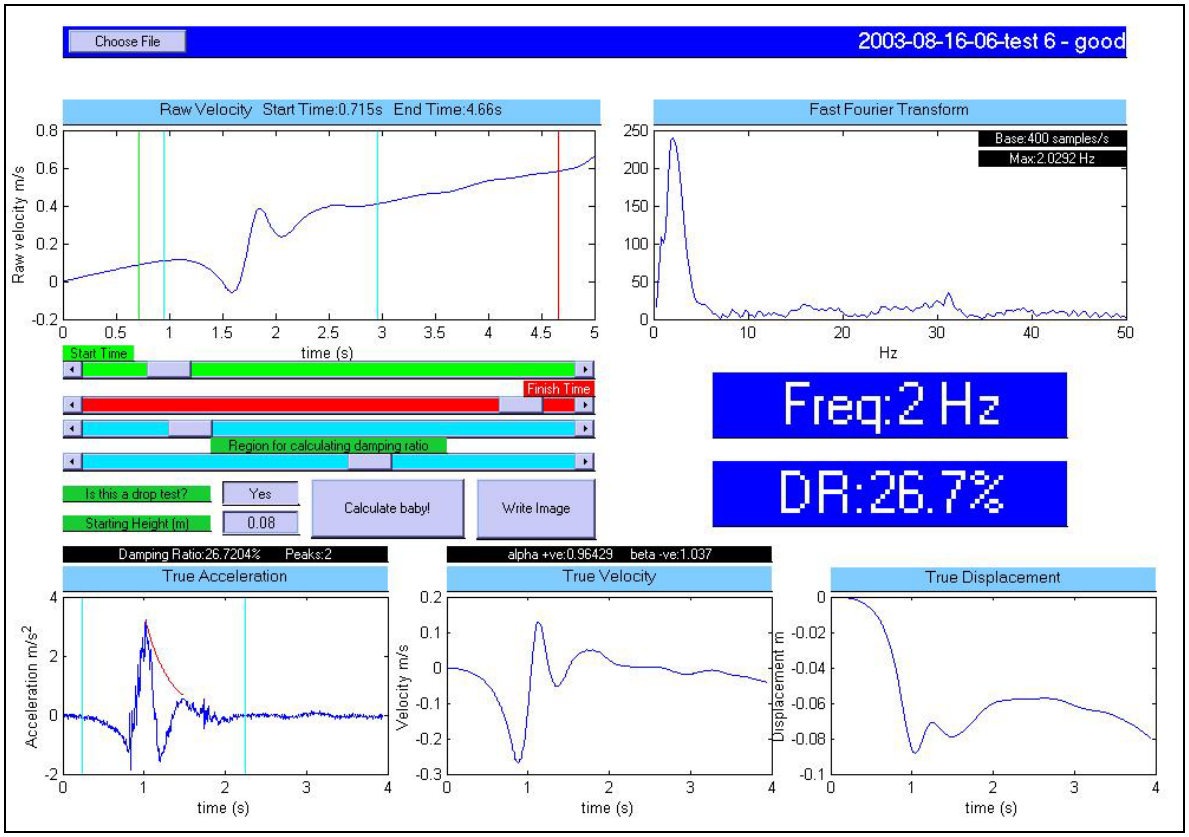

Testing session 3

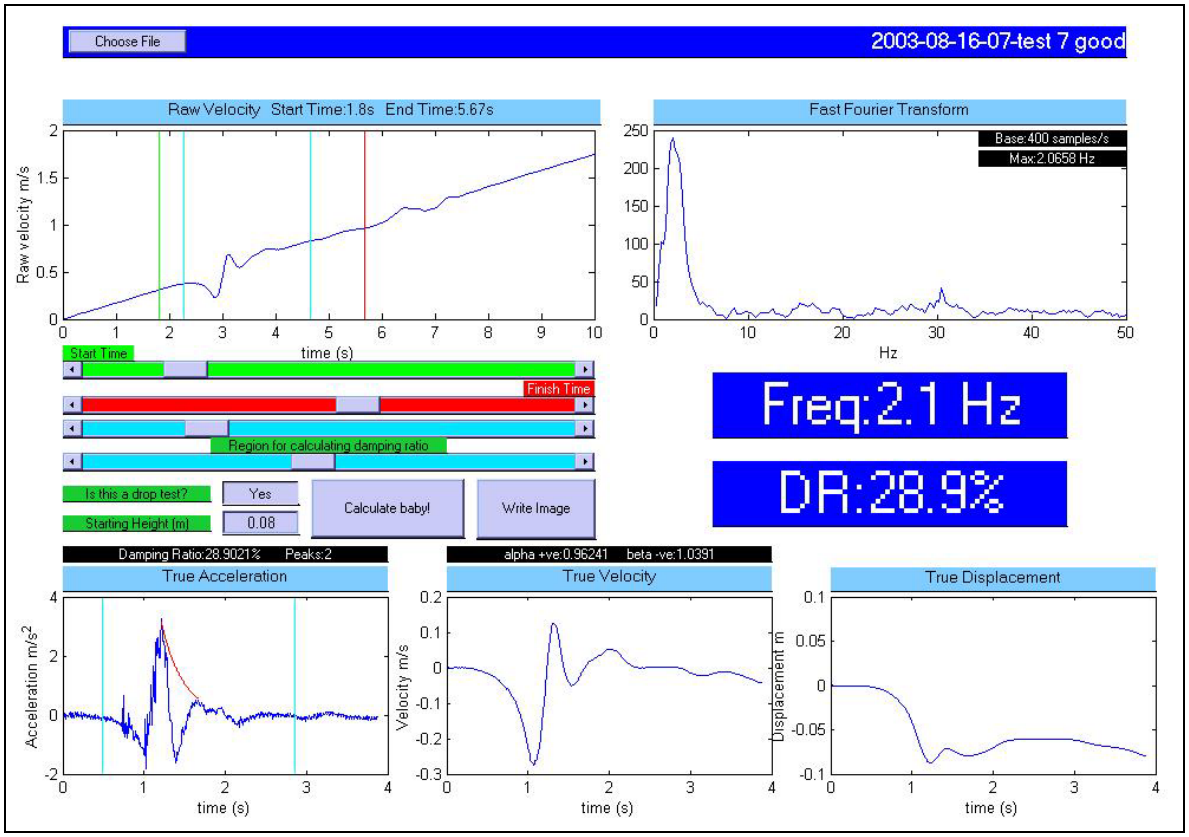

Testing session 3

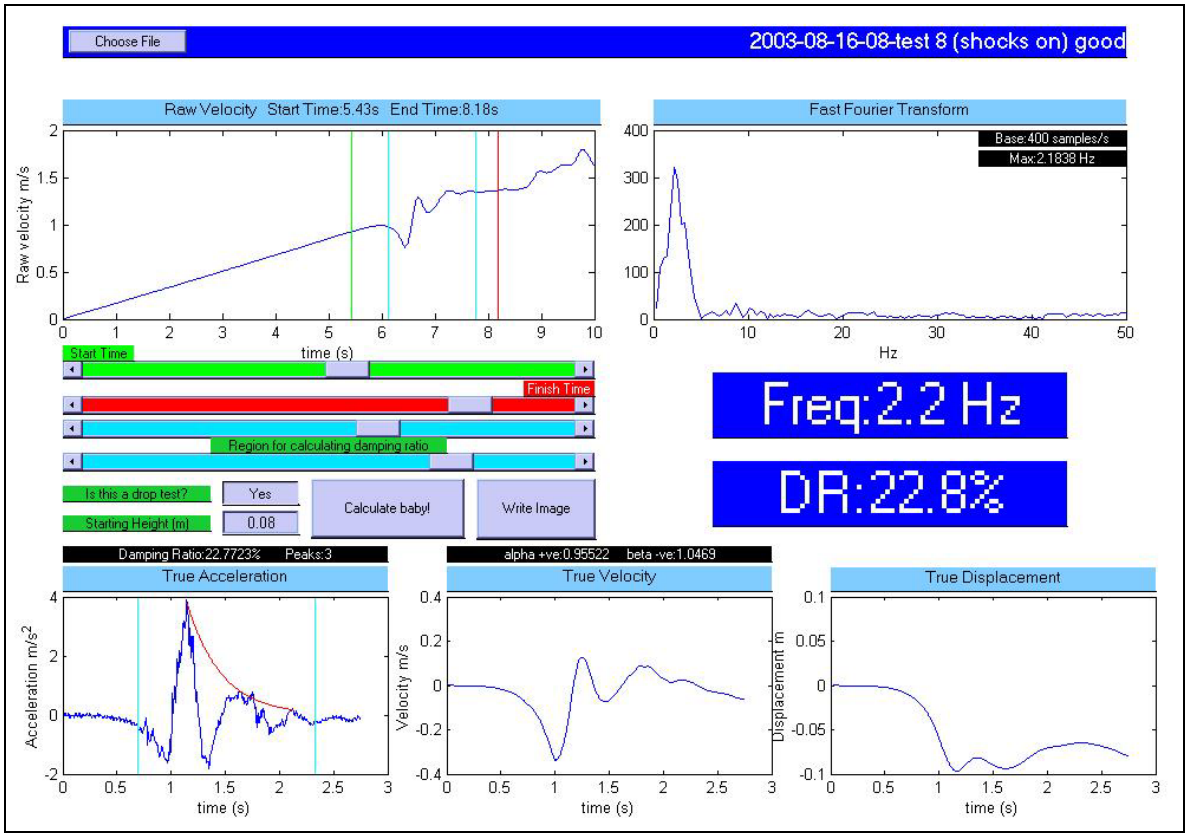

Testing session 3

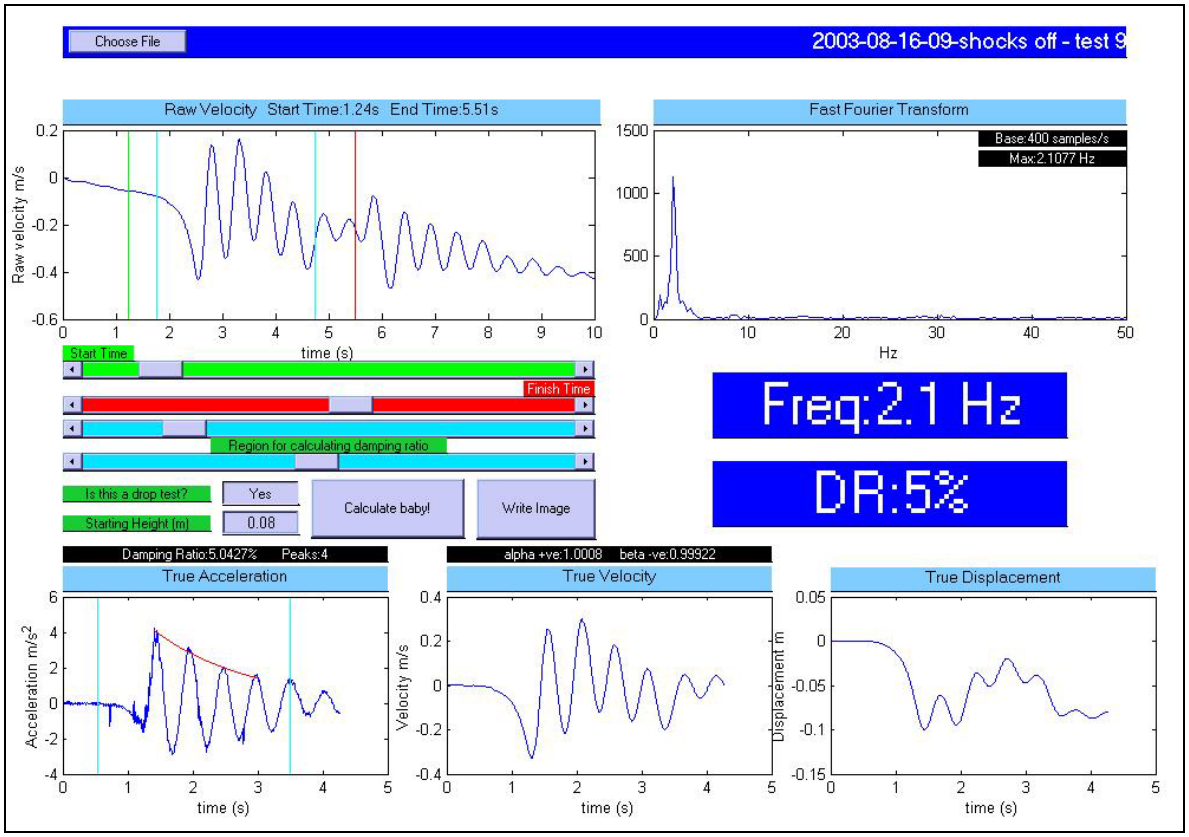

Testing session 3

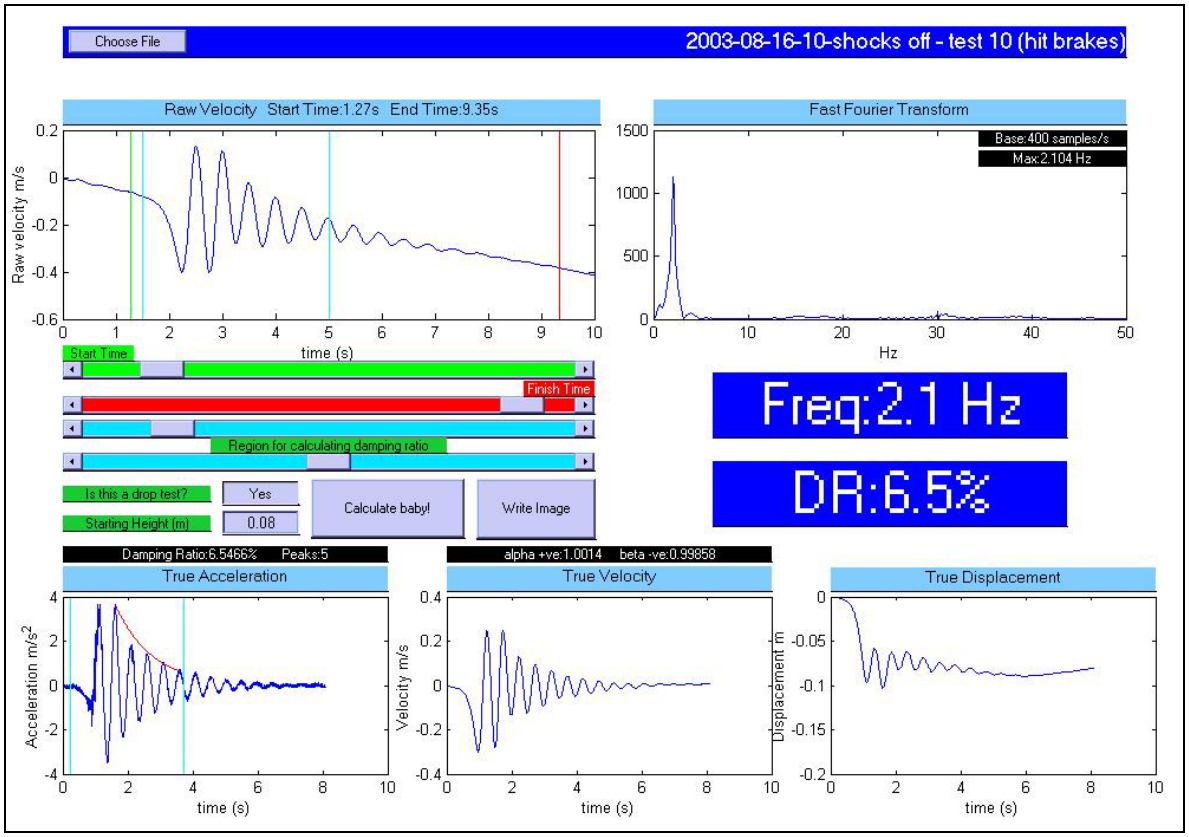

Testing session 3

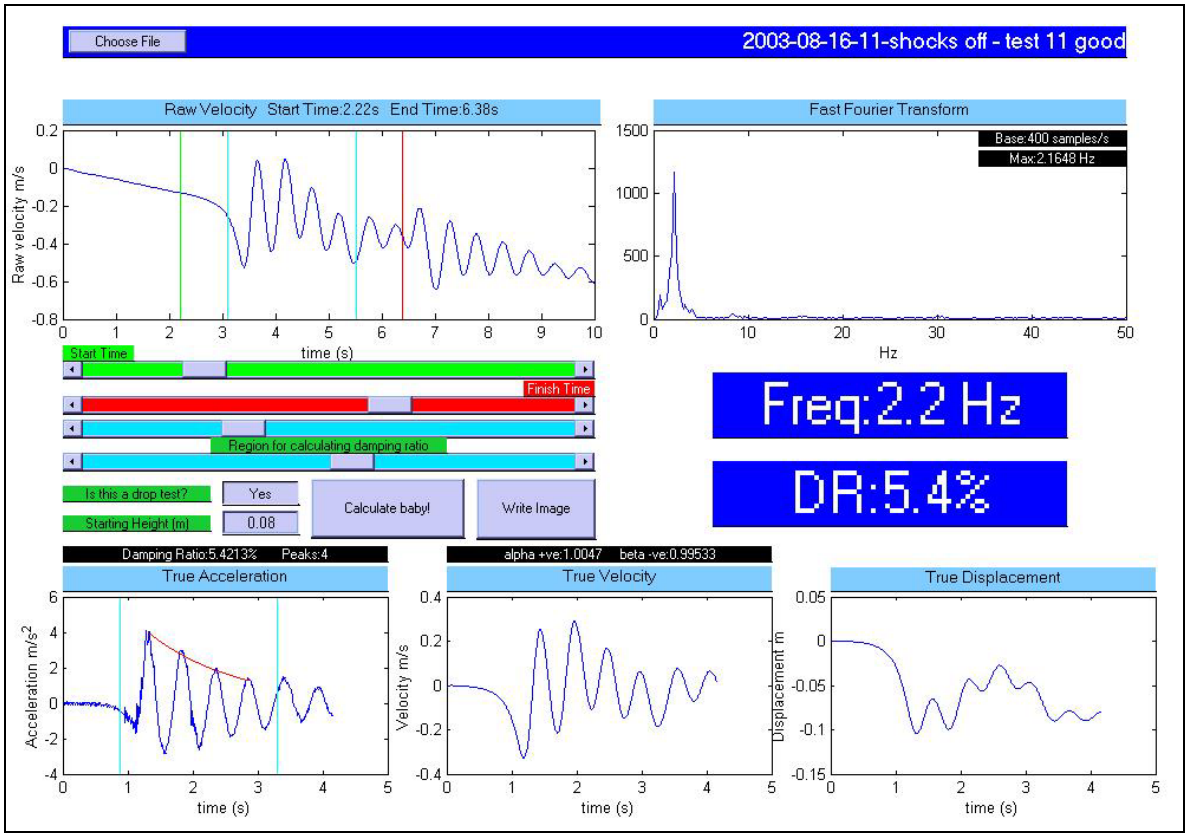

Testing session 3

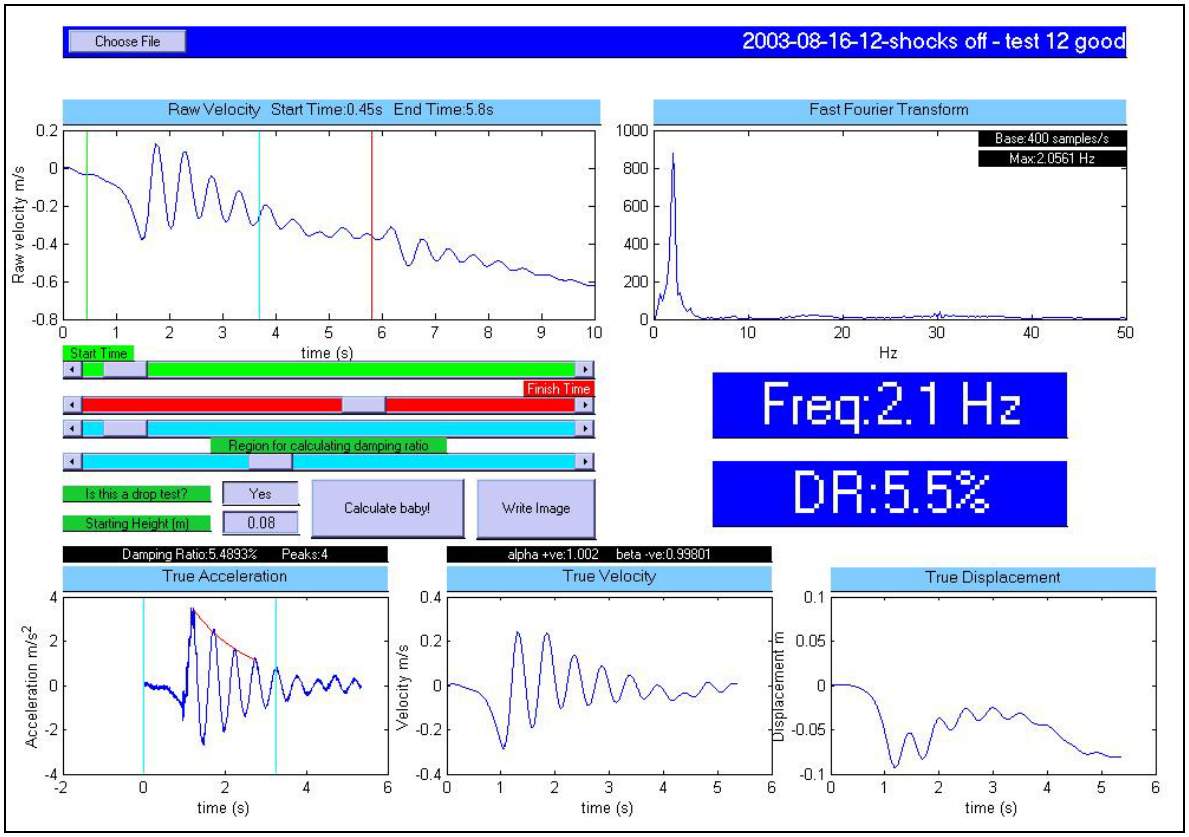

Testing session 3

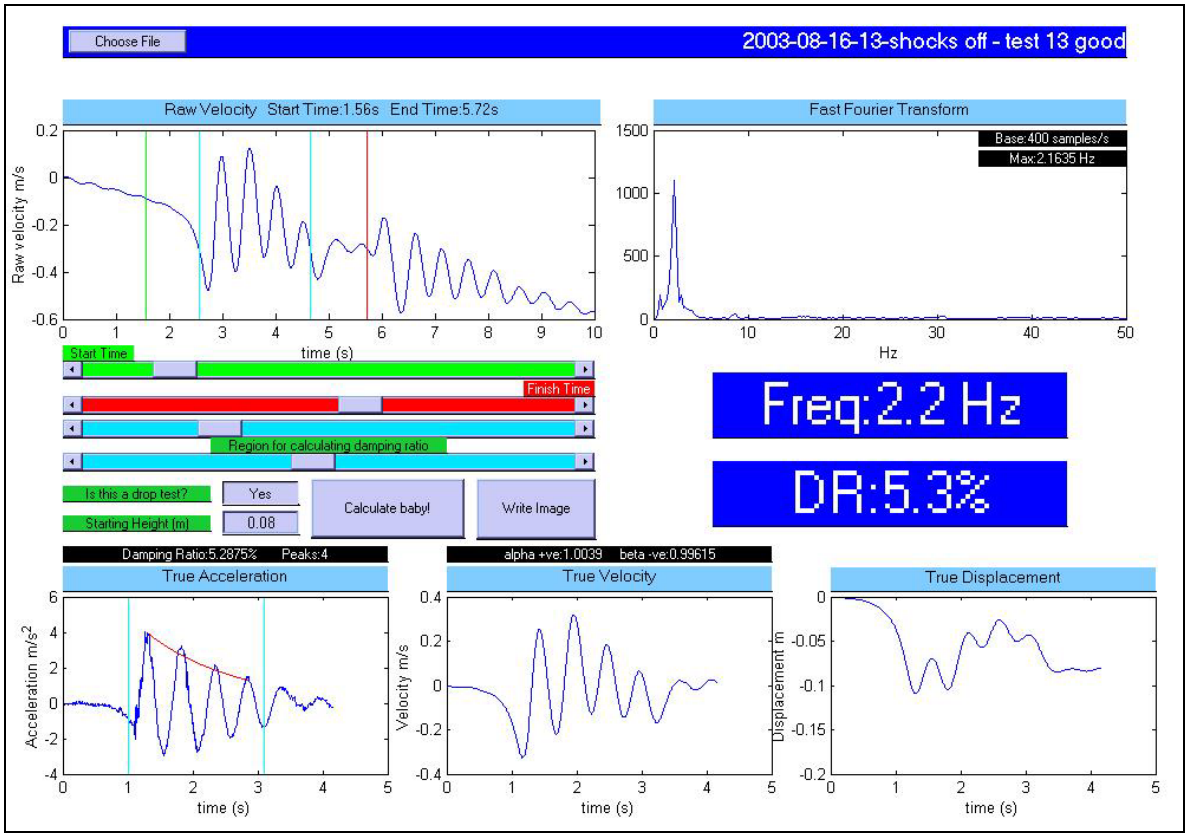

Testing session 3

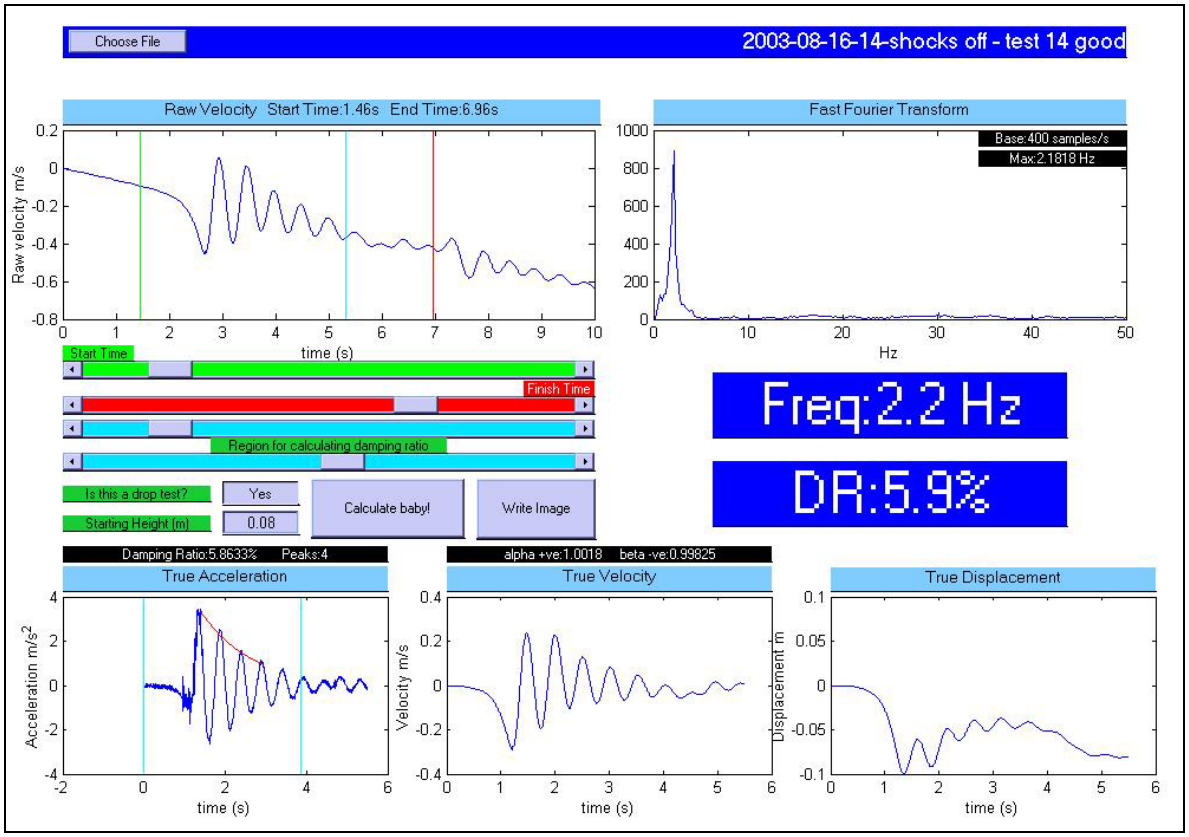

Testing session 3

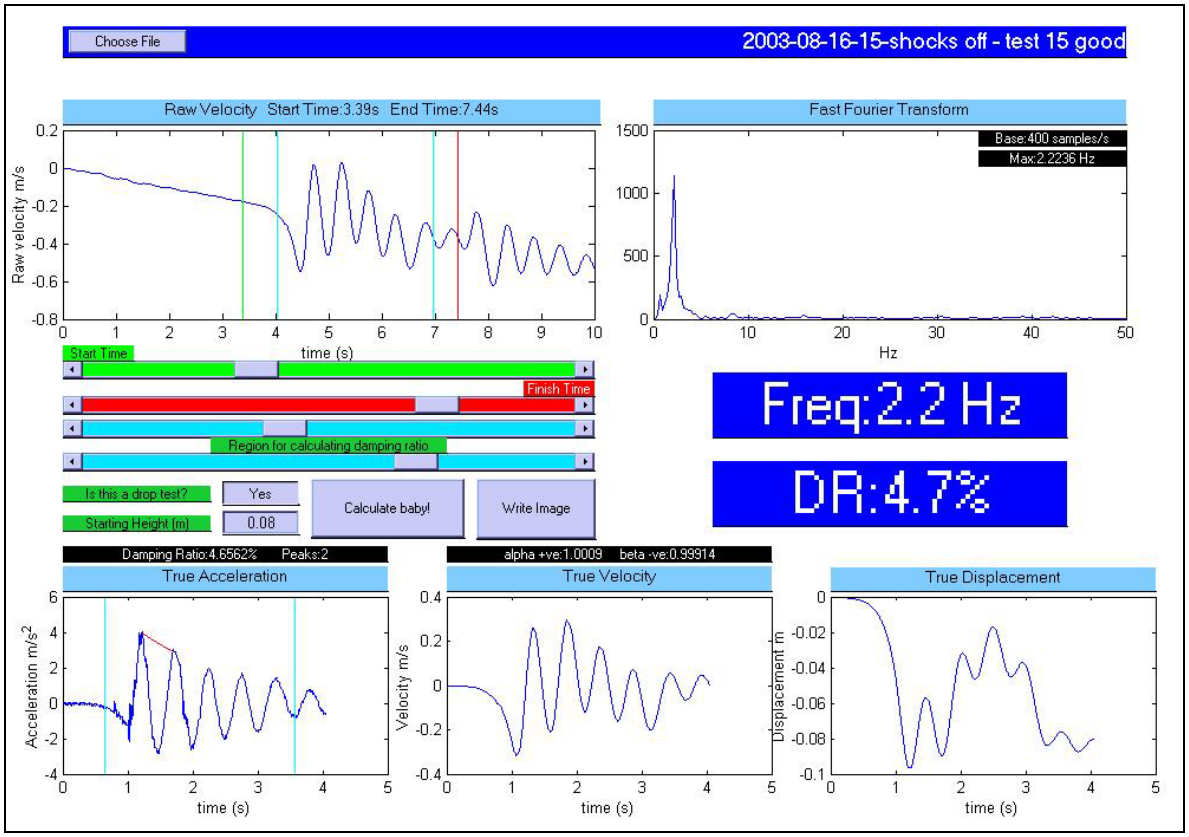

Testing session 3

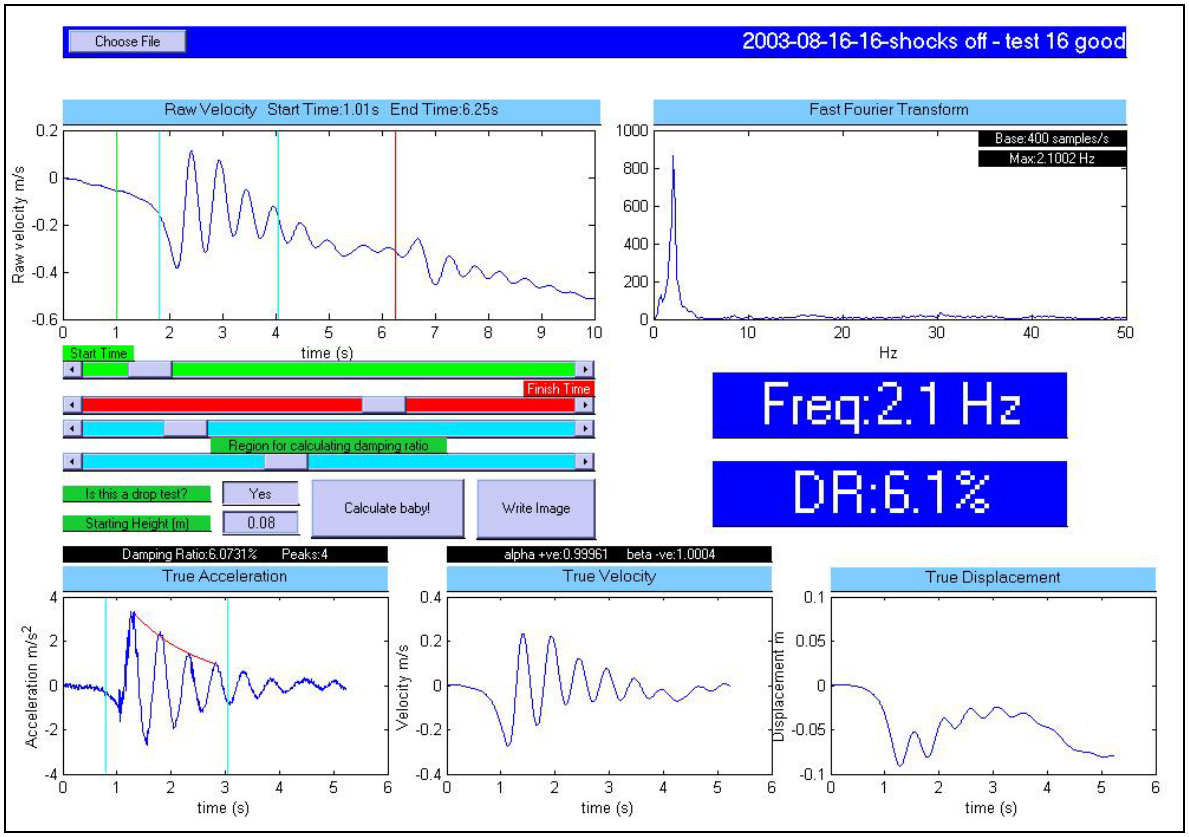

Testing session 4

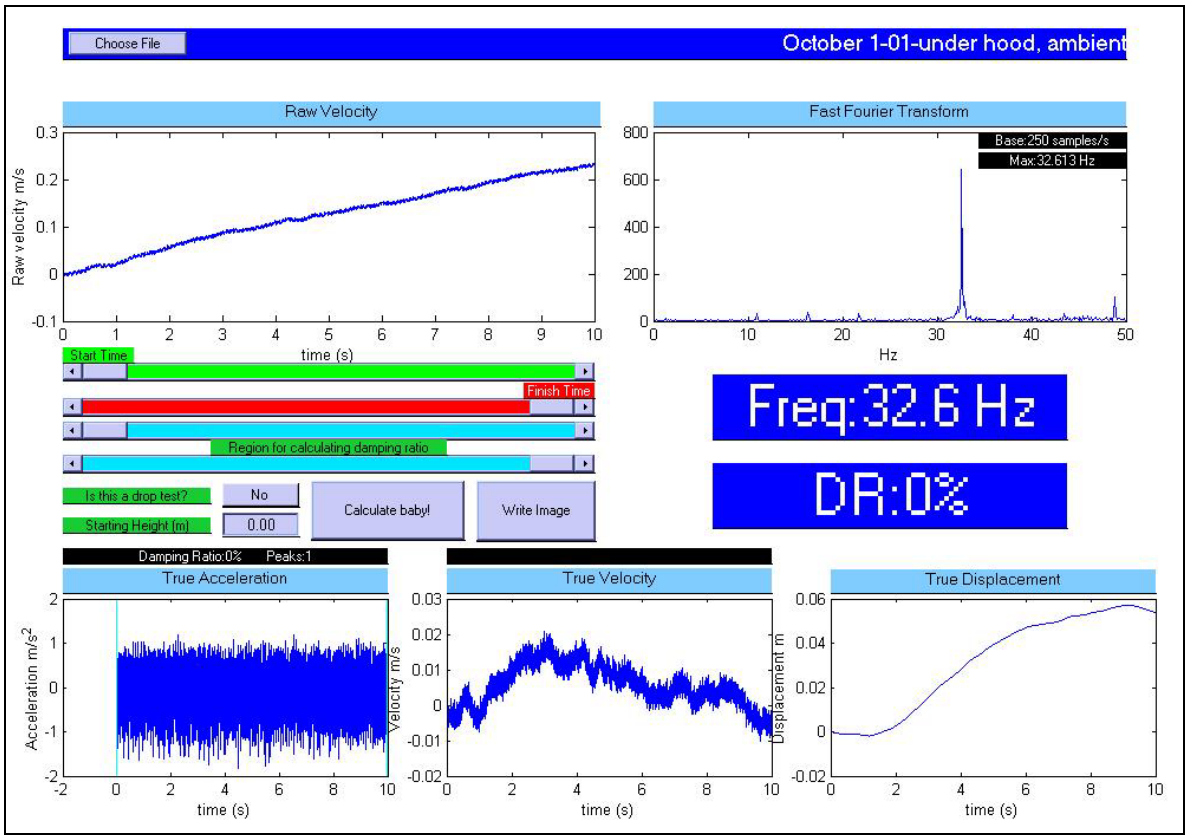

Testing session 4

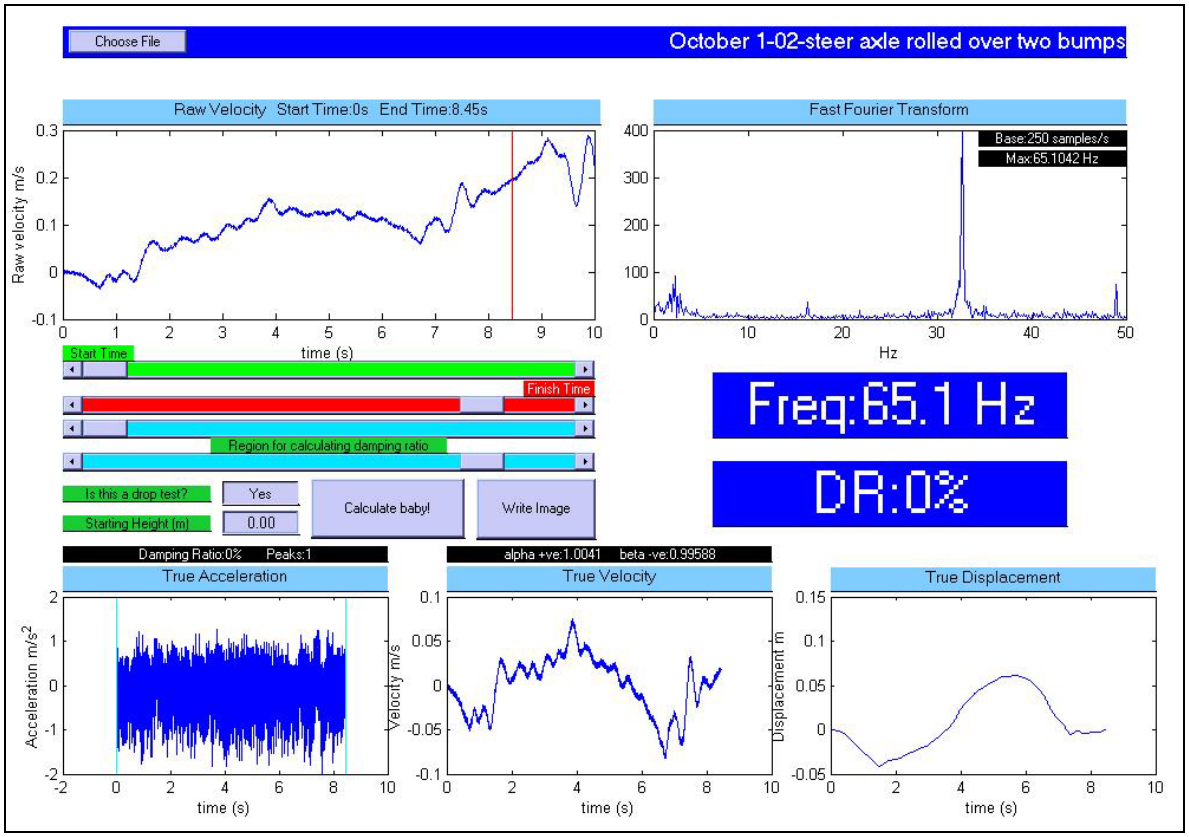

Testing session 4

Testing session 4

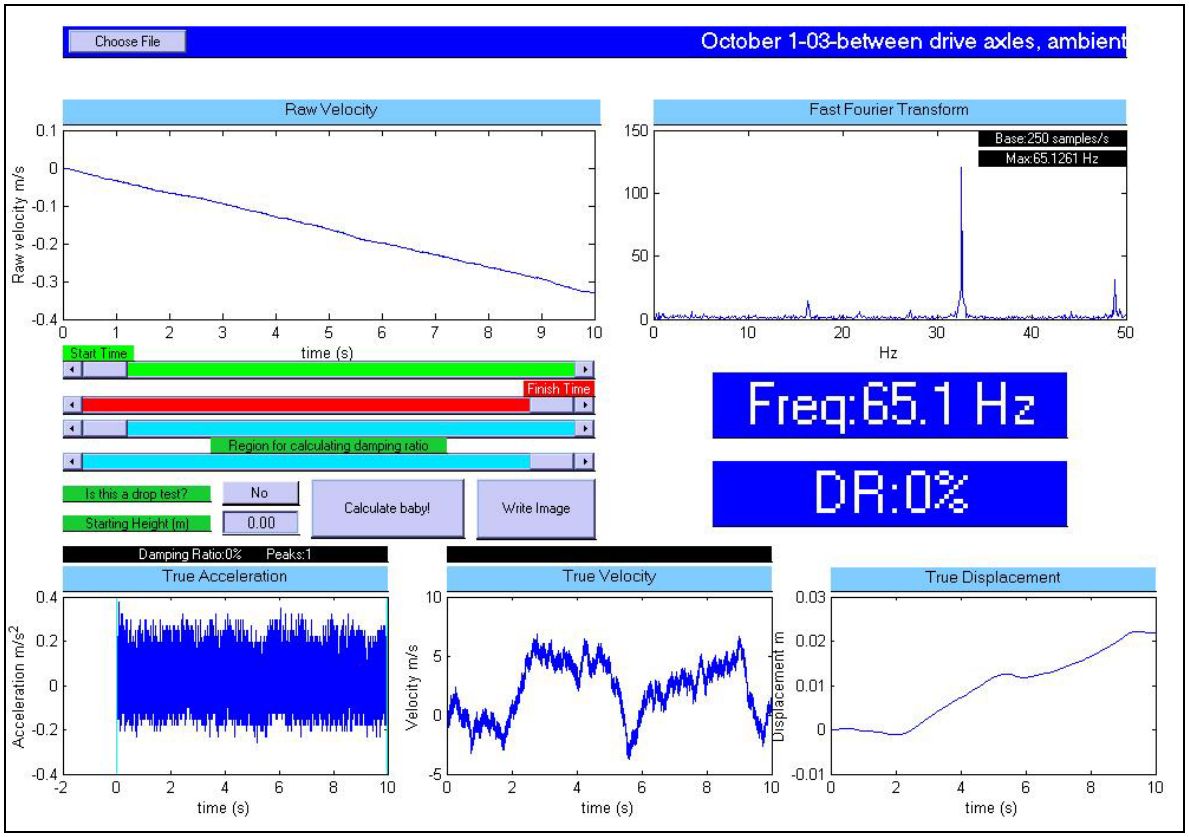

Testing session 4

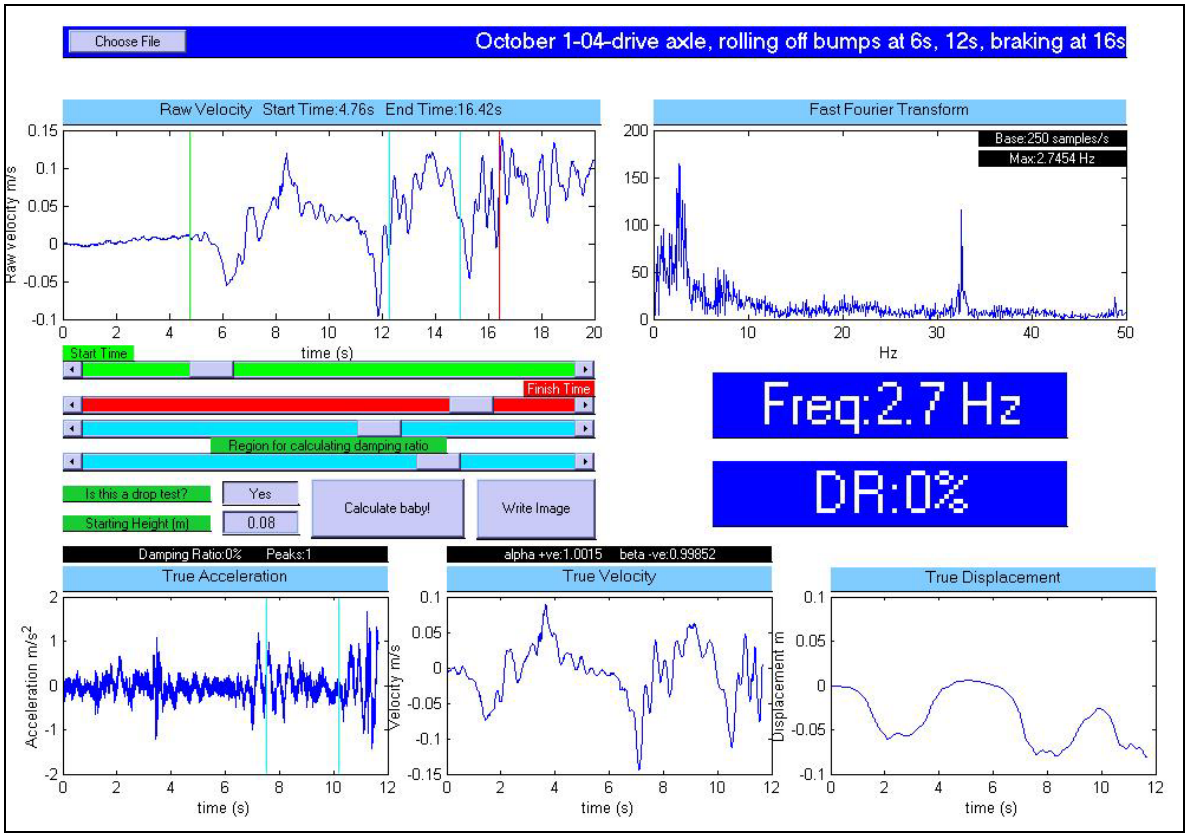

Testing session 4

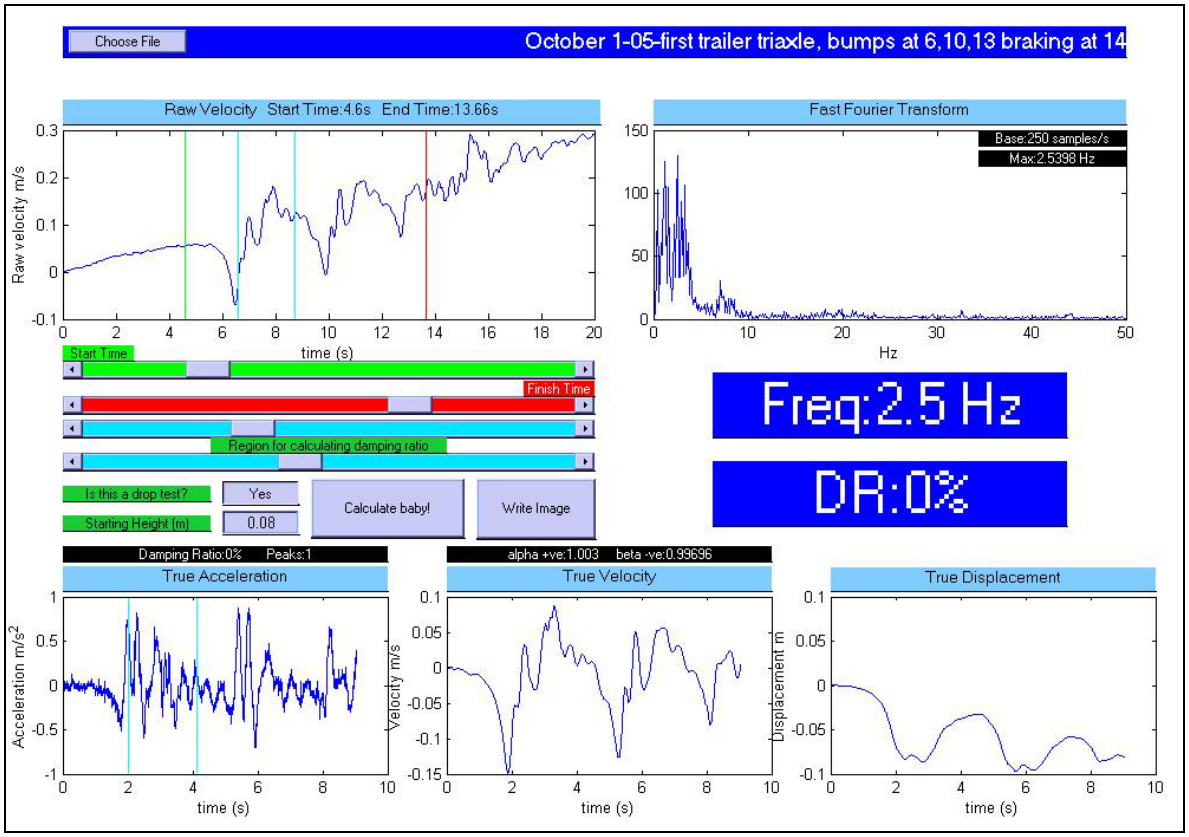

Testing session 4

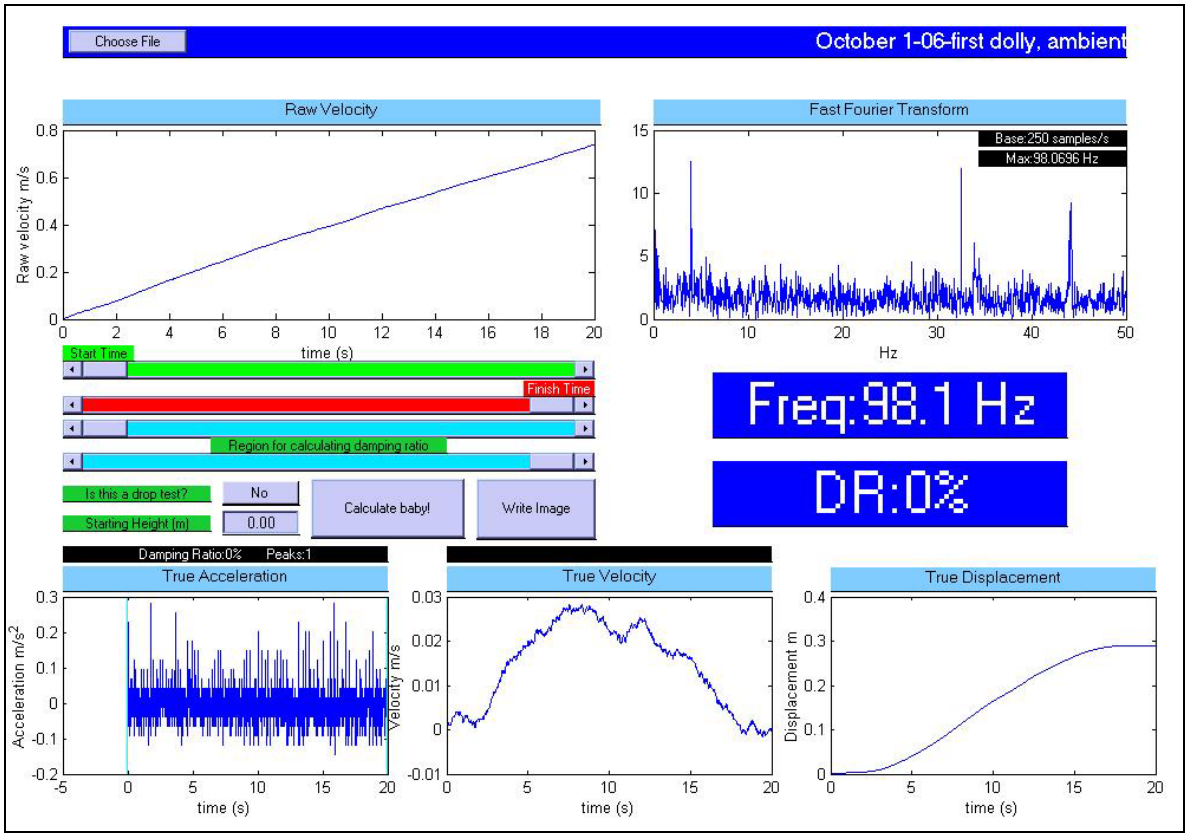

Testing session 4

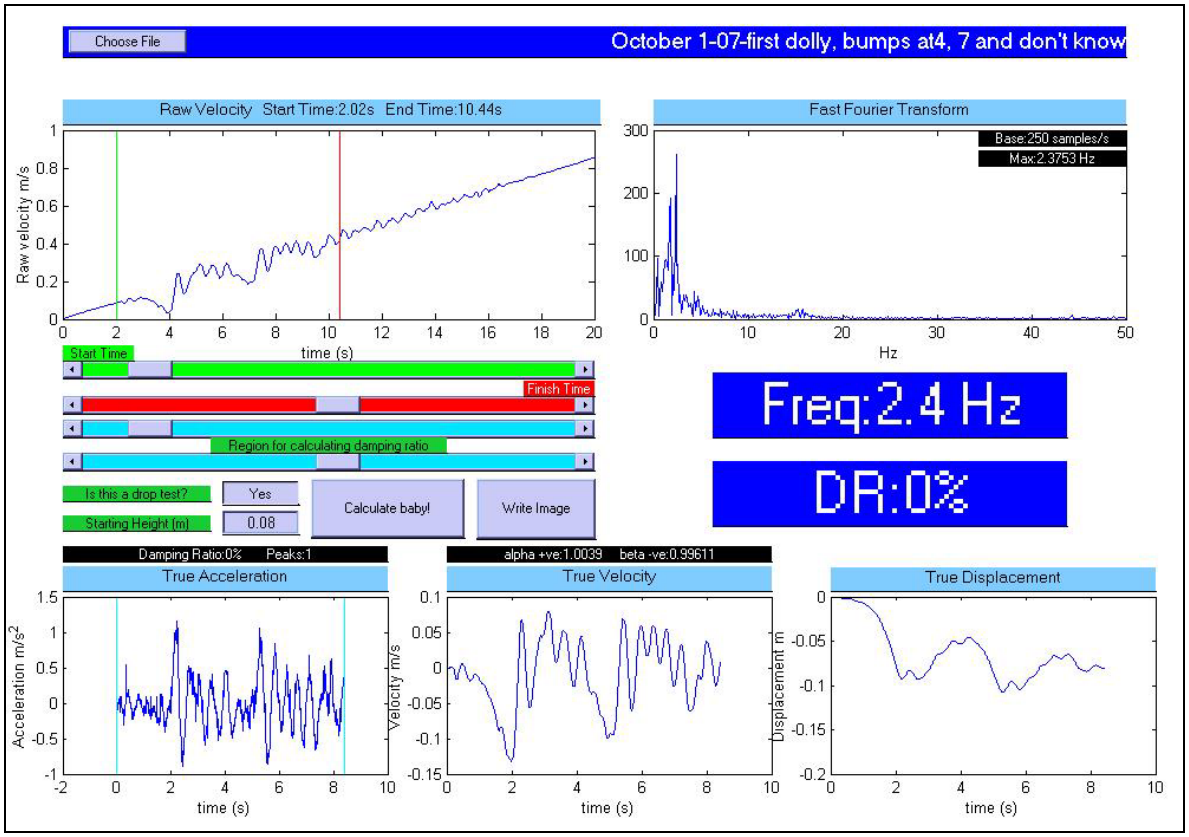

Testing session 4

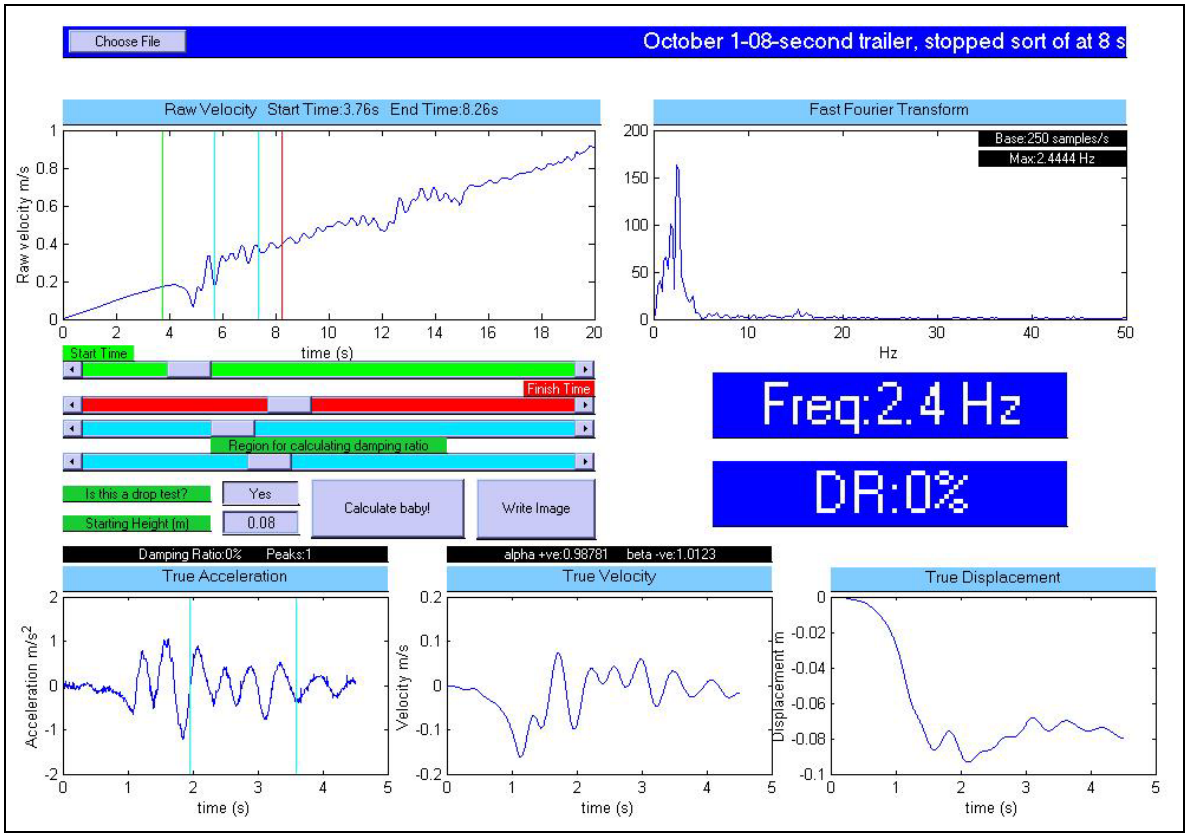

Testing session 4

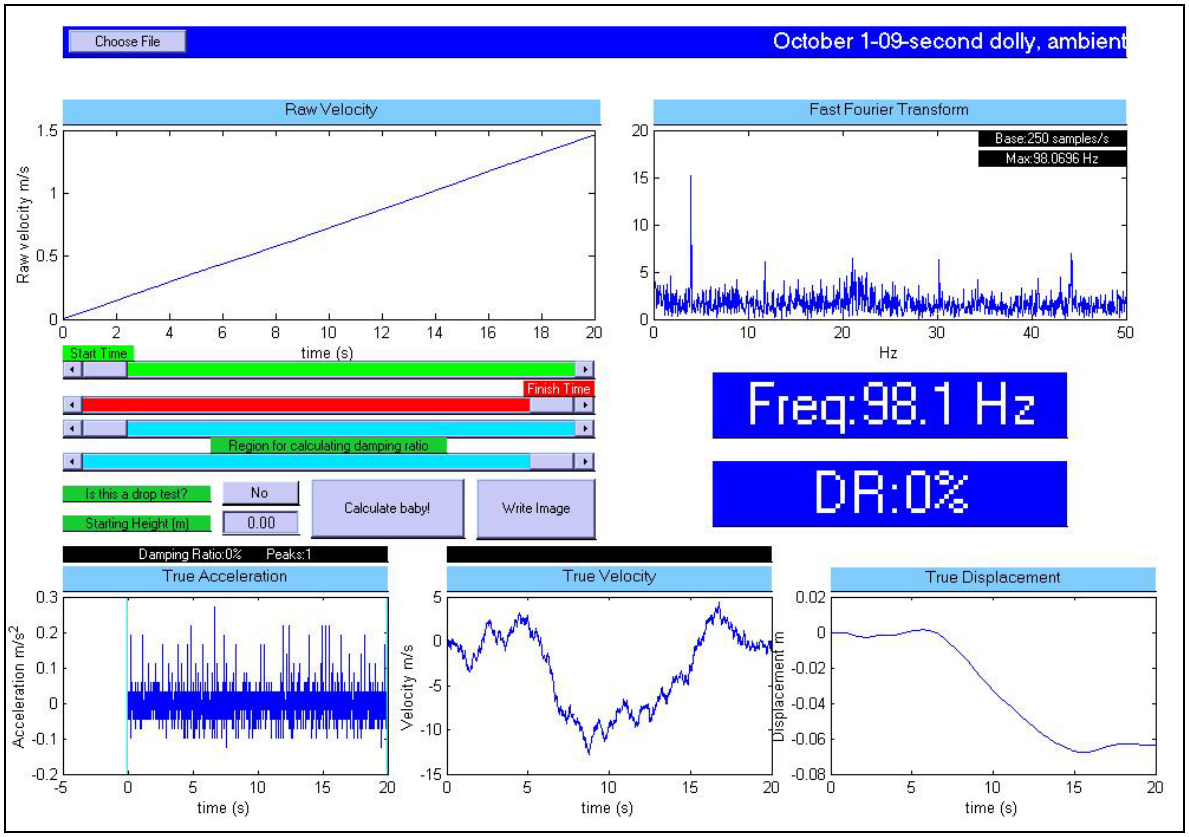

Testing session 4

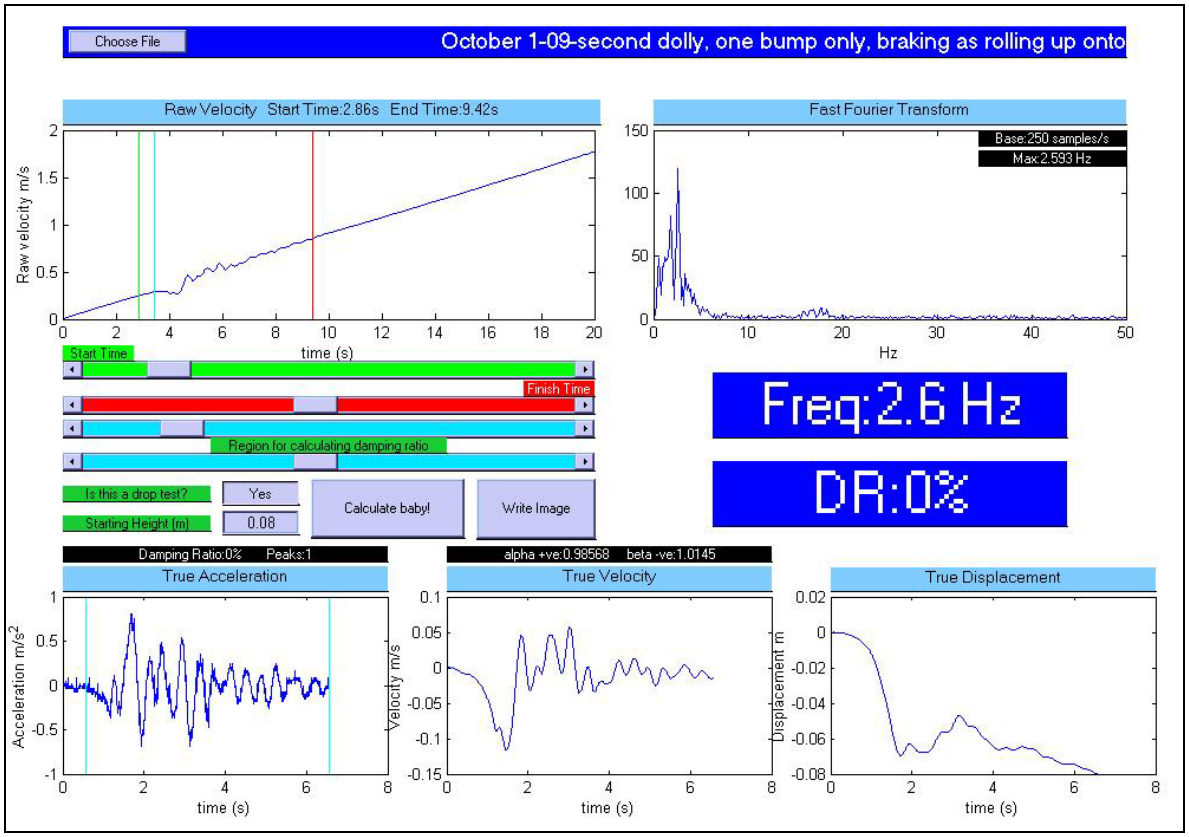

Testing session 4

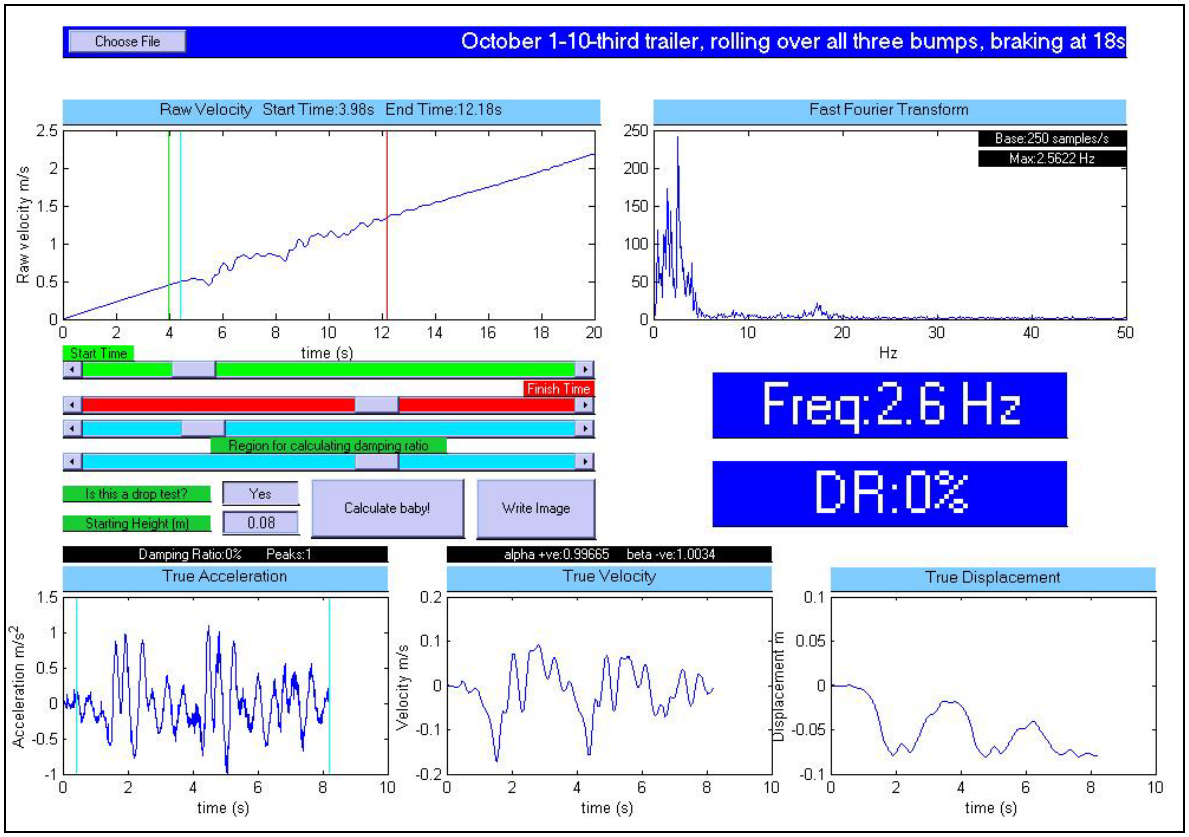

APPENDIX C

PHOTOS

The following photos were taken during the course of this investigation. They may prove useful for understanding of some of the concepts and equipment involved.

Figure C1: A typical Hendrickson-type suspension arrangement, with forward mounted shock absorber and short airbag. The operator of this vehicle was known to be unhappy with the general dynamic performance of the trailer to which this suspension was fitted.

Figure C2: A chassis under construction at the premises of Danteng (courtesy Dante Travaglini). This suspension is shown to with shock absorbers mounted rearwards of the axle.

Figure C3: Testing session 1 in progress, with tandem axle semi trailer vehicle.

Figure C4: The bumps, without frame, as used for testing session 1

Figure C5: The non-rigid clamp device, used to attach the accelerometer to the vehicle for testing session 1. It was consequently discarded for accelerometer attachment purposes in favour of a rigid magnet.

Figure C6: The rigid vehicle with mechanical leaf suspension used for testing session 2.

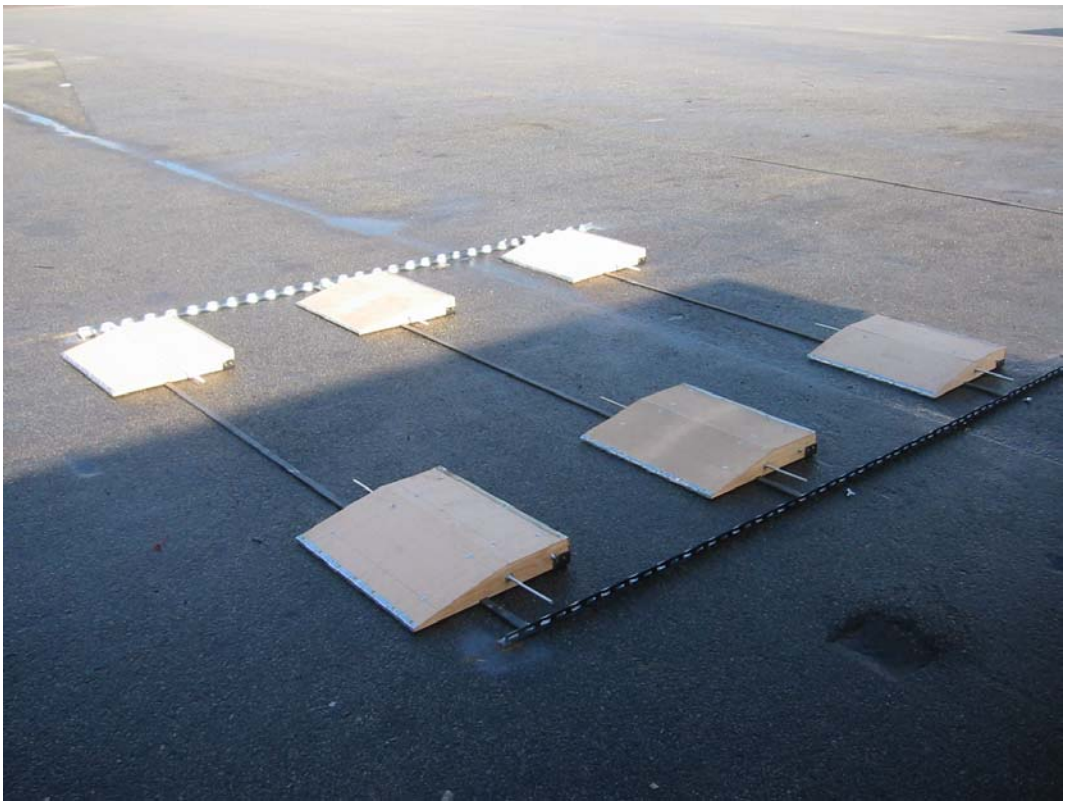

Figure C7: The bumps-in-frame arrangement used for testing session 3 and 4.

Figure C8: Location of the accelerometer on magnet, attached to the chassis between the axles.

Figure C9: Testing session 3 in progress. Note the non-rigid attachment device is being used to guide cables away from the wheel area.

Figure C10: The tripe road train used in testing session 4.

Figure C11: Detailed view of the accelerometer. Size is 2.5cm by 2.5cm.

Figure C12: Labpro data collection device.